Novel Oxovanadium Complexes with Alkoxy, Ketone, and Alcohol Ligands: Syntheses, Characterization and Catalysis

vorgelegt von

Master of Science

Huiling Cui

aus Hebei/V. R. China

von der Fakultät II - Mathematik und Naturwissenschaften

der Technischen Universität Berlin

zur Erlangung des akademischen Grades

Doktor der Naturwissenschaften

- Dr. rer. nat. -

genehmigte Dissertation

Promotionsausschuss:

Vorsitzender: Prof. Dr. Roderich Süßmuth

1. Berichter: Prof. Dr. Herbert Schumann

2. Berichter: Prof. Dr. Andreas Grohmann

Tag der mündlichen Prüfung: 20.04.2006

Berlin 2006

D 83

Abstract

Cui, Huiling

Neue Oxovanadium-Komplexe mit Alkoxy-, Keton- und Alkoholliganden: Synthese, Charakterisierung und Katalyse.

Eine Reihe von Vanadiumkomplexen mit chelatisierenden Alkoxyalkoholat-Liganden wurde synthetisiert. Zum Vergleich wurden einfache Vanadiumalkoxy-Komplexe hergestellt und der Effekt verschiedener Ausgangsverbindungen wurde studiert. Die Reaktion von $VOCl_3$ mit zwei Äquivalenten oder einem Überschuss CH_3OH in Pentan führt zu $[VOCl_2(OCH_3)(HOCH_3)_2]$ (**1**), wogegen die Reaktion von $VOCl_3$ mit zwei Äquivalenten CH_3ONa in Pentan $[VOCl(\mu\text{-}OCH_3)(OCH_3)]_2$ (**2**) ergibt. Die Reaktion ist lösungsmittelabhängig: $VOCl_3$ reagiert mit C_2H_5ONa in Tetrahydrofuran zu $[\{VOCl(\mu\text{-}OC_2H_5)(OC_2H_5)\}_2(\mu\text{-}THF)]$ (**3**). Die chlorverbrückten Komplexe $[VO(\mu\text{-}Cl)Cl\{\eta^2\text{-}OC(CH_3)_2CH_2OCH_3\}]_2$ (**4**) und $[VO(\mu\text{-}Cl)Cl\{\eta^2\text{-}OCH_2(cyclo\text{-}C_4H_7O)\}]$ (**5**) wurden durch die Reakion von $VOCl_3$ mit einem Äquivalent des entsprechenden Alkohols erhalten. **4** unterliegt der Reduktion und führt zu $[VOCl\{\mu,\eta^2\text{-}OC(CH_3)_2CH_2OCH_3\}]_2$ (**15**). Die monomeren Komplexe $[VOCl_2(\eta^2\text{-}OCH_2CH_2OR)(THF)]$ (R = Me (**6**), Et (**7**), ^{i}Pr (**8**)), $[VOCl_2\{\eta^2\text{-}OC(CH_3)_2CH_2OCH_3\}(THF)]$ (**9**) wurden durch Reaktion der entsprechenden dimeren Komplexe mit Tetrahydrofuran erhalten. $[VOCl_2(\eta^3\text{-}OCH_2CH_2OCH_2CH_2OC_4H_9)]$ (**10**) wurde durch Reaktion von $VOCl_3$ mit einem Äquivalent des entsprechenden Alkohols erhalten. $[VOCl_2\{OCH_2(cyclo\text{-}C_4H_7O)\}\{HOCH_2(cyclo\text{-}C_4H_7O)\}]$ (**11**) wurde durch Reaktion von $VOCl_3$ mit zwei Äquivalenten Alkohol erhalten. **11** reagiert in Toluol bei 70 °C und vermindertem Druck zu $[VOCl\{OCH_2(cyclo\text{-}C_4H_7O)\}_2]$ (**12**). $[VO\{OC(CH_3)_2CH_2OCH_3\}_3]$ (**13**) wurde durch Reaktion von $VOCl_3$ mit zwei Äquivalenten des entsprechenden Lithiumalkoxids erhalten. Die Behandlung von $HOC(C_6H_5)_2C(C_6H_5)_2OH$ mit einem Äquivalent $VOCl_3$ führt zu einem C–C-Bindungsbruch und Reduktion des Vanadium(V)-Kerns zu $[VOCl_2(O{=}CPh_2)_2]$ (**14**). $[VO(\mu\text{-}Cl)Cl(\eta^2\text{-}OCH_2CH_2OCH_3)]_2$ wurde durch PPh_3 reduziert und es wurde $[VOCl_2(OPPh_3)_2]\cdot CH_2Cl_2$ erhalten. Die Alkylierung von $[VO(\mu\text{-}Cl)Cl(\eta^2\text{-}OCH_2CH_2OCH_3)]_2$ mit $(CH_3)_3SiCH_2MgCl$ führt zu $[VO\{CH_2Si(CH_3)_3\}_3]$, während die Reaktion von $(CH_3)_3CCH_2Li$ und $PhCH_2MgCl$ zu Vanadium(IV)-Komplexen führt. $[VO(\mu\text{-}Cl)Cl(\eta^2\text{-}OCH_2CH_2OCH_3)]_2$ reagiert mit Acetonitril zu $[VOCl_2(\eta^2\text{-}OCH_2CH_2OCH_3)(CH_3CN)]$ (**16**) das im Sonnenlicht oder unter UV-Bestrahlung zu $[VOCl_2(\eta^2\text{-}HOCH_2CH_2OCH_3)(CH_3CN)]$ (**17**) reagiert. Auf die gleiche Weise wurden $[VOCl_2(\eta^2\text{-}HOCH_2CH_2OC_2H_5)(CH_3CN)]$ (**18**) und $[VOCl_2\{\eta^2\text{-}HOCH_2(cyclo C_4H_7O)\}(CH_3CN)]$ (**19**) erhalten. Die Komplexe **1**–**10**, **14**–**19**, und $[VOCl_2(OPPh_3)_2]\cdot CH_2Cl_2$ wurden kristallographisch untersucht. Es wurden katalytische Ethenpolymerisationen mit $[VO(\mu\text{-}Cl)Cl(\eta^2\text{-}OCH_2CH_2OCH_3)]_2$ in Kombination mit Methylaluminoxan oder Diethylaluminiumchlorid als Cokatalysator und Methyltrichloracetat als Promotor durchgeführt. Das System $[VO(\mu\text{-}Cl)Cl(OCH_2CH_2OCH_3)]_2$/Diethylaluminiumchlorid zeigt eine bedeutend höhere Aktivität als das Vergleichssystem $VOCl_3$/Diethylaluminiumchlorid. Die erzeugten Polymere besitzen eine höhere Molmasse bei enger Molmassenverteilung. $[VO(\mu\text{-}Cl)Cl(\eta^2\text{-}OCH_2CH_2OR)]_2$ (R = Me, Et, Ph) wurden in der Oligomerisierung von Styrol in Kombination mit Methylaluminoxan als Cokatalysator und Methyltrichloracetat als Promotor getestet. Mit $[VO(\mu\text{-}Cl)Cl(\eta^2\text{-}OCH_2CH_2OCH_3)]_2$ und $[VOCl_2(OCH_2CH_2Ph)]$ wurden Oligomerisierungen von 1-Decen in Kombination mit Methylalumoxan als Cokatalysator und Methyltrichloracetat als Promotor durchgeführt. $[VO(\mu\text{-}Cl)Cl(\eta^2\text{-}OCH_2CH_2OR)]_2$ (R = Me, Et, ^{i}Pr), **5**, **7**, **8** und $[VOCl_2(OCH_2CH_2OPh)]$ initiieren die Oligomerisierung von 1-Hexen in Kombination mit Methylaluminoxan als Cokatalysator und Methyltrichloracetat als Promotor. Die katalytische Epoxidierung von *cis*-Cycloocten durch *tert*-Butylhydroperoxid unter Verwendung von $[VO(\mu\text{-}Cl)Cl(\eta^2\text{-}OCH_2CH_2OR)]_2$ (R = Me, Et, ^{i}Pr), **4**, **5**, **10** und $[VOCl_2(OCH_2CH_2OPh)]$ als Katalysator wurde mit mäßigen Ausbeuten durchgeführt.

Abstract

Cui, Huiling

Novel Oxovanadium Complexes with Alkoxy, Ketone, and Alcohol Ligands: Syntheses, Characterization and Catalysis

A series of vanadium complexes is synthesized.
The effects of the reactants ratio, starting materials, and reaction media on the formation of the oxovanadium alkoxides are studied. Complexes $[VOCl_2(OCH_3)(HOCH_3)_2]$ (**1**), $VOCl(\mu\text{-}OCH_3)(OCH_3)]_2$ (**2**), and $[\{VOCl(\mu\text{-}OC_2H_5)(OC_2H_5)\}_2(\mu\text{-THF})]$ (**3**) are synthesized. $[VO(\mu\text{-Cl})Cl\{\eta^2OC(CH_3)_2CH_2OCH_3\}]_2$ (**4**) and $[VO(\mu\text{-Cl})Cl\{\eta^2\text{-}OCH_2(cyclo\text{-}C_4H_7O)\}]$ (**5**), which bear bridging chloro ligands, are prepared by the reaction of $VOCl_3$ with 1 equivalent of the corresponding alcohol. **4** undergoes reduction to afford $[VOCl\{\mu,\eta^2\text{-}OC(CH_3)_2CH_2O\text{-}CH_3\}]_2$ (**15**). $[VOCl_2(\eta^2\text{-}OCH_2CH_2OR)(THF)]$ (R = Me (**6**), Et (**7**), ^{i}Pr (**8**)), $[VOCl_2\{\eta^2\text{-}O\text{-}C(CH_3)_2CH_2OCH_3\}(THF)]$ (**9**) are obtained by reaction of the corresponding dimeric complexes with tetrahydrofuran. $[VOCl_2(\eta^3\text{-}OCH_2CH_2OCH_2CH_2OC_4H_9)]$ (**10**) is obtained from the reaction of $VOCl_3$ with 1 equivalent of the corresponding alcohol. $[VOCl_2\{OCH_2(cyclo C_4H_7O)\}\{HOCH_2(cyclo\text{-}C_4H_7O)\}]$ (**11**) is prepared by reaction of $VOCl_3$ with 2 equivalents of alcohol. Complex **11** is converted into $[VOCl\{OCH_2(cyclo\text{-}C_4H_7O)\}_2]$ (**12**) under reduced pressure. $[VO\{OC(CH_3)_2CH_2OCH_3\}_3]$ (**13**) is synthesized by the reaction of $VOCl_3$ with 3 equivalents of the corresponding alkoxide. Treatment of $HOC(C_6H_5)_2C\text{-}(C_6H_5)_2OH$ with 1 equivalent of $VOCl_3$ leads to cleavage of the C–C bond to give $[VOCl_2(O{=}CPh_2)_2]$ (**14**). $[VO(\mu\text{-Cl})Cl(\eta^2\text{-}OCH_2CH_2OCH_3)]_2$ is reduced by PPh_3 to give $[VOCl_2(OPPh_3)_2]\cdot CH_2Cl_2$. Alkylation of $[VO(\mu\text{-Cl})Cl(\eta^2\text{-}OCH_2CH_2OCH_3)]_2$ with $(CH_3)_3SiCH_2MgCl$ affords $[VO\{CH_2Si(CH_3)_3\}_3]$, while alkylation with $(CH_3)_3CCH_2Li$ and $PhCH_2MgCl$ leads to vanadium(IV) complexes. When $[VO(\mu\text{-Cl})Cl(\eta^2\text{-}OCH_2CH_2OCH_3)]_2$ reacts with acetonitrile, $[VOCl_2(\eta^2\text{-}OCH_2CH_2OCH_3)(CH_3CN)]$ (**16**) is isolated, which is reduced to $[VOCl_2(\eta^2\text{-}HOCH_2CH_2OCH_3)(CH_3CN)]$ (**17**) in the sunlight or by UV radiation. Similarly, $[VOCl_2(\eta^2\text{-}HOCH_2CH_2OC_2H_5)(CH_3CN)]$ (**18**) and $[VOCl_2\{\eta^2\text{-}HOCH_2(cyclo\text{-}C_4H_7O)\}(CH_3CN)]$ (**19**) are produced. Complexes **1**–**10**, **14**–**19**, and $[VOCl_2(OPPh_3)_2]\cdot CH_2Cl_2$ are studied by X-ray crystallography. Catalytic ethylene polymerizations for $[VO(\mu\text{-Cl})Cl(\eta^2\text{-}OCH_2CH_2OCH_3)]_2$ in combination with methyl alumoxane or diethylaluminum chloride as cocatalyst and methyl trichloroacetate as promoter are performed. The $[VO(\mu\text{-Cl})Cl(OCH_2CH_2OCH_3)]_2$/diethylaluminum chloride system exhibits remarkably higher activity than the $VOCl_3$/diethylaluminum chloride system. The polymers have high molecular masses with rather broad polydispersities. $[VO(\mu\text{-Cl})Cl(\eta^2\text{-}OCH_2CH_2OR)]_2$ (R = Me, Et, Ph) are tested for styrene oligomerization in combination with methyl alumoxane as cocatalyst and methyl trichloroacetate as promoter. $[VO(\mu\text{-Cl})Cl(\eta^2\text{-}OCH_2CH_2OCH_3)]_2$ and $[VOCl_2(OCH_2CH_2Ph)]$ are tested for 1-decene oligomerization with methyl alumoxane as cocatalyst and methyl trichloroacetate as promoter. $[VO(\mu\text{-Cl})Cl(\eta^2\text{-}OCH_2CH_2OR)]_2$ (R = Me, Et, ^{i}Pr), **5**, **7**, **8**, and $[VOCl_2(OCH_2CH_2OPh)]$ initiate 1-hexene oligomerization in combination with diethylaluminum chloride or methyl alumoxane as cocatalyst and methyl trichloroacetate as promoter. The catalytic epoxidation of *cis*-cyclooctene is performed with *tert*-butyl hydroperoxide employing $[VO(\mu\text{-Cl})Cl(\eta^2\text{-}OCH_2CH_2OR)]_2$ (R = Me, Et, ^{i}Pr), **4**, **5**, **10**, and $[VOCl_2(OCH_2CH_2OPh)]$ as catalysts, wherein moderate yields of cyclooctene oxide are obtained.

The work described in this dissertation has been carried out at the Institut für Chemie der Technischen Universität Berlin between July 2002 and April 2006.

I would like to give my sincere appreciation to Dr. Esther C. E. Rosenthal for her continuous guidance, suggestions, discussion, and encouragement throughout the course of this thesis. I also thank her for the help and care during my stay in Berlin.

I sincerely appreciate Prof. Dr. Herbert Schumann for his constant instruction, suggestions, and discussion during the course of this work. I would also like to thank him for the personal kindness and care during my stay in Berlin.

I am grateful to Prof. Dr. Andreas Grohmann for his acceptance of the second commentatorship.

Acknowledgements are given to Dr. Sebastian Dechert, Dr. Markus Hummert, Ms. Marina Borowski for X-ray crystal structure determinations and resolution; Dr. Alexandra Steffens, Prof. Dr. Bart Hessen for GPC measurement. Thanks are also extended to Ms. Sigrid Imme (CHN, IR), Dr. Heinz-Jürgen Kroth and Mr. Manfred Dettlaff (NMR), Mr. Martin Kempf, Ms. Semiha Schwarz, and Ms. Alice Stöckel (MS), Prof. Dr. Igor L. Fedushkin, and Dr. Friedhelm Lendzian (ESR).

I owe my special thanks to my colleague Mr. Nils Meyer for his friendship and help during his stay in this laboratory. Also I want to say thanks to all the group members of Prof. Schumann for the help and kindness they offered.

My thanks are due to Prof. Dr. Miao Du, Mr. Xing-Guo Chen, and Dr. Zhijian Li for reading and correcting the manuscript.

I am heartfully grateful to my parents and my wife Zhenzhen Wen for years of selfless affection and encouragement.

This work was supported by the Deutsche Forschungsgemeinschaft (Graduiertenkolleg “Synthetische, mechanistische und reaktionstechnische Aspekte von Metallkatalysatoren”).

List of Abbreviations, Acronyms and Symbols

acac	acetylacetonate
Am	amyl, $CH_2C(CH_3)_3$
Anal.	Analysis
br	broad
Calc.	calculated
C.N.	coordination number
d	doublet
DEAC	diethylaluminum chloride
δ	chemical shift (ppm)
Δ	difference
equiv	equivalent
GPC	gel permeation chromatography
J	coupling constant
KRS-5	TlBr-40%/TlI-60%
λ	wavelength
M^+	molecular ion
m	multiplet (NMR), medium (IR)
MAO	methyl alumoxane
mmp	1-methoxyl-2-methyl-2-propanolate
M.p.	melting point
MTCA	methyl trichloroacetate
m/z	mass/charge
ppm	parts per million
Pr	propyl
q	quartet
s	singlet
t	triplet
τ	angular parameter
TBHP	*tert*-butyl hydroperoxide
thffo	2-tetrahydrofuranylmethanolate
TMEDA	tetramethylethylendiamine
Z	number of molecules in the unit cell

1 Introduction 1

1.1 General Remarks 1

1.2 Preparation of Oxovanadium Alkoxides 1

1.3 Solution and Solid State Properties of Vanadates 3

1.4 Neutral Lewis Base Adducts of Oxovanadium(V) Complexes 6

1.5 Vanadium Catalysts for Olefin Polymerization 8

1.5.1 General Features of Homogeneous Vanadium Catalysts 8

1.5.2 Active Species and Polymerization Mechanism 9

1.5.3 Vanadium Catalysts 11

1.6 Vanadium Catalysts for Olefin Epoxidation 19

1.7 Aim and Objectives of the Present Work 20

2 Results and Discussion 21

2.1 Oxovanadium Methoxides and Ethoxides 21

2.1.1 Syntheses and Spectroscopic Characterization 21

2.1.2 X-ray Crystallographic Studies 23

2.2 Oxovanadium(V) Alkoxides with Chelating Ligands 27

2.2.1 Dimeric Oxovanadium(V) Alkoxides with Bidentate Ligands 27

2.2.2 THF Solvates of Oxovanadium(V) Alkoxyalkoxides 31

2.2.3 Reaction of $[VOCl_2(OCH_2CH_2OCH_3)]_2$ with Metal Alkyls and PPh_3 34

2.2.4 An Oxovanadium Alkoxide with a Tridentate Ligand 37

2.2.5 Oxovanadium Alkoxides with Two Tetrahydrofurfuroxo Ligands 40

2.2.6 An Oxovanadium Trisalkoxide 41

2.3 Oxovanadium(IV) Complexes 44

2.3.1 An Oxovanadum(IV) Dichloride with Benzophenone as Ligand 44

2.3.2 An Alkoxyalkoxo Chloro Oxovanadium(IV) Complex 47

2.4 Acetonitrile Solvates of Oxovanadium Complexes 49

2.4.1 Syntheses and Spectroscopic Characterization 49

2.4.2 X-ray Crystallographic Studies 52

2.5 Catalytic Studies 57

2.5.1 Ethylene Polymerization 57

2.5.2 1-Hexene Oligomerization 58

2.5.3 Styrene Oligomerization and 1-Decene Oligomerization 59

2.5.4 Cyclooctene Epoxidation 60

3 Experimental Section 61

3.1 General Remarks 61

3.2 Materials 62

3.3 Syntheses of Complexes 63

3.3.1 $[VOCl_2(OCH_3)(HOCH_3)_2]$ (**1**) 63

3.3.2 $[VOCl(\mu\text{-}OCH_3)(OCH_3)]_2$ (**2**) 63

3.3.3 $[\{VOCl(\mu\text{-}OC_2H_5)(OC_2H_5)\}_2(\mu\text{-THF})]$ (**3**) 64

3.3.4 $[VO(\mu\text{-}Cl)Cl(\eta^2\text{-}OC(CH_3)_2CH_2OCH_3)]_2$ (**4**) 64

3.3.5 [VO(μ-Cl)Cl{η²-OCH₂*cyclo*-(C₄H₇O)}]₂ (**5**) 66
3.3.6 [VOCl₂(η²-OCH₂CH₂OCH₃)(THF)] (**6**) 66
3.3.7 [VOCl₂(η²-OCH₂CH₂OC₂H₅)(THF)] (**7**) 67
3.3.8 [VOCl₂{η²-OCH₂CH₂OCH(CH₃)₂}(THF)] (**8**) 68
3.3.9 [VOCl₂(η²-OC(CH₃)₂CH₂OCH₃)(THF)] (**9**) 68
3.3.10 Alkylation of [VOCl₂(OCH₂CH₂OCH₃)]₂ 69
3.3.11 Reaction of [VOCl₂(OCH₂CH₂OCH₃)]₂ with PPh₃ 70
3.3.12 [VOCl₂(η³-OCH₂CH₂OCH₂CH₂OC₄H₉)] (**10**) 70
3.3.13 [VOCl₂{OCH₂*cyclo*-(C₄H₇O)}{HOCH₂*cyclo*-(C₄H₇O)}] (**11**) 71
3.3.14 [VOCl{OCH₂*cyclo*-(C₄H₇O)}₂]₂ (**12**) 72
3.3.15 [VO(OC(CH₃)₂CH₂OCH₃)₃] (**13**) 72
3.3.16 [VOCl₂(O=CPh₂)₂] (**14**) 73
3.3.17 [VOCl(μ,η²-OC(CH₃)₂CH₂OCH₃)]₂ (**15**) 74
3.3.18 [VOCl₂(η²-OCH₂CH₂OCH₃)(CH₃CN)] (**16**) 74
3.3.19 [VOCl₂(η²-HOCH₂CH₂OCH₃)(CH₃CN)] (**17**) 75
3.3.20 [VOCl₂(η²-HOCH₂CH₂OC₂H₅)(CH₃CN)] (**18**) 76
3.3.21 [VOCl₂{η²-HOCH₂(*cyclo*-C₄H₇O)}(CH₃CN)] (**19**) 77
3.4 Polymerization and Oligomerization 77
3.4.1 Ethylene Polymerization 77
3.4.2 1-Hexene Oligomerization 78
3.4.3 Styrene and 1-Decene Oligomerization 79
3.5 Cyclooctene Epoxidation 80
3.5.1 Handling of TBHP 80
3.5.2 Epoxidation Procedure 80
4 Summary and Outlook 82
5 Appendix 87
5.1 Crystal Data and Refinement Details 87
5.2 Packing Diagrams of Single Crystals 91
5.3 Experimental Details for Ethylene Polymerization 99
5.4 Experimental Details for Styrene Oligomerization 101
6 References 102

1 Introduction

1.1 General Remarks

Vanadium alkoxides have been of continuous interests in a wide range of fields since they were synthesized.[1,2] They are valuable precursors for electronic and ceramic materials,[3] prominent source materials for sol-gel techniques, and attractive precursors for chemical vapor deposition of metal oxides.[3] Due to their structural and electronic analogy to phosphate, Oxovanadium alkoxides have been proven to be the best analogues to phosphate with similar protonation reactions for mimicking cellular metabolites in biology.[4] Mixed hydroxo oxovanadium alkoxides $[VO(OH)_{3-n}(OR)_n]$ (n = 1 or 2) are found to be inhibitors for alkaline and acid phosphatases.[4,5] Depending on the oxidation state and coordination sphere of the vanadium centers, vanadium alkoxides can be used to develop numerous novel and selective redox organic reactions.[6] Since vanadium was employed by Carrick for ethylene polymerization,[7] an increased interest focused on vanadium alkoxides and related compounds as catalysts in Ziegler-Natta polymerization of olefins.[8,9] In the following part, the syntheses of the oxovanadium complexes as well as the catalytic reactivities of vanadium complexes will be discussed in detail.

1.2 Preparation of Oxovanadium Alkoxides

General approaches for oxovanadium trisalkoxides or mixed alkoxo vanadium chlorides formulated as $[VOCl_{3-n}(OR)_n]$ can be summarized in the types described in Scheme 1.1. Prandtl and Hess synthesized a series of oxovanadium alkoxides by refluxing V_2O_5 and the alcohols HOR (R = Et, ^{n}Pr, ^{n}Bu, ^{i}Bu, ^{t}Bu, ^{i}Am, and ^{t}Am, respectively).[2] An improved methodology for the synthesis of trisesters $[VO(OR)_3]$ is removal of the water produced in the reaction as an azeotrope with benzene to push the reaction to completion.[10,11] However, this method is not practicable for the synthesis of mixed vanadate chlorides $[VOCl_{3-n}(OR)_n]$. Reflux of a mixture of NH_4VO_3, a large excess of alcohol, and solvent such as toluene and cyclohexane and continuous removal of the H_2O by azeotropic distillation with the solvent yielded vanadium trisalkoxides. This approach is especially useful for vanadates with bulky alkoxo group like ^{i}Pr, ^{t}Bu or ^{t}Am.[12] Interestingly, $[VO\{OCH(CH_3)CH_2OCH_3\}_3]$ with an extra donor atom in the alkoxo moiety was prepared by this means.[13]

Funk employed $VOCl_3$ and alcohols for the synthesis of vanadates. It was found that the reaction patterns of $VOCl_3$ with ROH are rather complex.[14] For instance, $VOCl_3$ reacted with CH_3OH in 1:1 ratio in CCl_4 solution to produce $[VOCl_2(OCH_3)]$ as expected; however, attempts to prepare $[VOCl(OCH_3)_2]$ or $[VO(OCH_3)_3]$ were not successful regardless of the

$VOCl_3$ to CH_3OH ratio, a compound of the composition $[VOCl(OMe)_2 \cdot HCl \cdot MeOH]$ was isolated as the major product instead.[14] Similarly, the reaction of $VOCl_3$ and an excess C_2H_5OH was found to yield only a mixture of $[VOCl_2(OC_2H_5)]$ and $[VOCl(OC_2H_5)_2]$ rather than $[VO(OC_2H_5)_3]$ no matter how much C_2H_5OH was employed.[15] In the presence of a scavenger such as ammonia, HCl evolved in the reaction of $VOCl_3$ with ROH can be consumed by the formation of NH_4Cl to produce $[VO(OR)_3]$ in good yield. This method is applicable for the synthesis of a number of vanadium triesters.[14,16,17] Preparation of vanadium alkoxides from the stoichiometric reaction of $VOCl_3$ and ROLi or RONa *via* LiCl or NaCl elimination has been proven to be feasible because alcoholates are much more resistant toward oxidation by pentavalent vanadium. This method is practical for both trisalkoxides and mixed alkoxo oxovanadium alkoxides.[11]

Later on, the reaction between $VOCl_3$ and CH_3OH was studied using matrix isolation technique.[18] The reactive intermediates were isolated and characterized. The initial intermediate in the mechanism was identified as a weakly bound molecular complex of $VOCl_3$ and CH_3OH. $[VOCl_2(OCH_3)]$ is the second intermediate in the reaction sequence through the elimination of HCl from the initial complex, which decomposed above 150 °C leading to the formation of CH_2O and CH_3Cl.

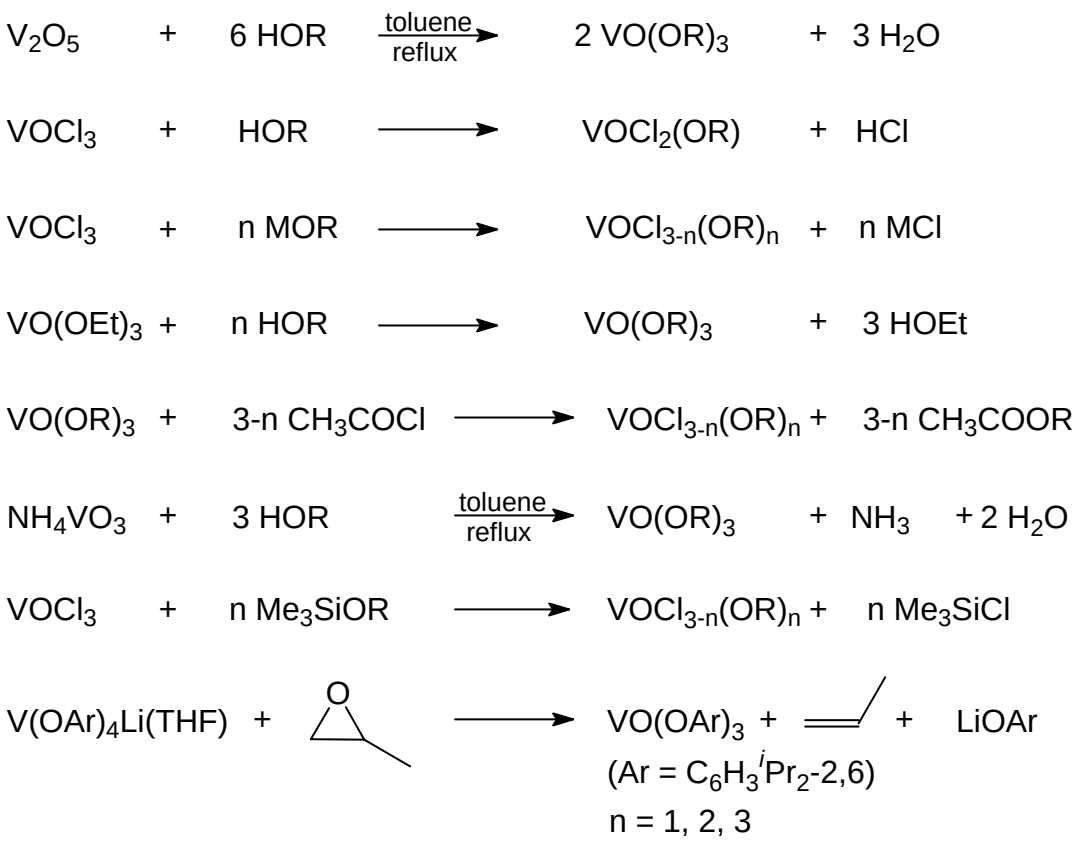

Scheme 1.1. Preparation of oxovanadium alkoxides.

Another practical technique for the synthesis of oxovanadium trisalkoxides [$VO(OR)_3$], especially with bulky alkyl substituents, is the ester exchange reaction.[19] [$VO(OC_2H_5)_3$] was refluxed with slight excess of higher alcohol and benzene. Ethanol liberated in the reactions was fractionated off azeotropically with benzene yielding orthovanadates (R = Me, ^{i}Pr, ^{t}Bu, ^{n}Bu, ^{s}Am, ^{t}Am, ^{s}Hex, ^{t}Hex, and cyclohexyl) in about 70% yield. Compared with other paths, the ester exchange reaction has several advantages: 1, the ethanol produced is continuously distilled off pushing the reaction to completion; 2, only slight excess of the higher alcohol is required which is of great importance due to the reductive properties of alcohols towards pentavalent vanadium; 3, side reactions like formation of alkyl chloride and water are avoided; 4, the oxidation of the alcohol is much less by ethyl vanadate than by oxovanadium trichloride or vanadium pentoxide.

In addition, mixed alkoxo vanadium halides [$VOCl_{3-n}(OR)_n$] have been prepared by reaction of [$VO(OR)_3$] with acetyl chloride *via* ligand metathesis.[15] It has been found that the reactions in the cases of primary and secondary alkoxides were facile while they became slow in the case of tertiary alkoxides. The disadvantage of this reaction is that the acetyl ester byproducts coordinate to the vanadium center.

A complementary method is to employ trimethylsiloxy derivatives to react with $VOCl_3$.[20] By this method vanadium aryloxides [$VOCl_{3-n}(OC_6H_4OMe\text{-}4)_n$] (n = 1 or 2) have been readily synthesized in good yields.[21] Oxidation of [$V(OC_6H_3{}^{i}Pr_2\text{-}2,6)_4Li(THF)$] with propylene oxide produced [$VO(OC_6H_3{}^{i}Pr_2\text{-}2,6)_3$] in good yield.[22] However, compared to the rapid development of oxovanadium alkoxides, less vanadium aryloxides have been reported due to the extensive reduction of pentavalent vanadium to poorly characterized species.[14]

1.3 Solution and Solid State Properties of Vanadates

Promoted by their fundamental and applied significance, numerous oxovanadium alkoxides with versatile functional groups and chelating ligands have been synthesized. They have been extensively studied by means of ^{1}H-,[10] ^{51}V-NMR,[11,23,24] IR spectroscopy,[25] mass spectrometry,[26] thermolytic characterizations,[27] and especially by X-ray diffraction oxovanadium alkoxides have been extensively studied. However, the structures characterized in the solid state may not be the same as the structures in solution, since exchange and fluxional processes occur in solution. Therefore the combination of characterizations, both in solution and in the solid state is important as direct correlation between solution and solid-state structures of vanadium alkoxides is unavailable.

Cryoscopic measurements[27] and mass spectrometric studies have indicated that the molecules of [$VO(OR)_3$] tend to form dimers and/or oligomers jointed by bridging alkoxide oxygens in

solution. Moreover, due to its low quadrupole moment, the ^{51}V nucleus may be considered the most favorable for NMR analysis among transition metal nuclei of spin > 1/2. NMR parameters obtained from vanadium spectra (shift values, nuclear spin-spin coupling constants, line widths and quadrupole splittings) have been employed in structural analyses and discussions of the electronic interactions in the coordination sphere of the metal nucleus.[11,23b,28,29,30] It has been revealed that simple oxovanadium alkoxides undergo rapid ligand exchange in solution,[24] and several species associated to different extent are in equilibrium.

^{51}V shielding depends on steric and electronic factors. It is now known that the shielding of vanadium nucleus has the features as follows: Crowding around the vanadium center leads to additional shielding;[23a,23c,23d, 29] an increase of the coordination number, *e.g.*, on going from tetrahedral to trigonal-bipyramidal or octahedral geometry leads to a decrease of shielding.[28,31,32] Therefore ^{51}V shielding increases with the bulk of the alkyl substituent, and an increase in concentration leads to a higher degree of oligomerization featured by a decrease of ^{51}V shift or at least a discrepancy in the relative ratio of different oligomers.[30] This discrepancy is more pronounced for $[VO(OCH_3)_3]$ and less demonstrated for esters with bulky R substituents, because the former tends to associate more readily than the latter.[11]

In view of the electronic factor, an inverse electronegativity dependence of ^{51}V shielding in the d^0 configuration has been observed. Specifically, the ^{51}V shielding of vanadium complexes increases with increasing electronegativity of the ligand attached to the metal center: namely the shielding of the vanadium nucleus increases in the order $VOBr_3 \leq VOCl_3 < VOF_3$ between coordinating atoms in the same group,[23a] while in the same period, the shielding increases with the increasing nucleus charge, *e.g.*, $[VO(NEt)_3] < [VO(OR)_3] < [VOF_3]$.[23a]

Interests in the X-ray diffraction of vanadate esters have been evoked by the structural similarity of vanadate with phosphate. However, the first structurally characterized trisalkoxides $[VO(OCH_3)_3]$ did not provide much similarity since vanadium in $[VO(OCH_3)_3]$ is in an highly distorted octahedral environment achieved by intersheet interaction between the V and O atoms to generate a wide network with six coordinate vanadium.[33] Redetermination of the molecular structure of $[VO(OCH_3)_3]$ with a better solution shows that the central vanadium is in an octahedral environment.[34] In tuning the ligand, vanadates with various steric bulk have been prepared. The synthesis of a silyl derivative $[VO(OSiPh_3)_3]$ shows that vanadium can exist in a tetrahedral coordinate geometry.[35] Norborenoxide and adamantanoxide complexes considered to be tetrahedral coordinate have been prepared in

solution, but none of them has been characterized by X-ray crystallography.[16] $[VO(O^tBu)_3]$,[34] $[VO(OC_6H_3{}^iPr_2\text{-}2,6)_3]$[22] containing tetrahedrally coordinate vanadium are structurally characterized. Still solid state structural information through X-ray crystallography was rather difficult to obtain due to the disorder or twinning of the crystals. When substituting a chlorine atom for an alkoxy group, it was found that the rates of rapid exchange reactions of vanadium alkoxides were significantly decreased. Thus, several mixed alkoxo/aryloxo chlorides with well defined solid structures containing bidentate ligands were reported.[20,36,37,38,39] Scheme 1.2 lists some of the structurally characterized vanadates with tetrahedrally coordinated vanadium.

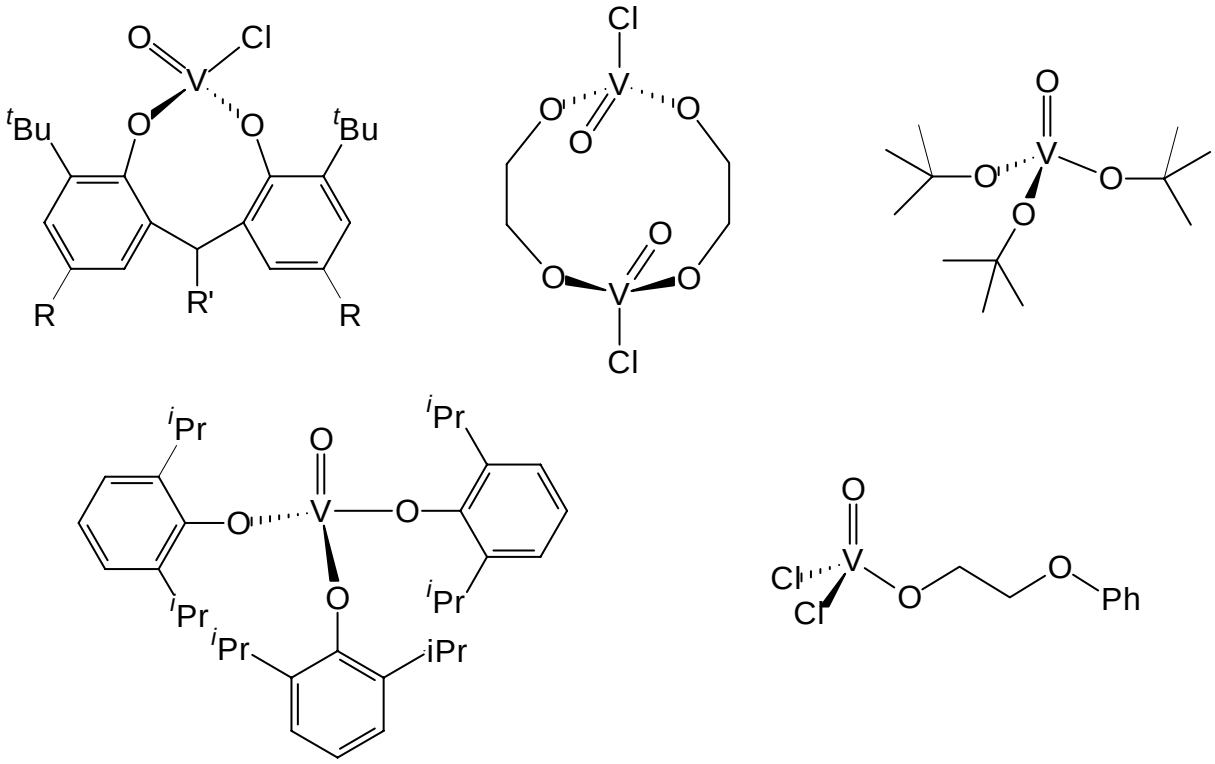

Scheme 1.2. Tetrahedrally coordinated oxovanadium(V) alkoxides. [20,24,34,36,37]

Regardless of the aforementioned complexes, vanadates tend to adopt pentacoordinate geometry either through alkoxide bridging as revealed in the cases of $[VO(OCH_2CH_2Cl)_3]_2$[11] and $[VO(OC_5H_9)_3]_2$[30] or through chelating ligands as for $[VOCl\{\mu,\eta^2OC(Me)_2C(Me)_2O\}]_2$,[40] $[VO\{OCH(Me)CH_2\}_3N]$,[41] and $[VO\{(OCH(Et))_3CH\}]_2$.[42]

A theoretical evaluation of the effects of ligands on vanadium coordination geometry in these simple systems suggested that electronic effects did not induce the coordination differences, but that subtle ligand effects such as the *gem*-dimethyl effect were invoked.[43] Thereafter several trisalkoxides of chiral triolates with either trigonal bipyramidal or tetragonal

pyramidal environment were successfully characterized by X-ray crystallography.[41,42] Scheme 1.3 presents some pentacoordinate vanadium alkoxides.

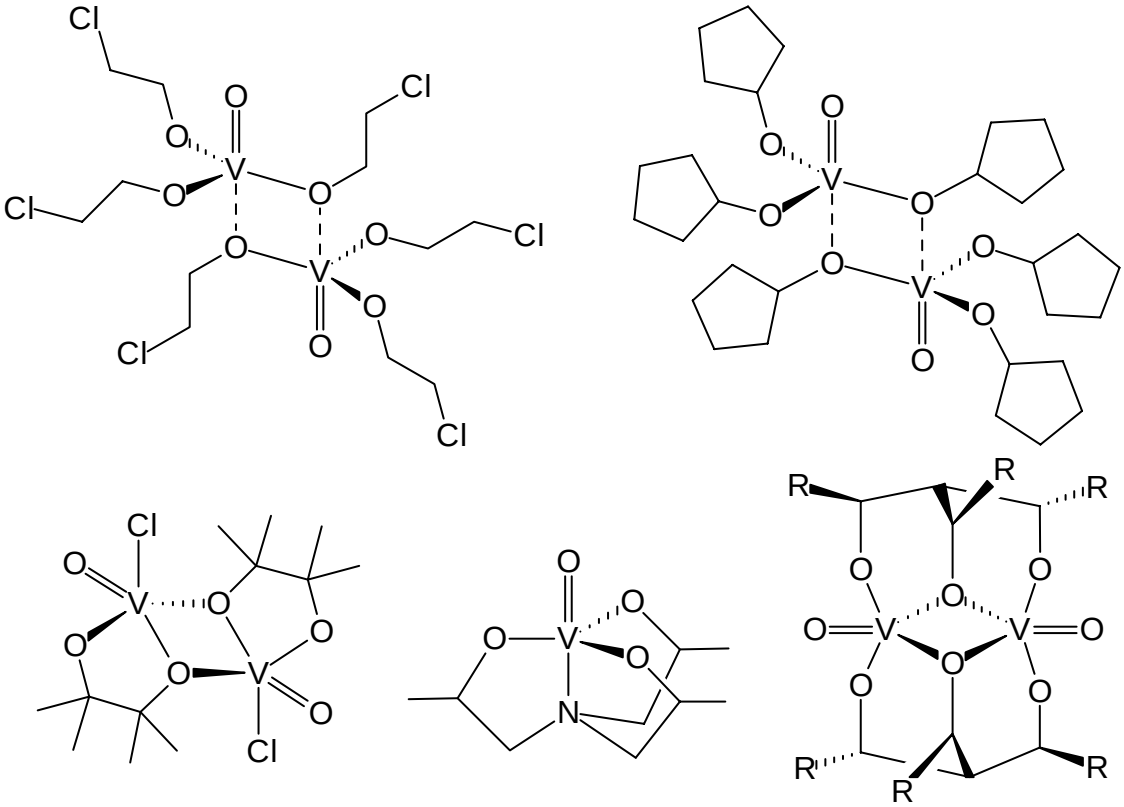

Scheme 1.3. Examples of pentacoordinate oxovanadium alkoxides.[11,30,40,41,42]

Besides tetracoordinate and pentacoordinate, hexacoordinate vanadates have been reported.[44,45,46] To achieve octahedral configuration, blocking of two coordination sites with ligands containing two additional donor atoms have been employed. In this regard, N-containing chelating ligands are preferential.[47] In conclusion, the coordination geometries of oxovanadium alkoxides depend on the R group, physical conditions, and auxiliary donor ligands.

1.4 Neutral Lewis Base Adducts of Oxovanadium(V) Complexes

Herein the survey is restricted to THF, nitrile, phosphine, and phosphine oxide and ketone containing complexes. Reaction of $VOCl_3$ with oxygen and nitrogen containing ligands gives $[VOCl_3L_n]$ (n = 1 or 2) adducts, reduction to vanadium(IV) complexes sometimes occurs.[14,48,49] Chloro oxovanadium alkoxides $[VOCl_{3-n}(OR)_n]$ are species formally similar to $VOCl_3$. They can behave as Lewis acids, giving $[VOCl_{3-n}(OR)_nL]$ or $[VOCl_{3-n}(OR)_nL_2]$ adducts with oxygen and nitrogen containing neutral ligands (L),[50] and similarly to $VOCl_3$, readily interact with Cl^- to give $[VOCl_{4-n}(OR)_n]^-$.[50] The VO unit in the $VOCl_4^-$ ion[51] and the

$[VOCl_3L]$ compounds are similar in bond length and stretching frequency to those in VO^{2+} complexes.[48]

Reaction of $VOCl_3$ with CH_3CN and C_6H_5CN in CCl_4 was found to give black moisture sensitive $[VOCl_3(CH_3CN)_2]$ and $[VOCl_3(C_6H_5CN)_2]$, respectively.[14] Afterwards, the crystal structures of $[VOCl_3(CH_3CN)]$,[52] $[VOCl_3(C_6H_5CN)]$, and $[VOCl_3(C_6H_5CH_2CN)]$ were reported.[53] In all cases, the vanadium atom is surrounded by a tetragonal pyramid formed by one oxygen, one nitrogen and three chlorine atoms. The crystal structure of $[VOCl_3(C_6H_5CN)_2]$ with the vanadium in an octahedral coordination sphere was also reported.[54] $[VOCl_2(OMe)]$ reacts with THF to afford the 1:1 adduct while under the same conditions no solid complex could be isolated from the reaction with $[VOCl_2(O^tBu)]$.[50] Reaction of $[VOCl_2(OMe)]$ with CH_3CN yields 1:1 adduct $[VOCl_2(OMe)(CH_3CN)]$. The reaction has to be carried out under mild conditions, otherwise reduction to vanadium(IV) takes place.[50] Rehder studied THF solutions of $VOCl_3$ and $[VOCl_2(OR)]$ (R = Me, Et, ^{i}Pr, ^{t}Bu) by ^{51}V-NMR.[23a] It was found that there is a considerable solvent shift for $VOCl_3$ dissolved in THF. Two signals were observed for this solution. This suggests an equilibrium between a solvated species $[VOCl_3(THF)_n]$ and a species containing THF molecules incorporated into the first coordination sphere, probably with partial or complete removal of coordinated Cl, thus giving rise to structural units $[\{VOCl_m(THF)_n\}Cl_{3-m}]$ (m = 0, 1 or 2).

The study of phosphine complexes of transition metals includes a diversity of products depending on the oxidation state of the metal and its position in the periodic table. Research on the reaction of $VOCl_3$ with phosphine has reached controversial conclusion in the literature. The early study on reactions of $VOCl_3$ and PPh_3 in petroleum ether came to the conclusion of formation of a 1:1 adduct $VOCl_3(PPh_3)$, a complex decomposing in the presence of moisture but being stable in dry O_2.[55] Subsequent studies on the oxidation of PPh_3 by O_2 catalyzed with $VOCl_3$ revealed the formation of VO^{2+} species as characterized by ESR spectroscopy.[56] Cotton and coworkers investigated the reaction of $VOCl_3$ with PEt_3 and PMe_2Ph. In contrast to what was reported by Osaka and Kanai, $[HPEt_3][VCl_4(PEt_3)_2]$ was isolated in the case of PEt_3, while $[HPMe_2Ph][VCl_4(PMe_2Ph)(OPMe_2Ph)]$ was obtained in the case of PMe_2Ph.[57] In both reactions, the VO entity, being very stable in most cases, was cleaved and reduced to vanadium(III) species; meanwhile, the phosphine was presumably oxidized to phosphine oxide. Henderson and coworkers conducted the reaction between PMe_2Ph and $VOCl_3$.[58] The addition of PMe_2Ph to a toluene solution of $VOCl_3$ resulted in rapid precipitation of salmon-pink *trans,mer*-$[VCl_3(OPMe_2Ph)(PMe_2Ph)_2]$, clearly demonstrating the cleavage of the VO entity by reducing agent PMe_2Ph.

1.5 Vanadium Catalysts for Olefin Polymerization

1.5.1 General Features of Homogeneous Vanadium Catalysts

The discovery of Ziegler-Natta catalysts for olefin polymerization made by Ziegler and Natta in the 1950s explored a principal area of catalysis.[59] Following this breakthrough, vanadium compounds in combination with alkyl aluminum halides at low temperature were shown to produce soluble active species promoting homo- and copolymerization of ethylene and propylene.[7] Higher α-olefins, such as 1-butene, copolymerize with either ethylene or propylene with high α-olefin content, but homopolymerization only affords low molecular weight materials.[60]

Typical vanadium compounds suitable as catalyst precursors are VCl_4 [61] and V(III) β-diketonates.[62,63] In combination with dialkylaluminum halides these compounds produced syndio-enriched polypropylenes.[61,64] At –78 °C the rate of polymerization was constant for a long reaction time and molecular weight increased with time linearly over a long time indicating the living feature of the polymerization. Investigations documented that the oxidation state of the active species in these catalytic systems was trivalent and that the inactive species was divalent.[65,66]

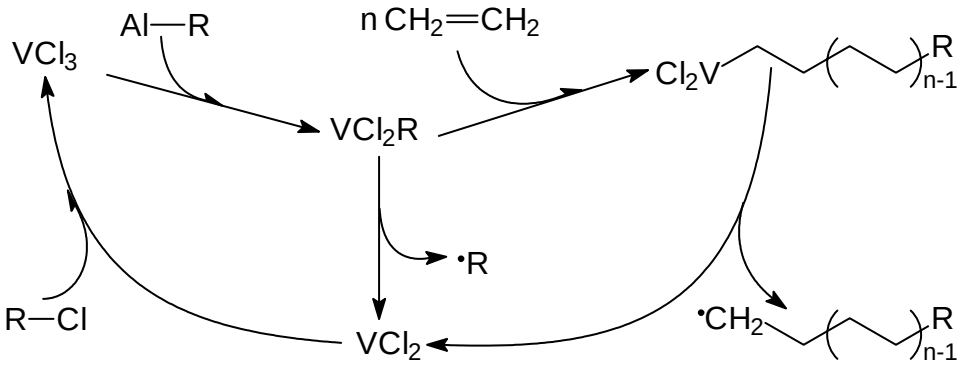

Scheme 1.4. Simplified pathway for the ethylene polymerization with vanadium catalysts and a chlorinated ester.

The current level of knowledge of vanadium catalyst can be summarized as follows: 1, the active species is a component containing both vanadium and aluminum. 2, at least one component should be halogen containing, either the vanadium precatalyst, the aluminum cocatalyst or the solvent. 3, no matter how it is prepared, the catalytic systems are thermolabile and quickly decompose at room temperature leading to a poorly characterized V(II) species, which are inactive for olefin polymerization. Therefore polymerization has to be performed either at low temperature or in the presence of a promoter (preferable a chlorinated ester) able to continuously reoxidize V(II) to vanadium species of higher

oxidation states during the polymerization (Scheme 1.4).[67] 4, in all cases the active species represents a fraction of the total amount of vanadium present in the catalytic systems. 5, the concentration of catalyst appears to affect only the rate of polymerization, not the properties of the polymer.

Although vanadium based catalysts are irreplaceable for the industrial manufacture of synthetic rubber, ethylene-propylene-diene elastomers,[68] and other polymers with unique quality, their utilization is highly restricted. This is due to their overall low activity arising from ligand abstraction and reduction of V(III) to V(II), which is considered to be the main obstacle for the development of a competitive single-site catalyst. Therefore the search for long-lasting vanadium based catalytic systems should be oriented toward design of new ligand systems.

1.5.2 Active Species and Polymerization Mechanism

Despite the fact that homogeneous and heterogeneous catalysts of olefin polymerization are of great commercial and industrial importance, relatively little is known about the influence of particular compounds of the catalysts on their performance. The vast majority of outstanding catalysts, for instance those developed by Kaminsky,[69] Grubbs and coworkers,[70] and Brookhart and coworkers[71] were developed as a result of experimental work. Accordingly, the elucidation of the mechanism of polymerization is mainly empirical.

The deactivation of the catalyst by reduction to V(II) species at room temperature, the composition of the precipitate arising from decomposition of the catalyst[64,72,73] and the identity of the polymer end groups derived from the initiation step, suggest that the polyinsertion might occur on σ vanadium-carbon bonds owing to ligand exchange between vanadium and aluminum. In that case chlorine, from either the vanadium precatalyst or from ligand exchange with alkylaluminum chloride, should provide additional anionic ligands to the active vanadium. The oxidation state of catalytically active vanadium should be III. Of course this does not mean that the active species is simply VCl_2R. Such a highly coordinative unsaturated species could easily acquire additional neutral ligands by dimerization or, more likely, by the coordination of organoaluminum compounds such as $[AlClR_2]$ or $[AlR_3]$. Less unsaturated Al-V bimetallic species, such as those in Scheme 1.5, have been proposed in attempts to rationalize the regiospecificity and, possibly, the stereospecificity of the propagation.[74,75,76,77]

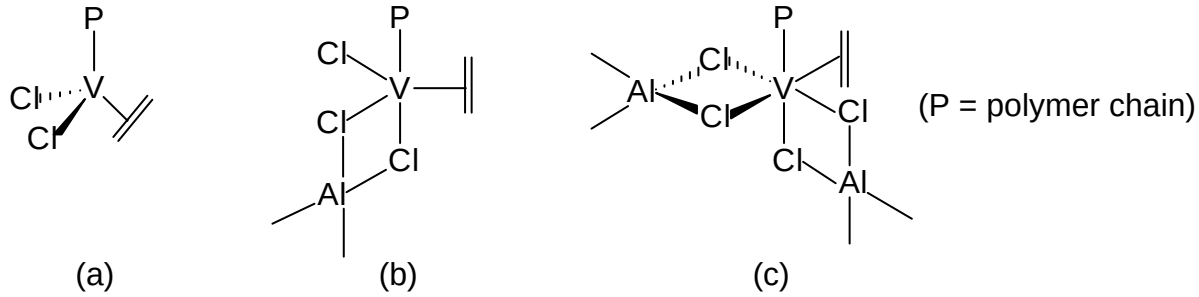

Scheme 1.5. The hypothetical active species of vanadium catalysts.

No matter what the original compound of vanadium is, once it functions as an active site, the active species should be trivalent and is reactivated repeatedly by the same reaction (or reactions) to give an identical catalyst site in a named system. Therefore polymers produced by reaction of vanadium precatalysts and alkylaluminum chlorides should have a relatively narrow molecular mass distribution in truly homogeneous polymerization systems.

The three models of complexes proposed in the literature (Scheme 1.5) assume that the catalytic center is a V(III), coordinating an olefin, a growing polymer chain, and two to four chlorine atoms, so the coordination number of vanadium is the distinguishing feature of the models. Each was able to rationalize some experimental data arising from an NMR interpretation of the polypropene microstructure.[74,76,77]

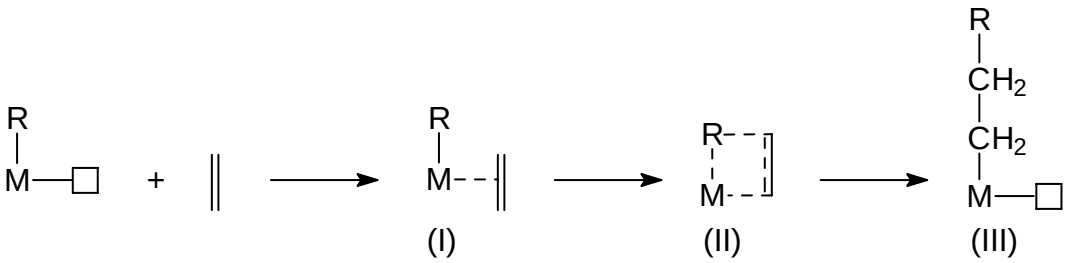

Scheme 1.6. Chain propagation according to Cossee and Arlman.

The widely accepted mechanism of polymerization developed by Cossee and Arlman,[78,79] shown in Scheme 1.6, assumed that the catalytic active sites bind olefin molecules to form a π-complex (I). The π-complex undergoes insertion *via* four-membered transition state (II) to form product (III). The difference between the energy of (I) and the substrates is called olefin uptake energy or energy of complexation, whereas the insertion barrier is defined as the difference between energy of (II) and (I). The magnitude of olefin uptake energy, insertion and termination barriers as well as insertion energy determines the overall activity of a particular catalyst. It is known that the polymerization process should be characterized by low insertion barrier and high termination barrier.[80]

1.5.3 Vanadium Catalysts

Advantages and Disadvantages of Vanadium Catalysts

While V-based catalysts possess many desirable properties as single-site catalysts, *e.g.*, the production of high molecular weight polymers, high incorporation ability for α-olefins and dienes, and living polymerization behavior for propylene, they show low catalytic activities particularly at elevated temperatures because of catalyst deactivation. Therefore a large number of vanadium complexes have been developed in order to improve catalytic activity and gain control over the polymer formed. Herein different catalyst precursors will be classified according to the ligand system.

Oxygen Based Lewis Adducts of Vanadium Trichloride

Sobota and coworkers first tested ethylene polymerization activity of two acetate adducts $[V_2(\mu\text{-}Cl)_2Cl_4(MeCO_2Et)_4]$ and $[VOCl_2\{CH_2(CO_2Et)_2\}_4]$ as well as THF adduct $[V_2(\mu\text{-}Cl)_2Cl_4(THF)_4]$.[81,82] High catalytic activities were found for these complexes in combination with $MgCl_2$ and DEAC (> 10000 kg PE (mol[V])$^{-1}$ h^{-1}, 50 °C). The activities were comparable since they are all oxygen-based Lewis adducts of vanadium trichloride.

Aryloxides

Oxygen based ligands such as aryloxides have been known to support a very high level of catalytic activity. In view of this fact novel monomeric vanadium catalysts containing bulky 2,6-diisopropylphenoxide ligand were synthesized by Sobota and coworkers (Scheme 1.7).[22] The catalytic activities of systems **a** and **b** for ethylene polymerization were 1570 and 1040 kg PE (mol[V])$^{-1}$ h^{-1} bar^{-1}, respectively (6 bar, 50 °C, Al:Mg:V = 500:10:1), which reached 2060 and 1360 kg PE (mol[V])$^{-1}$ h^{-1} bar^{-1} at 70 °C for **a** and **b**, respectively. In sharp contrast to DEAC as cocatalyst, the systems with MAO as cocatalyst gave a much lower activities (830 and 470 kg PE (mol[V])$^{-1}$ h^{-1} at 70 °C, respectively). The addition of $[MgCl_2(THF)_2]$ to the vanadium catalyst precursors did not raise the activity significantly but prevents the reactor from being fouled. Moreover, vanadium complexes containing both bulky phenoxide and chelating 2,2'-oxydiethanethiolate were prepared. They showed tenfold activity in ethylene polymerization relative to metallocenes catalysts.[83] Complexes **c** and **e** showed activities of 330 and 170 kg PE (mol[V])$^{-1}$ h^{-1} bar^{-1} (6 bar, 50 °C, Al:Mg:V = 500:10:1) for ethylene polymerization.

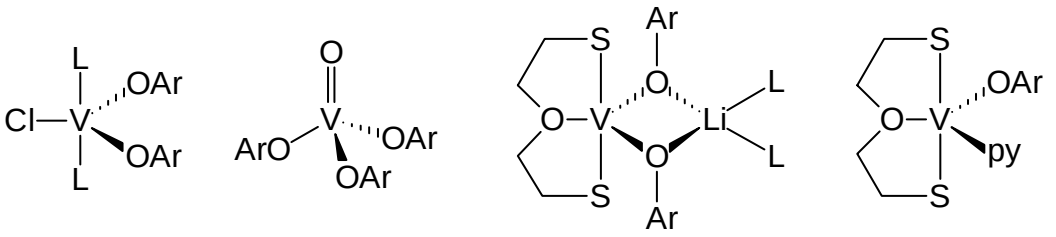

a L = THF **b** **c** L = THF **d** L = MeCN **e** py = pyridine

Ar = 2,6-^{i}Pr-C_6H_3

Scheme 1.7. Vanadium catalysts containing bulky phenoxide used by Sobota *et al*..

Sobota and coworkers studied the catalytic activity of $[V^{II}(CH_3CN)_6][V^{III}Cl_2\{O(CH_2\text{-}CH_2S)_2\}]_2$ for ethylene polymerization in combination with DEAC and $MgCl_2$.[84] This system was shown to give only low activity of 42 kg PE $(mol[V])^{-1}$ h^{-1} bar^{-1} (6 bar, 50 °C, Al:Mg:V = 250:10:1). Interaction of $[V^{II}(CH_3CN)_6][V^{III}Cl_2\{O(CH_2CH_2S)_2\}]_2$ and $[AlMe_3]$ indicated that, under the influence of an excess of $[AlMe_3]$, the abstraction and transformation of the $\{O(CH_2CH_2S)_2\}_2$ ligand from the vanadium(III) center occurred resulting in the formation of a dimeric organoaluminum complex $[Al_2\{\mu,\eta^3\text{-}(OCH_2CH_2SCH_2CH_2S)\}_2Me_2]$. This result revealed that during the catalytic cycle the $\{O(CH_2CH_2S)_2\}^{2-}$ ligand migrated to an aluminum atom of the activator and a V(II) species was formed, which was considered to be inactive in the ethylene polymerization process. Recently, a vanadyl precatalyst containing a thiobisphenoxo ligand was reported to produce polypropylene with narrow molecular weight distribution in combination with MAO as cocatalyst (Scheme 1.8).[85]

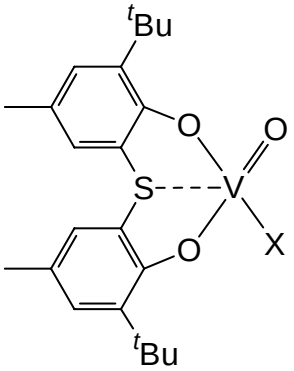

a X = Cl
b X = Bu

Scheme 1.8. Vanadyl precatalysts containing a thiobisphenoxo ligand.

Very recently, a class of novel, exceptionally active vanadium-based catalysts was explored using bi- and triphenolate ancillary ligands (Scheme 1.9).[86] Vanadium complexes with chelating aryloxide ligation in the form of $[OV(\mu^2\text{-}O^{n}Pr)L^1)]_2$ (**a**, **b**) and $[OVL^2]_2$ (**c**, **d**) (where L^1 and L^2 are the deprotonated forms of the di- and triphenols, respectively) were prepared from the reaction of the alkoxide $[VO(O^{n}Pr)_3]$ and the parent di- and triphenol,

respectively. In the presence of ethyl trichloroacetate as promoter and dimethylaluminum chloride, activities for **a** and **b** readily reached $3 \cdot 10^5$ kg PE (mol[V])$^{-1}$ h^{-1} bar^{-1} (7 bar, 80 °C, Al:V = $1.5 \cdot 10^5$:1), whilst for **c** and **d** activities of the order $6.4 \cdot 10^5$ kg PE (mol[V])$^{-1}$ h^{-1} bar^{-1} were observed. It was shown that the activity of the system was a function of the Al:V molar ratio, increasing with the amount of dimethylaluminum chloride used. At higher temperatures, high activities were possible for much smaller cocatalyst loadings, for example at 55 °C, activities of over 3500 kg PE (mol[V])$^{-1}$ h^{-1} bar^{-1} were observed using Al:V in 50:1. In the absence of a promoter, there was a remarkable decrease in activity. Significantly, the systems have shown the highest observed activities reported to date for any vanadium-based ethylene polymerization system.

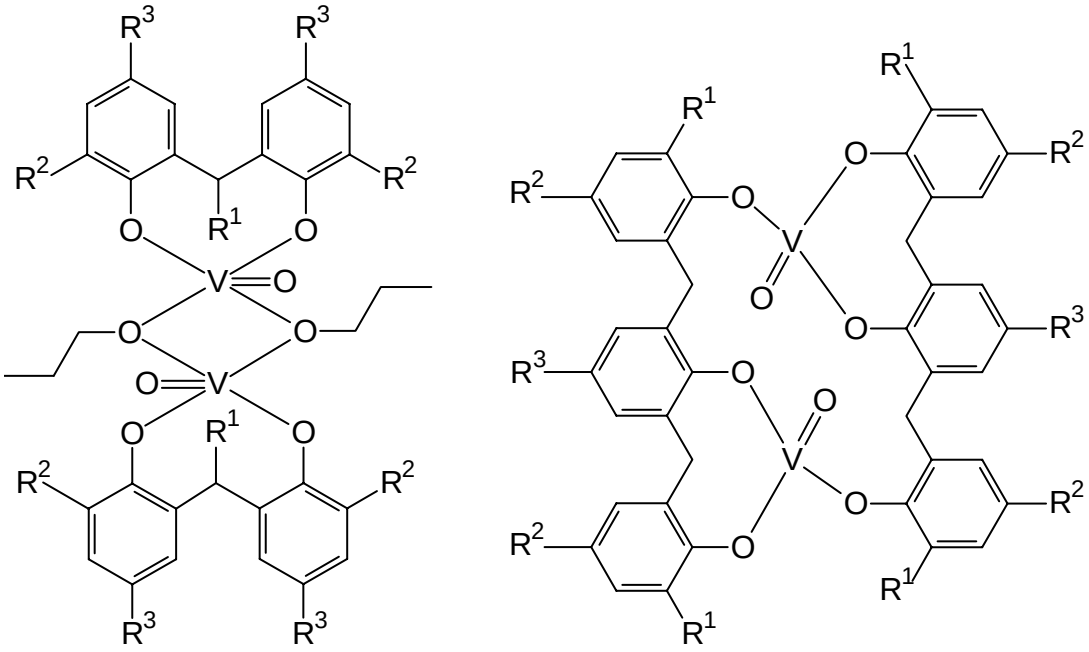

a R^1 = Me, R^2, R^3 = ^{t}Bu
b R^1 = H, R^2 = ^{t}Bu, R^3 = Me
c R^1 = ^{t}Bu, R^2, R^3 = Me
d R^1, R^2 = ^{t}Bu, R^3 = Me

Scheme 1.9. Vanadium catalysts with bi- and triphenolate ancillary ligands.

Chelating Aminoaryloxides and Pyridinyl Alkoxides

Van Koten and coworkers developed *o*-aminophenolate [N,O] and [N,O,N] chelating ligands and pyridyl alcoholate [N,O] ligands for the preparation of vanadium catalyst systems (Scheme 1.10). Complexes **a** and **b** derived from ligands of **a'** and **b'** type were well-defined by X-ray crystallography and tested for ethylene and propylene copolymerization. The activities varied between 21 and 222 kg PE (mol[V])$^{-1}$ h^{-1} bar^{-1}. The big difference in activity was tentatively attributed to their different solubilities.[87] Ligand **a'** failed to serve as a pincer type ligand. Complexes derived from ligand **c'** showed either no activity or only low activity for ethylene polymerization.[88]

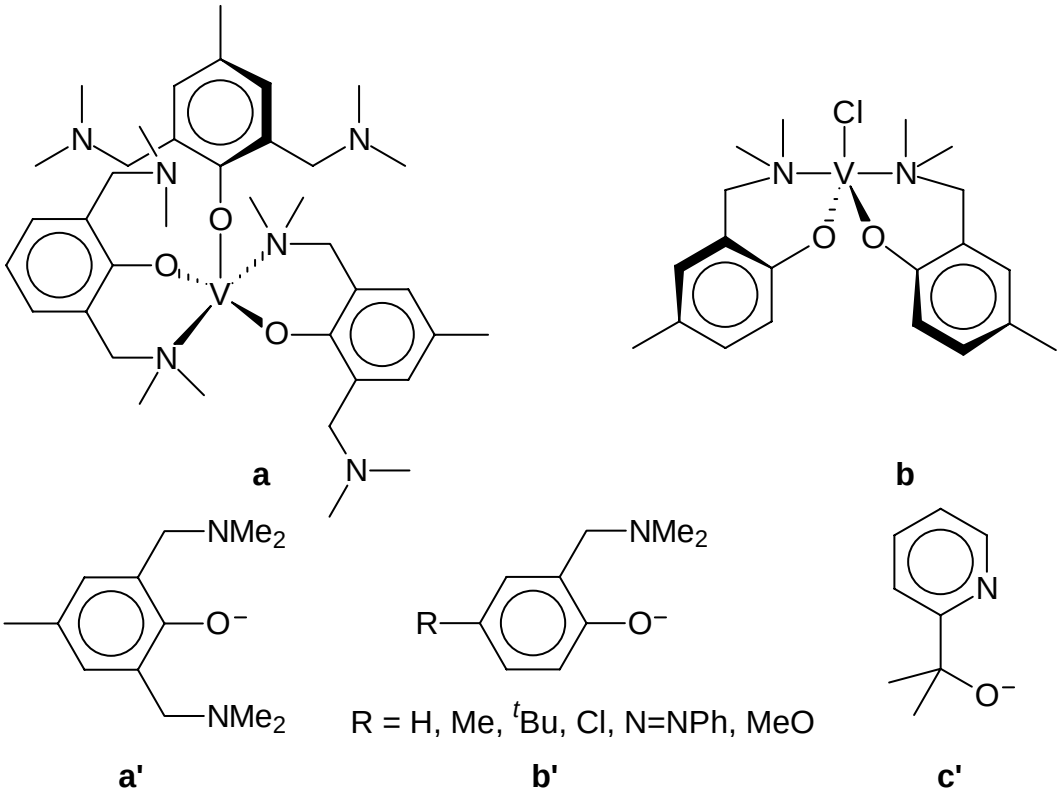

Scheme 1.10. Vanadium catalysts with *o*-aminophenolate and pyridyl alcoholate ligands.

Imido-Containing Complexes

Vanadium(V) complexes containing arylimido ligands have attracted considerable attention because this ligand moiety should be more stable at high temperature relative to the V=O moiety. Studies focused on arylimido vanadium complexes as catalysts have been carried out by Gibson and other research groups (Scheme 1.11).[88, 89] Half-sandwich compound **I** displayed an activity of 27 kg PE (mol[V])$^{-1}$ h^{-1} bar^{-1} when activated with MAO.[89a] The low activity was probably due to bimolecular deactivation, since immobilizing the catalyst on a polystyrene resin led to remarkable enhancement in the lifetime and productivity of the supported catalysts compared with their unsupported analogues.[89c,89d] Compound **II** explored not only the isolobal relationship between Cp and the dianionic imido group but also that of Cp with the monoanionic trispyrazolylborate ligand. Rather low activity of 14 kg PE (mol[V])$^{-1}$ h^{-1} bar^{-1} for ethylene polymerization was shown, and propylene was polymerized to a low molecular weight material.[89b]

Choukroun and coworkers reported a class of vanadium(IV) arylimido complexes for olefin polymerization.[90] When activated with [$AlCl_2Et$], complexes **IIIa** and **IIIb** displayed high activities of 220 and 1200 kg PE (mol[V])$^{-1}$ h^{-1} bar^{-1}, respectively, whilst in combination with MAO compound **IIIb** showed a much lower activity.

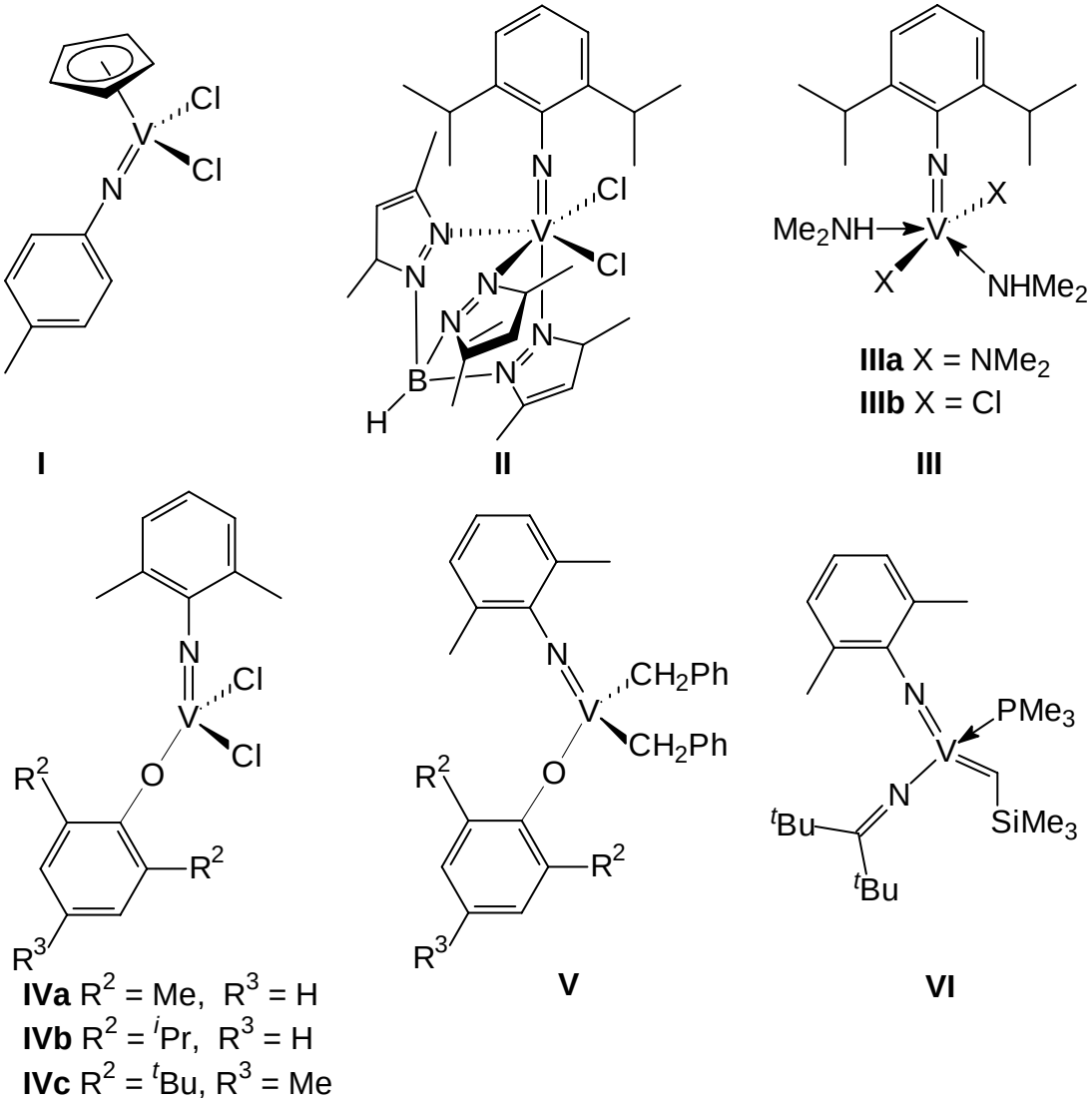

Scheme 1.11. Vanadium catalysts containing arylimido ligands.

Nomura and coworkers reported that the (arylimido)(aryloxo)vanadium(V) compounds **IV** exhibited remarkable catalytic activities for ethylene polymerization in the presence of MAO.[91] Complex **IVb** displayed an activity of 120 kg PE (mol[V])$^{-1}$ h^{-1} bar^{-1}, affording high molecular weight polymer with unimodal molecular weight distribution (M_w = 2.92 · 10^6, M_w/M_n = 2.88).[92] Complex **V** initiated ring-opening metathesis polymerization (ROMP) of norbornene without cocatalyst, giving high molecular weight polymer with unimodal molecular weight distribution (M_w = 4.69 · 10^6, M_w/M_n = 1.93). When treated with $AlMe_3$ complexes **IVb** and **IVc** catalyzed ROMP of norbornene, whilst in combination with DEAC the highest activity of 1040 kg PE (mol[V])$^{-1}$ h^{-1} bar^{-1} was observed for **IVb**. Very recently,[93] an imido-alkylidene vanadium complex **6** was reported to initiate ROMP of norbornene, yielding a high molecular weight polymer with unimodal polydispersity (M_w = 1.15 · 10^6, M_w/M_n = 1.6) in 98% yield. The most attractive merit of this catalyst is its highly thermal stability even at 80 °C, providing potential industrial application.

Imine-Aryloxide

Fujita reported the olefin polymerization behavior of imine-aryloxy ligated vanadium complexes with $MgCl_2/R_mAl(OR)_n$ systems (Scheme 1.12).[94] Complexes **a** and **b** in association with $MgCl_2/R_mAl(OR)_n$ demonstrated very high activities of $6.51 \cdot 10^4$ and $4.38 \cdot 10^4$ kg PE $(mol[V])^{-1}$ h^{-1} bar^{-1} (1 bar, 75 °C) at elevated temperature, which represented the first reported examples of highly active, thermally robust single-site vanadium based olefin polymerization catalyst. Moreover, the polyethylenes formed from the $MgCl_2/R_mAl(OR)_n$ systems displayed good polymer morphology, indicating that complexes **a** and **b** were heterogenized on the surface of the $MgCl_2/R_mAl(OR)_n$, which not only worked as an excellent cocatalyst, but also was a good support for imine-aryloxy ligated vanadium complexes.

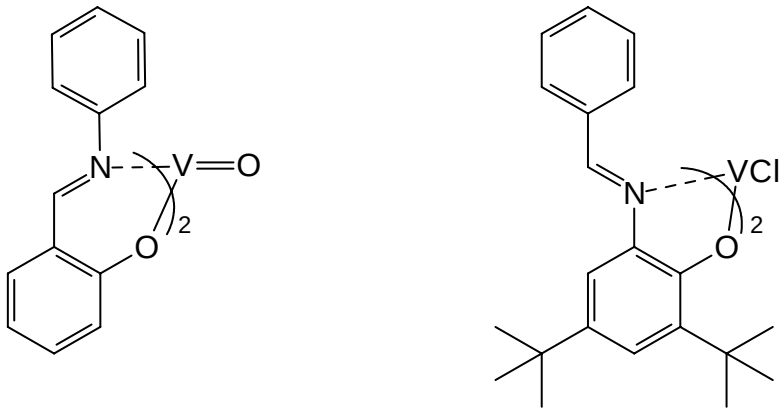

a **b**

Scheme 1.12. Imine-aryloxy ligated vanadium catalysts.

Alkoxides

By using a chelating oxygen-based 2-tetrahydrofurfuryl ligand (thffo) Sobota and coworkers synthesized trivalent $[V_2Mg_2(\mu_3,\eta^2\text{-thffo})_2(\mu,\eta^2\text{-thffo})_4Cl_4]_4 \cdot 2CH_2Cl_2$ and tetravalent $[V_2(\mu,\eta^2\text{-thffo})_2Cl_2O_2]$, both were very effective procatalysts for ethylene polymerization (Scheme 1.13).[95,96] High activities of 4330 and 3370 kg PE $(mol[V])^{-1}$ h^{-1} bar^{-1} were achieved for **a** and **b**, respectively (6 bar, 70 °C, Al:Mg:V = 500:10:1). Notably the catalytically active species were particularly stable during polymerization reaction. The highest activities were obtained after 2–3 min and did not decrease over 30 min. This indicates that there was no maximum in the relationship between activity and time of the polymerization reaction. The addition of $[MgCl_2(THF)_2]$ to the vanadium catalyst precursors did not significantly raise the activity and therefore was a nonessential component. However, the use of $[MgCl_2(THF)_2]$ could avoid reactor fouling.

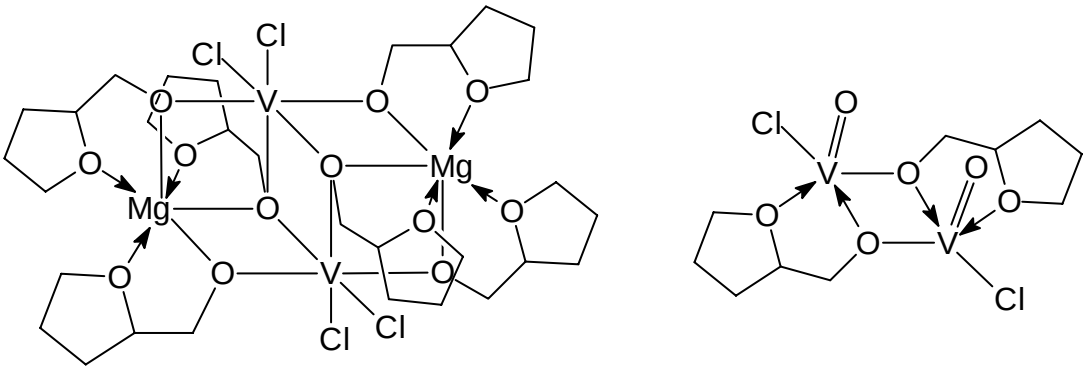

Scheme 1.13. Vanadium complexes containing chelating alkoxyalkoxide ligands.

β-Diketonates and β-Diminates

Gambarotta and coworkers reported a series of substituted [V(*β*-diketonate)$_3$] and tested the propylene and ethylene copolymerization in order to study the effect of the steric (^{t}Bu-acac) and electronic (F-acac) features of various ligands on catalytic activity (Scheme 1.14).[63] The cy-acac ligand was selected in consideration of obtaining higher solubility while preserving almost unchanged steric and electronic properties of the basic acac ligand. Polymerization results showed that the modifications introduced in the ligand system did not have a significant impact on the activity, polymer quality or composition. This indicated that the ligands have been completely abstracted from catalytically active vanadium derivatives, thus, implying that the primary role of the cocatalyst is to abstract ligand molecules and provide in return alkyl functions and halide atoms.

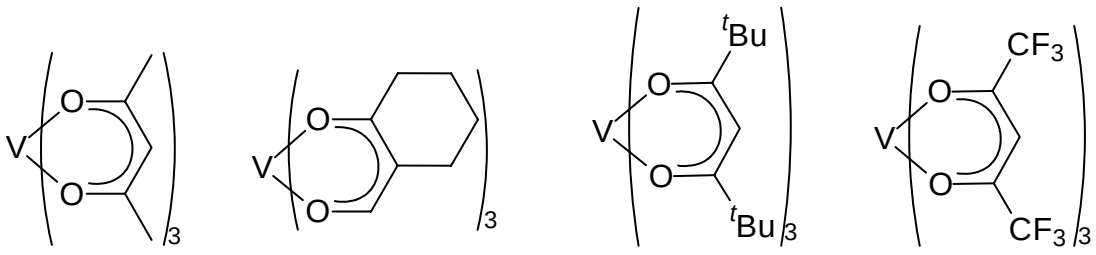

Scheme 1.14. Vanadium-acac complexes used by Gambarotta *et al*..

As an analogue of *β*-diketonate ligand system, *β*-diiminate was introduced in vanadium(III) chemistry. [L(**a**)VMe$_2$] and [L(**b**)V^{n}Bu$_2$] were tested as catalyst for ethylene and propylene homopolymerization but no obvious polymerization was observed (Scheme 1.15).[97a] However, [L(**c**)VCl$_2$] catalyzed ethylene polymerization in combination with MAO (Al:V = 130:1) giving high molecular weight polyethylene with a narrow polydispersity (M_w = 2.0 · 10^6, M_w/M_n = 1.75).[97b] It catalyzed ethylene/propylene copolymerization (M_w = 1.7 · 10^6, M_w/M_n = 3.46). Given the big difference between the activities of these complexes, it can be considered

that the steric bulk of the substituent on the nitrogen affects the catalytic performance strongly.

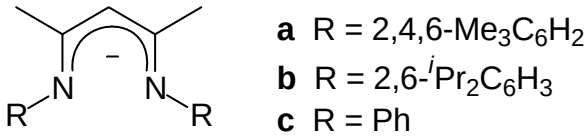

Scheme 1.15. *β*-diiminate ligands used for syntheses of vanadium catalysts.

[N,N] Amidinates

A second class of monoanonic N,N-chelating ligands are the amidinates introduced by Teuben and coworkers (Scheme 1.16).[98] Alkyl complexes [L_2(**a**)VR] (R = Me, Et, allyl) and [L_2(**b**)VR] (R = Me, allyl) were prepared. The neutral alkyl system [L_2(**a**)VCH_3] slowly catalyzed the oligomerization of ethylene at 80 °C to linear alkenes without the addition of cocatalysts. The productivity of the catalyst system was modest, which was likely due to the relatively low electrophilicity of the metal center. Therefore benzamidinate **c** with a more electron-withdrawing pentafluorophenyl group was employed. When exposed to ethylene (8 bar, 80 °C), [L_2(**c**)VMe] produced higher molecular weight oligomer (M_n = 1780, M_w/M_n = 2.3) with an activity of 8.1 kg PE (mol[V])$^{-1}$ h^{-1}, more than 5 times higher than the productivity of [L_2(**a**)VMe]. The M_n of the oligomer is more than two-fold higher than that produced by [L_2(**a**)VMe]. [L(**d**)VCl_2(THF)] derived from tridentate ligand **d** was employed in ethylene polymerization (6 bar, 30 °C, Al:V = 20:1) with DEAC as cocatalyst gaining an activity of 447 kg PE (mol[V])$^{-1}$ h^{-1} bar^{-1}.[99] The molecular mass distribution of the product indicated the presence of a single active site.

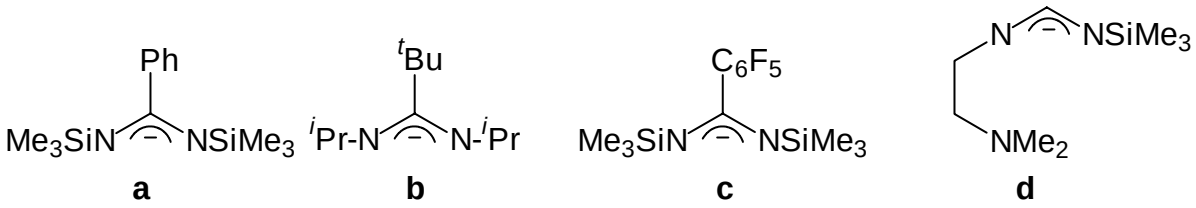

Scheme 1.16. Vanadium amidinate complexes used by Teuben *et al*..

In addition to the ligand system mentioned above, some other systems such as silsesquioxanes, oxocyclosiloxanes, amides, and imines were investigated in context of vanadium based olefin polymerization.[100] In summary, the vanadium based catalysts for olefin polymerization have undergone significant development over the past decades, with some of the most important recent advances occurring for aryloxide and alkoxide systems. It is reasonable to predict that with more fine-tuneable ligand systems the olefin polymerization catalysis, the process of catalyst discovery and development will gain more and more success.

1.6 Vanadium Catalysts for Olefin Epoxidation

Vanadium(V) centers are usually strong Lewis acids as a consequence of low radius/charge ratio, which makes them suitable for the activation of peroxidic reagents.[101] Accordingly, vanadium(V) complexes have been found to act as catalyst precursors in various oxidation reactions like brominations, epoxidations of alkenes and allylic alcohols.[102] The active species has been identified in some stoichiometric reactions as mononuclear oxoperoxovanadium(V) complexes, a few examples of which have been structurally characterized in the case of epoxidation.[103] In all cases the peroxide is bound in a η^2-manner in the equatorial plane relative to the axial oxo ligand. Additionally, vanadium(IV) complexes are readily converted to the oxoperoxovanadium(V) complexes in the presence of excess peroxide. By this means, they can also be precursors in the oxidation reactions. However, owing to ligand exchange reactions, systematical studies elucidating the actual structures of V(V) catalysts are yet absent.[104]

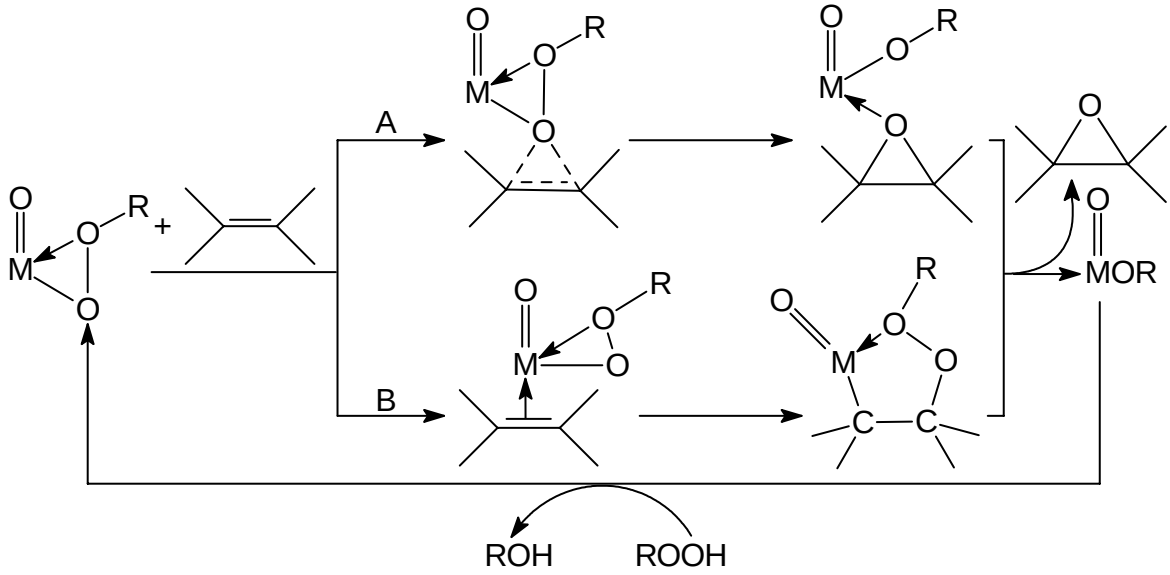

Scheme 1.17. Proposed mechanisms of catalyzed epoxidation of olefins.

Oxoperoxovanadium complexes containing pyridine-2-carboxylato, pyrazine-2-carboxylato, or *N*-(2-oxidophenyl)salicylidenaminato ligands are known to catalyze the oxidation of unfunctionalized olefins.[103,105] It is generally accepted that the epoxidation proceeds *via* a heterolytic rather than a homolytic mechanism. Two alternative mechanisms, A and B as shown in Scheme 1.17, which involve d^0 metal alkylperoxidic intermediates, emerge from the numerous interpretations proposed:[106] (A) nucleophilic attack of olefin on the electrophilic oxygen atom covalently bonded to the metal. For this mechanism, the oxidations are best carried out in nonprotic solvents such as CH_2Cl_2 or CH_3CN, in which the reaction rates are almost the same. Instead, protic solvents such as CH_3OH strongly retard the reaction. (B)

coordination of the olefin to the metal followed by its insertion in the metal-oxygen bond, forming a five-membered pseudocyclic dioxametallocyclopentane, which decomposes by a 1,3-dipolar cycloreversion mechanism to the epoxide and the metal alkoxide, a process referred to as pseudocyclic peroxy metalation.[107] The reaction is inhibited by water, alcohols, and basic ligands or solvents.

It was proposed that when a vacant site on the vanadium center is present, the olefins are able to coordinate to the vanadium center, leading to the formation of epoxides with high selectivity.[108] However, when coordination of the olefin is not possible, one-electron oxidation processes often play a role, which proceed in a nonstereoselective manner.

1.7 Aim and Objectives of the Present Work

Given the aforementioned background materials, vanadium alkoxides are highly interesting concerning solution and solid state properties, catalysis in olefin polymerization and epoxidation. The aims of this thesis are the following by using chelating alkoxyalcoholate systems:

• To synthesize oxovanadium alkoxides and investigate their solution properties and solid state structures;

• To study the reactivity of oxovanadium alkoxyalkoxides, *e.g.*, dimer cleavage reactions in the presence of nucleophilic reagents and disproportionations in coordinating solvents and in the solid state;

• To design highly active vanadium based olefin polymerization procatalysts with good thermal stability.

2 Results and Discussion

2.1 Oxovanadium Methoxides and Ethoxides

2.1.1 Syntheses and Spectroscopic Characterization

$[VOCl_2(OCH_3)]$[14] and $[VO(OCH_3)_3]$[33] were synthesized decades ago. However, the reactions between $VOCl_3$ and CH_3OH have not been fully elucidated. Funk *et al.* synthesized an extremely moisture sensitive complex $[VOCl(OCH_3)_2{\cdot}HCl{\cdot}CH_3OH]$, wherein they postulated the formula to be $[CH_3OH_2]^+[VOCl_2(OCH_3)_2]^-$.[14] Moreover, there is no well-defined crystallographic data of oxovanadium methoxides except for that of $[VO(OCH_3)_3]_n$. $[VOCl_2(OC_2H_5)]$ and $[VOCl(OC_2H_5)_2]$ were reported in the literature.[14,15,17] However, X-ray diffraction of both complexes have been pending. In order to study the effect of the starting materials and the solvent on the final product, two methoxy complexes **1**, **2**, and a THF coordinated oxovanadium ethoxide **3** have been synthesized and structurally characterized (Scheme 2.1).

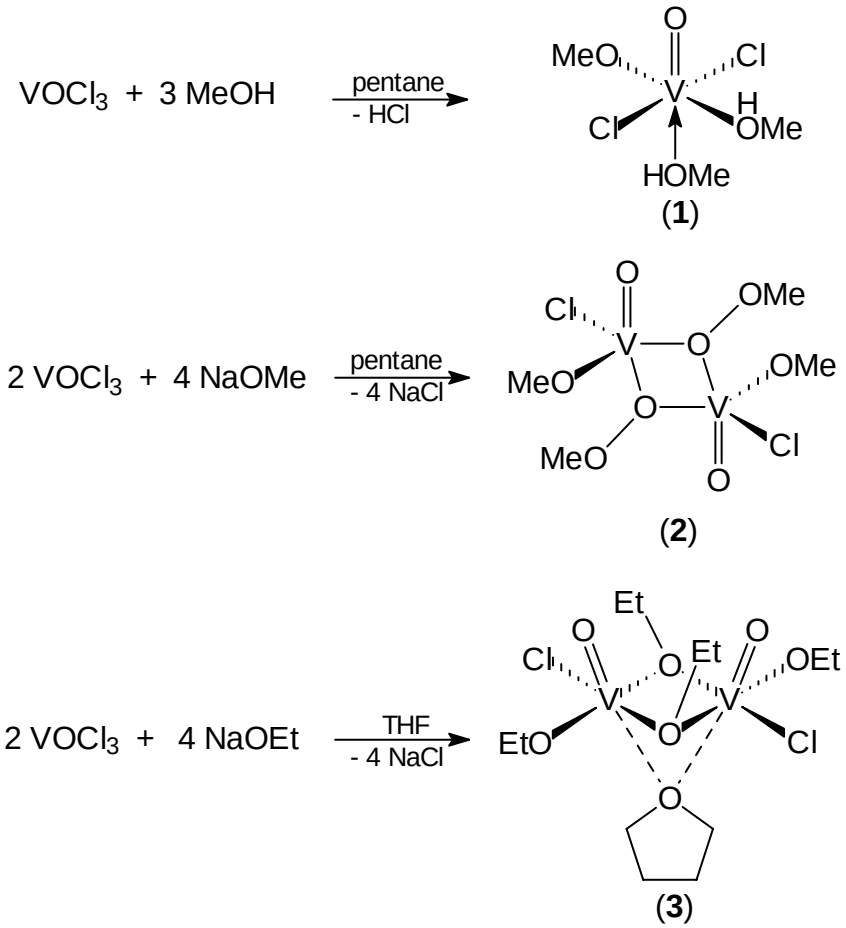

Scheme 2.1. Preparation of oxovanadium methoxides **1**–**2** and ethoxide **3**.

Complex **1** was prepared in relatively low yield of 23% from the reaction of $VOCl_3$ with at least 2 equiv of CH_3OH in pentane at ambient temperature. Notably, when $VOCl_3$ was treated

with more than 2 equiv of CH_3OH, complex **1** rather than $[VOCl(OCH_3)_2]$ or $[VO(OCH_3)_3]$ was the only isolated product. In accordance with the literature,[14] this orange-red crystalline material is extremely moisture sensitive and melts at 20 °C. It crystallizes from cold pentane and is stable at –30 °C for several months. The complex dissolves very well in organic solvents such as pentane, toluene, and dichloromethane. It undergoes slow decomposition at 0 °C within several weeks to afford green vanadium(IV) species both in solution and in the solid state.

Complex **2** was synthesized *via* salt elimination starting from $VOCl_3$ and 2 equiv of CH_3ONa in pentane in good yield. It was isolated as brown viscous oil and crystallized slowly at 0 °C to afford light yellow crystals suitable for X-ray diffraction within several months. The pure complex is colorless crystalline solid melting at 63 °C, traces of moisture lead to a color change to orange or red. It is much more stable than complex **1** as it can be stored under an inert atmosphere at room temperature for 24 h without appreciable decomposition.

Complex **3** was prepared from $VOCl_3$ and 2 equiv of C_2H_5ONa in THF. The weak coordination of THF to the vanadium center was confirmed by X-ray single crystal diffraction. Purification of the complex under reduced pressure led to THF dissociation from the vanadium center. Complex **3** is a brown liquid at room temperature. When exposed to sunlight at room temperature, the complex turns to dark brown and decomposition to green oil takes place within 24 h.

Complexes **1**–**3** have been characterized by ^{1}H-, ^{13}C-, ^{51}V-NMR, IR spectroscopy, mass spectrometry, and X-ray diffraction. Complexes **1** and **2** display almost the same chemical shifts for both ^{1}H- and ^{13}C-NMR at 5.2 and 76 ppm, respectively. Both ^{1}H- and ^{13}C-NMR signals are considerably broadened. Compared with CH_3ONa, ^{1}H resonances for **1** and **2** shift to lower field by 1.7 ppm. Complex **3** shows the expected number of signals for the ethoxo and THF ligand in both ^{1}H- and ^{13}C-NMR spectra. For ^{1}H spectrum, the signal at lower field at 5.48 ppm in $CDCl_3$ is due to the $VOCH_2$ protons while those at 3.90 ppm and 1.90 ppm are ascribed to CH_2OCH_2 and CH_2CH_2 protons of the THF ligand. The signal at 1.51 ppm is assigned to the CH_3 protons. For ^{13}C spectrum, the four signals at 86.2, 69.8, 25.3 and 17.6 ppm are attributed to $VOCH_2$, CH_2OCH_2, CH_2CH_2, and CH_3 carbon atoms, respectively. ^{51}V-NMR spectrum for **1** exhibits a signal at –443 ppm while **2** displays a main signal –436 ppm and a minor signal –388 ppm. The ^{51}V-NMR signal for **3** appears at –303 ppm.

IR spectra of the CS_2 solutions of **1**–**3** were carried out between KBr plates. Characteristic stretching frequencies for V=O are observed at 1025 cm^{-1} for **1**, 1017 cm^{-1} for **2**, and 1014 cm^{-1} for **3** as very strong and sharp signals. These data are in good agreement with the

empirical rule reported by Rehder with respect to the alkoxylation degree of $VOCl_{3-n}(OR)_n$ that V=O vibration appears between 1025–1028 cm^{-1} for n = 1, 1014–1017 cm^{-1} for n = 2, and 1005–1008 cm^{-1} for n = 3.[11] The vibrations at 455 and 491 cm^{-1} for **1**, 492 and 455 cm^{-1} for **2**, 492 and 465 cm^{-1} for **3** are assigned to V–Cl stretching frequencies. Mass spectrometric data for **1** exhibits a fragment ion of $[VOCl_2(OCH_2)]$, formed by loss of two CH_3OH and one hydrogen atom. Complex **2** displays no molecular ion but the signal of $[VOCl(OCH_3)_2]$. Similarly, complex **3** gives a fragment of $[VOCl(OC_2H_5)_2]$.

2.1.2 X-ray Crystallographic Studies

A single crystal X-ray structure determination (Fig. 2.1, selected bond distances and bond angles are shown in Table 2.1) shows that **1** crystallizes in the monoclinic, space group $P2_1/n$. The vanadium atom is coordinated in an octahedral environment. The chloro ligands Cl(1) and Cl(2), O(2) from the methoxy group, O(3) from the methanol, and V form almost a perfect plane, as demonstrated by the sum of the angles around the vanadium center (357.0°). The terminal oxo ligand O(1) and O(4) occupy the *trans*- positions and the O(1)–V–O(4) angle is 171.62(8)°.

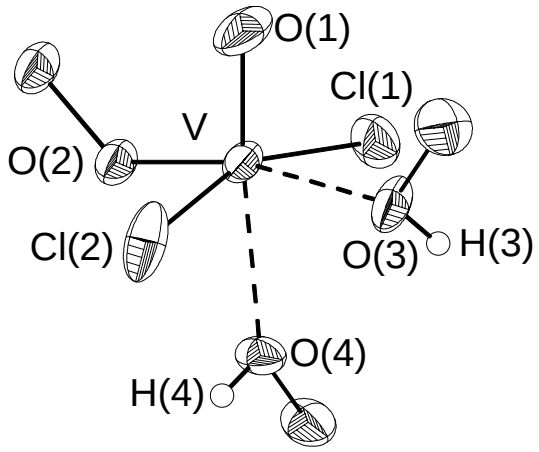

Fig. 2.1. Molecular structure of **1**. Hydrogen atoms are omitted for clarity except for the hydroxyl hydrogen.

The V=O bond length (1.578(16) Å) compares well to those observed for $[VOCl(OCH_2CH_2O)]_2$ (1.578(2) Å)[20] and $[VOCl\{OC(CH_3)_2\}_2]_2$ (1.576(1) Å).[40] The V–O(2) bond length of 1.7446(15) Å is consistent with those found for $[VOCl(OCH_2CH_2O)]_2$ (1.741(2) and 1.743(2) Å) and $[VOCl\{2,2'\text{-}CH_2(4\text{-}Me, 6\text{-}^tBu\text{-}C_6H_2O)\}_2]$ (1.734(3), 1.752(4) Å).[36] The bond length of V–O(3) 2.1132(16) Å is considerably longer than that of V–O(4) due to the *trans*-influence of V=O(1) on V–O(4). The bond lengths of V–Cl(1) (2.3108(7) Å) and V–Cl(2) (2.3442(8) Å) are considerably longer than those for $[VOCl\{2,2'\text{-}CH_2(4\text{-}Me,6\text{-}^tBu\text{-}C_6H_2O)\}_2]$ (2.199(2) Å), $[VOCl(OCH_2CH_2O)]_2$ (2.207(1) Å),

and $[VOCl\{OC(CH_3)_2\}_2]_2$ (2.219(1) Å) due to the different coordination spheres for vanadium centers. The chlorine ligands and hydroxyl groups are extensively involved in hydrogen bonding. One layer network of the complex is shown in Fig. 2.2. Four molecules constitute a centrosymmetric macrocycle by four alcohol-chlorine hydrogen bonds with distances of 3.07 and 3.36 Å, respectively.

Table 2.1. Selected bond lengths (Å) and angles (°) for **1**.

V–O(1)	1.5778(16)	V–O(2)	1.7446(15)
V–O(3)	2.1132(16)	V–O(4)	2.2286(16)
V–Cl(1)	2.3108(7)	V–Cl(2)	2.3442(8)
O(1)–V–O(4)	171.62(8)	O(2)–V–Cl(2)	94.64(5)
O(3)–V–Cl(1)	84.26(5)	O(3)–V–Cl(2)	81.38(5)
O(2)–V–O(3)	167.77(7)	Cl(1)–V–Cl(2)	160.54(3)
O(2)–V–Cl(1)	96.68(6)		

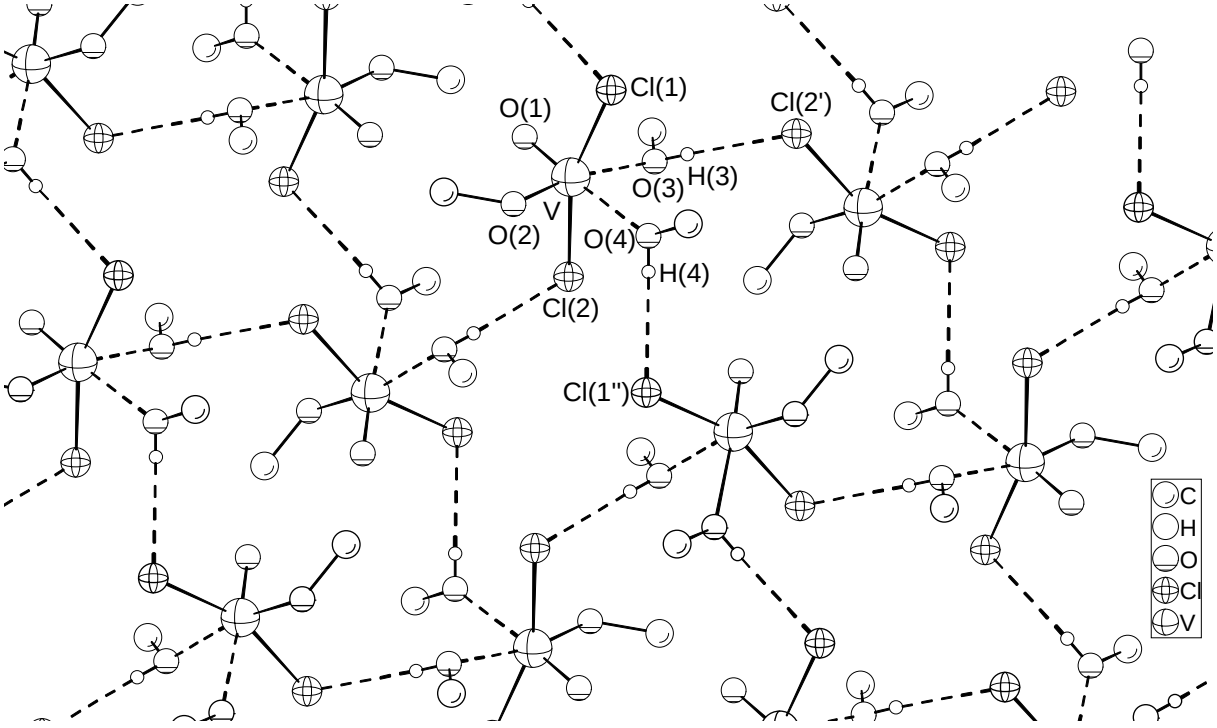

Fig. 2.2. One layer network of **1** through two hydrogen bondings. Symmetry transformations used to generate equivalent atoms: ' –x + 3/2, y + 1/2, –z + 3/2; " x + 1/2, –y + 3/2, z + 1/2. Bond lengths in Å: O(3)…Cl(2') 3.07; O(4)…Cl(1") 3.36.

Complex **2** crystallizes in triclinic space group $P\bar{1}$. A representation of **2** is shown in Fig. 2.3. Selected interatomic distances and angles are given in Table 2.2. Each vanadium atom in the centrosymmetric dimer is pentacoordinate in a trigonal-bipyramidal geometry (Fig. 2.3). The terminal oxo ligand and a bridging alkoxide ligand occupy the apical sites and the

O(1)–V–O(2') angle is 171.0°. One chloro ligand, one terminal and one bridging alkoxide ligand are located in equatorial positions. The sum of the angles around the vanadium atom formed by Cl(1), O(2), O(3) and V(1) is 349.3°, indicating some distortion of the trigonal-bipyramidal conformation to square pyramid. The τ value, which is 0 for ideal tetragonal and 1 for ideal trigonal arrangements, reaches τ = (the largest angle – the second largest angle)/60 = 0.86.[109] The V–V internuclear distance is 3.38 Å, clearly indicating the absence of any bonding interaction between the vanadium atoms. The bridging alkoxide ligands are arranged in a distinct unsymmetrical fashion, with the axial V(1)–O(2') bond length (2.331(2) Å) being 0.52 Å longer than that of the equatorial V(1)–O(2) bond (1.8116(18) Å). This is attributed to the V–O bonds in the *trans*-position to strong σ-donor ligands like oxo functions are repulsed considerably from the coordination sphere due to the *trans*-influence.

Table 2.2. Selected bond lengths (Å) and angles (°) for **2**.

V(1)–O(1)	1.580(2)	V(1)–Cl(1)	2.2190(18)
V(1)–O(2)	1.8116(18)	V(1)–O(3)	1.745(2)
V(1)–O(2')	2.331(2)		
O(1)–V(1)–O(3)	102.88(10)	O(2)–V(1)–Cl(1)	119.59(6)
O(1)–V(1)–O(2)	100.00(10)	O(1)–V(1)–O(2')	171.03(8)
O(3)–V(1)–O(2)	115.85(9)	O(3)–V(1)–O(2')	82.75(9)
O(1)–V(1)–Cl(1)	100.19(8)	O(2)–V(1)–O(2')	71.14(9)
O(3)–V(1)–Cl(1)	113.90(7)	Cl(1)–V(1)–O(2')	83.57(6)

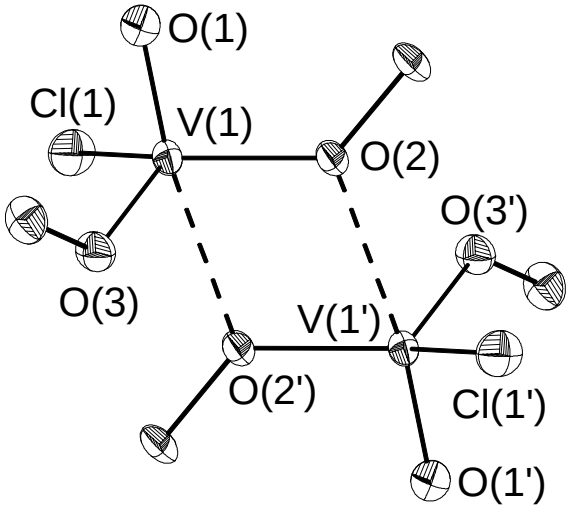

Fig. 2.3. Molecular structure of **2**. Thermal ellipsoids are drawn at 50% probability level. Hydrogen atoms are omitted for clarity. Symmetry transformations used to generate equivalent atoms: ' –x + 1, –y + 1, –z + 1.

A view of the crystal structure of complex **3** is shown in Fig. 2.4. Selected interatomic distances are listed in Table 2.3. Complex **3** crystallizes in monoclinic space group $P2_1/c$. The dimeric molecule is asymmetrical and the vanadium atoms are bridged by two ethoxides. The additional THF molecule is loosely coordinated to the vanadium atoms with distances for V(1)–O(7) and V(2)–O(7) of 2.527(1) Å and 2.658(1) Å, respectively. The vanadium coordination sphere can be viewed as a distorted octahedron with bond angles of 173.07(15) and 170.65(15)° for O(1)–V(1)–O(7) and O(2)–V(2)–O(7), respectively. The bond length of 1.574(4) for V(1)–O(1) matches that of 1.5778(16) Å in complex **1**, while the V(2)–O(2) bond length of 1.583(4) Å match that in complex **2** of 1.580(2). The V(1)–O(3) distance of 2.010(3) Å is slightly longer than V(1)–O(4) of 1.956(3) Å due to different *trans*-influence. The terminal ethoxide bond length of 1.753(3) for V(1)–O(5) is 0.21 and 0.26 Å shorter than the two bridging alkoxides. The V(1)–Cl(1) bond distance of 2.2830(14) Å is shorter than those of 2.3108(7) and 2.3442(8) Å in complex **1**, but considerably longer than that of 2.2190(18) Å in complex **2**.

Interestingly, *syn* configuration for the two V=O functions is found, thus the whole molecule adopts a butterfly configuration. So far, complex **3** represents the first structurally characterized oxovanadium(V) alkoxide with the two V=O groups *syn* to each other.[40,110] The V…V distance (3.1147(12) Å) is shorter than that found in complex **2**, but clearly excludes the possibility of any V…V interaction.

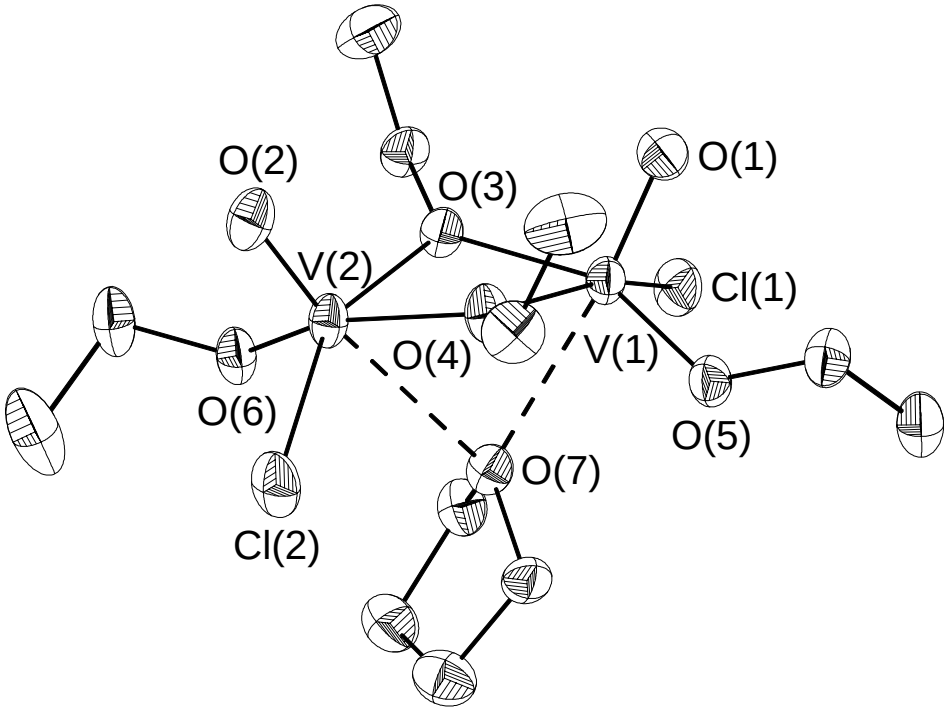

Fig. 2.4. Molecular structure of **3**. Thermal ellipsoids are drawn at 50% probability level. Hydrogen atoms are omitted for clarity.

Table 2.3. Selected interatomic distances (Å) and bond angles (°) for complex **3**.

V(1)–O(1)	1.574(4)	V(2)–O(2)	1.583(4)
V(1)–O(3)	2.010(3)	V(2)–O(3)	1.937(3)
V(1)–O(4)	1.956(3)	V(2)–O(4)	1.999(3)
V(1)–O(5)	1.753(3)	V(2)–O(6)	1.751(4)
V(1)–O(7)	2.529(1)	V(2)–O(7)	2.658(1)
V(1)–Cl(1)	2.2830(14)	V(2)–Cl(2)	2.2788(15)
V(1)...V(2)	3.1148(12)		
O(5)–V(1)–O(4)	92.16(15)	O(6)–V(2)–O(3)	91.42(15)
O(4)–V(1)–O(3)	72.27(13)	O(3)–V(2)–O(4)	72.88(14)
O(6)–V(1)–Cl(1)	97.16(13)	O(6)–V(2)–Cl(2)	96.16(12)
O(3)–V(1)–Cl(1)	89.90(10)	O(4)–V(2)–Cl(2)	89.13(10)
O(1)–V(1)–O(7)	173.07(15)	O(2)–V(2)–O(7)	170.65(15)

2.2 Oxovanadium(V) Alkoxides with Chelating Ligands

2.2.1 Dimeric Oxovanadium(V) Alkoxides with Bidentate Ligands

Syntheses and Spectroscopic Characterization

Treatment of corresponding alkoxyethanols with $VOCl_3$ in pentane at room temperature, followed by stirring for 2–4 h, removal of the HCl with a warm water bath, and storage at 0 °C for several days, afforded complexes **4** and **5** as orange and red crystals in yield of 69% and 58%. (Scheme 2.2).

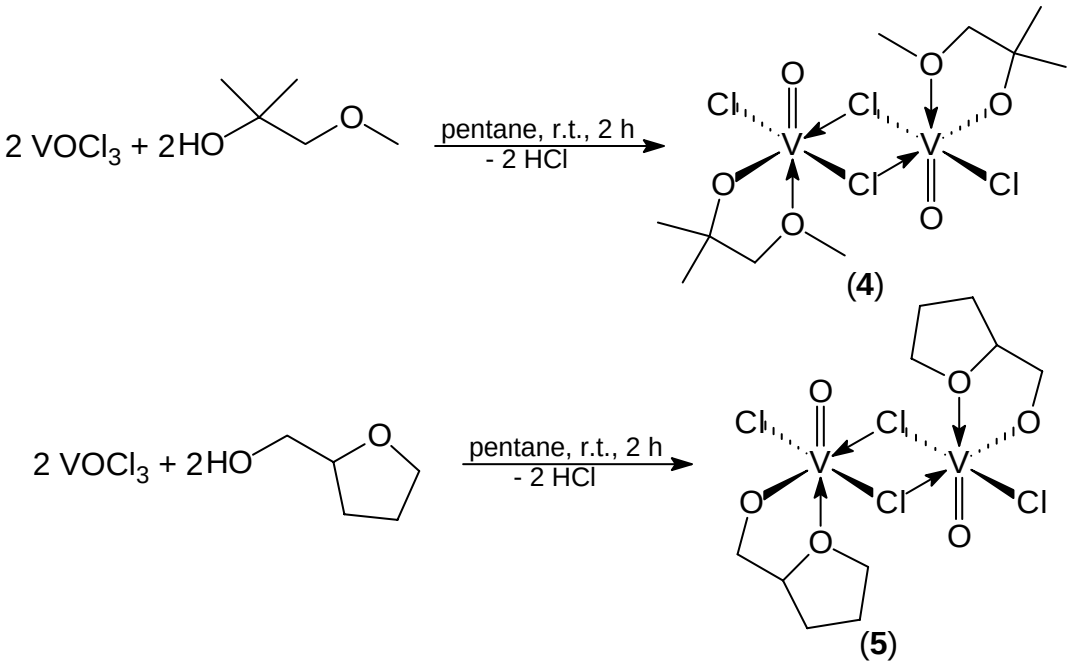

Scheme 2.2. Syntheses of chloride-bridged oxovanadium dimers **4** and **5**.

Different from mixed oxovanadium alkoxides [$VOCl_2(OR)$] (R = Me,[14] Et,[14] ^{i}Pr,[15] ^{t}Bu,[23c]) with simple R groups, complexes **4** and **5** are solids at room temperature with melting points of 48 and 73 °C, respectively. Complex **4** dissolves slightly in pentane, very well in toluene or dichloromethane and reacts with THF. Complex **5** does not dissolve in pentane, slightly in toluene, moderately in dichloromethane and reacts with THF and CH_3CN. This agrees with the tendency for $[VOCl_2(OCH_2CH_2OR)]_2$ complexes that the solubility in pentane increases with R changing from Me to ^{i}Pr. Complexes **4** and **5** are light and moisture sensitive and can be stored at –30 °C in the dark for several weeks without appreciable decomposition. At room temperature orange crystals of complexes **4** and **5** turn black within 24 h. After standing at room temperature for several weeks and dissolution in dichloromethane, a blue solution was obtained denoting the decomposition of vanadium(V) to tetravalent species.

Complexes **4** and **5** essentially fall into the scope of [$VOCl_2(OR)$]. Characteristic IR vibrations are listed in Table 2.4. IR spectra of both complexes in Nujol mull or CS_2 showed characteristic strong and sharp absorptions arising from V=O stretching frequencies for complex **4**; the terminal V–Cl stretching frequency for complex **4** is observed in both CS_2 solution and Nujol mull. Bands arising from the bridging V–Cl–V are observed. Mass spectrometry of complexes **4** and **5** showed fragments $[VOCl(OR)]_2$, which demonstrate their dimeric feature, formed by loss of two chlorine atoms from $[VOCl_2(OR)]_2$. The ^{1}H-NMR chemical shifts at 5.6 (in $CDCl_3$) and 4.8 ppm (in C_6D_6) for the VOC*H*$_2$ moiety in complex **5** are shifted downfield significantly upon vanadylation. More distant protons do not show significant downfield shift. The ^{13}C-NMR spectra show the VO*C* carbon shift 19 and 15 ppm downfield upon vanadylation for complexes **4** and **5**, respectively. The downfield shifts presumably can be ascribed to the deshielding of the carbon atom due to transfer of electron density to the metal atom. All the other carbons shift very little.

Table 2.4. Characteristic IR stretching frequencies for **4** and **5**.

		ν(V=O)	ν(V–OR)	ν(V–Cl)	ν(V–Cl–V)
4	Nujol	1026 s	653 m	487 w	436 w
4	CS_2	1023 vs	660 m	475 vs	431 s
5	Nujol	1021 s	637 s	460 w	431w

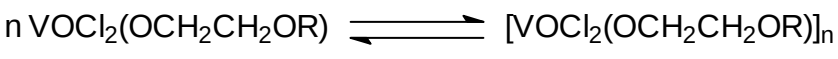

upfield vanadium in ^{51}V-NMR downfield vanadium in ^{51}V-NMR

Scheme 2.3. Monomer/Oligomer equilibrium of oxovanadium alkoxides in solution.

^{51}V shielding depends on electronic and steric factors. Crowding around the vanadium center leads to additional shielding as has been documented for the octahedral alkoxo compound $[VO(oxine)_2OR]$.[111] On the other hand an increase of the coordination number, *e.g.*, on going from tetrahedral to trigonal-bipyramidal environment or octahedral arrangements, is usually accompanied by a decrease of shielding (Scheme 2.3).[32] An increase of shielding takes place as the equilibrium shifts toward the monomer side with decreasing concentration. In case of compound **4**, the dilute solution in $CDCl_3$ exhibited two signals at –273 and –281 ppm in ratio of 24:1. The one at –273 ppm is ascribed to the dimeric species, while the one at –281 ppm is designated to a monomeric species. Complex **5** displayed one signal at –247 ppm due to the dimeric species $[VOCl_2(OR)]_2$.

X-ray Crystallographic Studies for **4** *and* **5**

Molecular structures for complexes **4** and **5** are shown in Fig. 2.5 and Fig. 2.6, respectively. Selected interatomic distances and bond angles are presented in Table 2.5. Complex **4** crystallizes in triclinic space group $P\bar{1}$, while complex **5** in monoclinic $C2/c$ space group. Structural determination shows that **4** and **5**, together with $[VOCl_2(OCH_2CH_2OR)]_2$ (R = Me, Et, ^{i}Pr)[38,39] are similar: both complexes are dimers formed through μ-chloro bridges across the crystallographic inversion center so that oxo groups and terminal chlorine atoms adopt an *anti* orientation. Each vanadium center is in an octahedral coordination geometry consisting of O_3Cl_3. The oxo groups and ether oxygens are situated in *trans*-position.

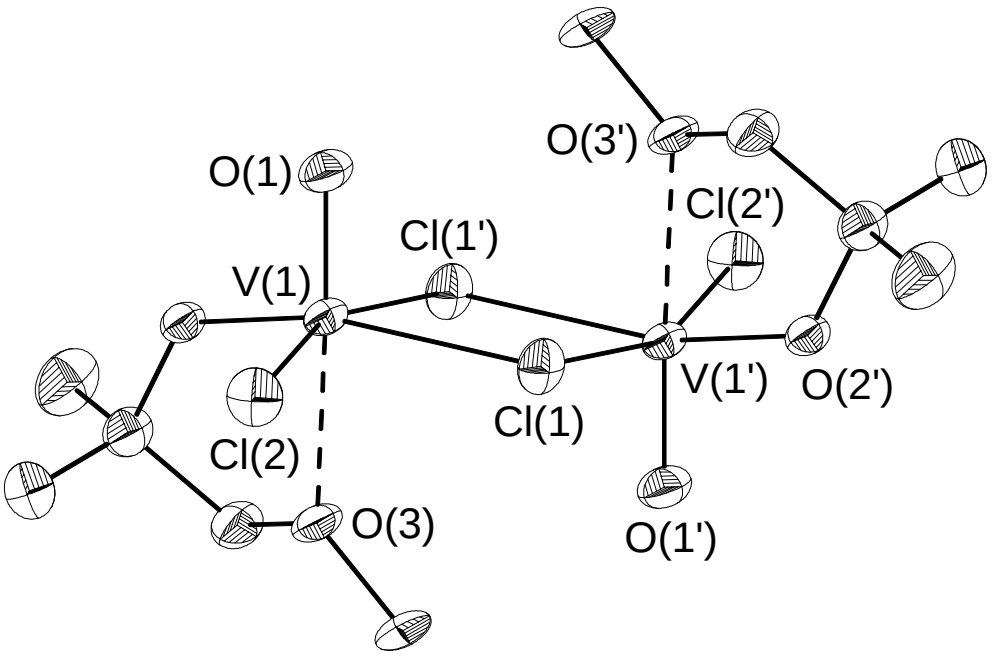

Fig. 2.5. Molecular structure of **4**. Thermal ellipsoids are drawn at 50% probability level. Hydrogen atoms are omitted for clarity. Symmetry transformations used to generate equivalent atoms: ' –x + 1, –y + 1, –z + 1.

The vanadium atoms deviate from the mean equatorial planes consisting of O(2)–Cl(2)–Cl(1)–Cl(1') by 0.265(1) Å and 0.282(2) Å toward the oxo ligand for **4** and **5**, respectively. The sum of the angles formed by O(2)–Cl(2)–Cl(1)–Cl(1') is 356.56° and 356.08° for **4** and **5**, respectively, defining a distorted octahedron. The bridging chlorine atoms and the vanadium atoms form a perfect rhombus with almost the same (μ-Cl)–V–(μ-Cl) angles in both cases (78.57(4)° for **4** and 79.35(4)° for **5**, respectively). These angles are significantly smaller than that for an ideal octahedron, which can be ascribed to the distortion imposed by the bridging formation. The chloride bridge in **4** and **5** is approximately symmetric with V(1)–Cl(1) and V(1)–Cl(1') distances ranging from 2.4331(11) to 2.4429(12) Å. The distances of the vanadium to the terminal chlorines are significantly shorter with the distances of 2.2501(12), 2.2447(12) Å. The oxygens are bound to V(1) with distinctly different bond distances in complexes **4** and **5**. The V(1)–O(1) bond distances of 1.581(3) and 1.587(3) Å clearly indicate the V=O character. The vanadium to alkoxo oxygen bonds distances of 1.762(3) and 1.768(3) Å are shorter than the vanadium to ether oxygen bonds and only about 0.2 Å longer than the formal double bonds to the oxo group, indicative of some multiple bond character. A *trans*-influence is evident with the vanadium to ether oxygen bond *trans* to the oxo group at distances of 2.2623(3) and 2.2453(3) Å for **4** and **5**, respectively.

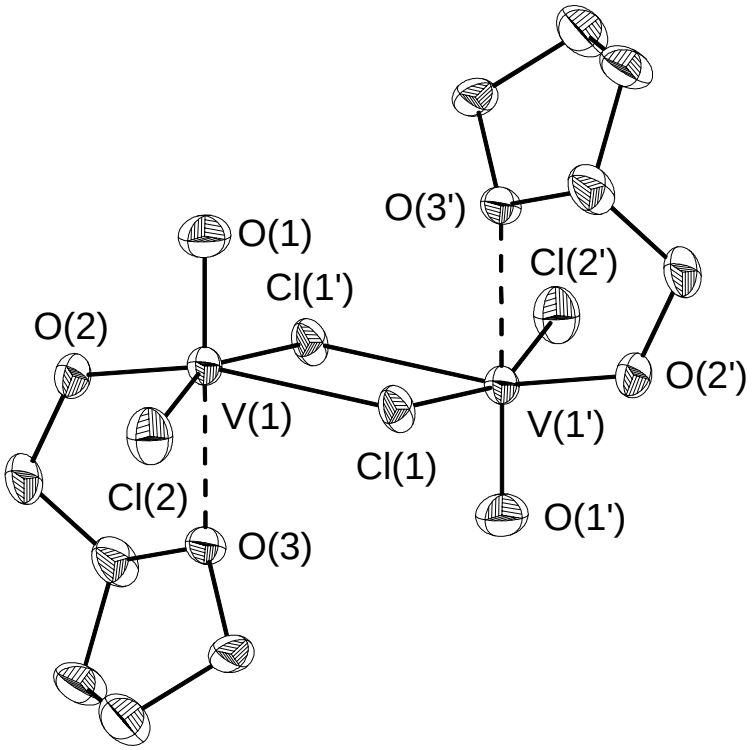

Fig. 2.6. Molecular structure of **5**. Thermal ellipsoids are drawn at 50% probability level. Hydrogen atoms are omitted for clarity. Symmetry transformations used to generate equivalent atoms: ' –x, –y + 1, –z.

Table 2.5. Selected interatomic distances (Å) and bond angles (°) for complexes **4** and **5**.

	4	**5**
V(1)–O(1)	1.581(3)	1.578(3)
V(1)–O(2)	1.762(3)	1.768(3)
V(1)–O(3)	2.262(3)	2.245(3)
V(1)–Cl(1)	2.4429(12)	2.4331(11)
V(1)–Cl(1')	2.4391(13)	2.4392(10)
V(1)–Cl(2)	2.2501(12)	2.2447(12)
O(1)–V(1)–O(3)	173.40(15)	172.29(14)
O(2)–V(1)–Cl(1)	161.25(11)	92.77(9)
O(2)–V(1)–Cl(1')	90.97(11)	162.12(10)
O(2)–V(1)–Cl(2)	100.78(11)	98.30(9)
Cl(2)–V–Cl(1')	161.88(6)	85.66(4)
Cl(1)–V–Cl(2)	86.24(5)	161.21(5)
Cl(1)–V–Cl(1')	78.57(4)	79.35(4)
V(1)–Cl(1)–V(1')	101.43(4)	101.42(5)

2.2.2 THF Solvates of Oxovanadium(V) Alkoxyalkoxides

The dimeric chloro-bridged complexes $[VO(\mu\text{-}Cl)Cl(\eta^2\text{-}OCH_2CH_2OR)]_2$ offer an entry into a series of complexes $[VOCl_2(OCH_2CH_2OR)(THF)]$ *via* bridge cleavage with the appropriate nucleophile. Herein THF was used for cleavage reactions of $[VOCl_2(OCH_2CH_2OR)]_2$ (R = Me, Et, ^{i}Pr), and **4**. In all cases the *cis* isomers are nearly quantitatively produced.

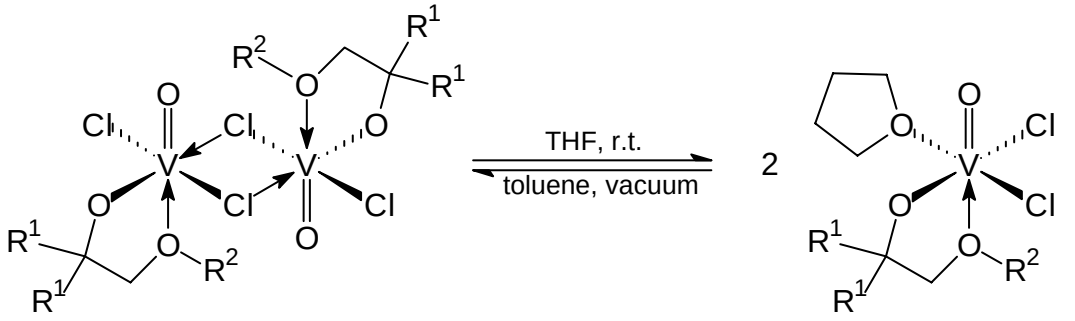

R^1 = H, R^2 = Me (**6**), Et (**7**), i-Pr (**8**)
$R^1 = R^2$ = Me (**9**)

Scheme 2.4. Preparation of THF solvates of oxovanadium alkoxyalkoxides.

Treatment of complexes $[VOCl_2(OCH_2CH_2OR)]_2$ (R = Me, Et, ^{i}Pr)[38,39] and **4** in either THF/toluene or THF/pentane, followed by crystallization at 0 °C, afforded complexes **6**–**9** as orange crystals in high yields. Particularly, in THF/pentane the complexes could be produced nearly quantitatively (Scheme 2.4). If the THF complexes are dissolved in toluene and all

solvent is removed in vacuum again, the chloride-bridged dimeric complexes are recovered. Complexes **6–9** turn into black oils within 24 h when exposed to sunlight. They are well soluble in THF, dichloromethane, and toluene, and slightly soluble in saturated hydrocarbons. Complex **8** dissolves moderately in pentane. At –30 °C the complexes are stable for several months, while at 0 °C they decompose slowly both in solution and in the solid state. No significant ^{1}H-, ^{13}C- or ^{51}V-NMR chemical shift discrepancy between **6–9** and the corresponding dimeric complexes is observed for a given resonance. The IR spectra show the characteristic, sharp, and strong V=O stretching band analogous to that of the dimeric complexes. Selected vibrations are listed in Table 2.6.

Table 2.6. Characteristic IR frequencies for complexes **6–9** in CS_2.

	ν(V=O)	ν(V–OR)	ν(V–Cl)
6	1024 vs	606 vw	484 w
7	1025 vs	667 w	484 m
8	1025 vs	668 m	482 s
9	1023 vs	659 vw	475 m

X-ray Crystallographic Studies

Molecular structures for complexes **6–9** are shown in Fig. 2.7 to Fig. 2.10. Selected interatomic distances and bond angles for **6–9** are presented in Table 2.7. Complex **6** crystallizes in monoclinic system, space group $P2_1/c$, **7** and **8** in orthorhombic system, space group $Pna2_1$, and **9** in monoclinic system, space group $P2_1/n$. The vanadium centers in all four complexes are octahedrally coordinated. Two chlorine atoms and the alkoxo and THF oxygen atoms are situated in the equatorial plane, the oxo function and the ether function from the chelating ligands occupy the *trans*-positions completing the octahedral geometry.

The vanadium atom deviates from the mean equatorial plane by 0.2811, 0.2733, 0.2620, and 0.2625 Å for **6–9**, respectively. The distances of V=O double bond range between 1.576(3) Å and 1.581(3) Å and are nearly the same as those in complexes **4** and **5**. The alkoxo group to vanadium distances in complex **9** is longer than that in complex **4** by 0.02 Å due to different *trans*-influence. The ether to vanadium distances between 2.288(4) and 2.348(3) Å in complexes **6–9** are considerably longer than those in complexes **4** and **5** (2.262(3) and 2.245(3) Å). Expectedly, the Cl–V–Cl bond angle of 90.92(4)° in **9**, is significantly larger than that of 78.57(4)° for **4** in the V–(μ-Cl)–V–(μ-Cl) rhombus. The average V–Cl distance of 2.29 Å is 0.04 Å longer than the average terminal V–Cl bond length in **4** and **5**. Significantly for complexes **6–9** only isomers with the chloro ligands in *cis* configuration were found. Since

these isomers are chiral they crystallize as racemic mixtures with two molecules of each enantiomer in the unit cell. Molecular structure of complex **7** is shown in the Δ-form, while complexes **6**, **8**, and **9** are shown in the Λ-form.

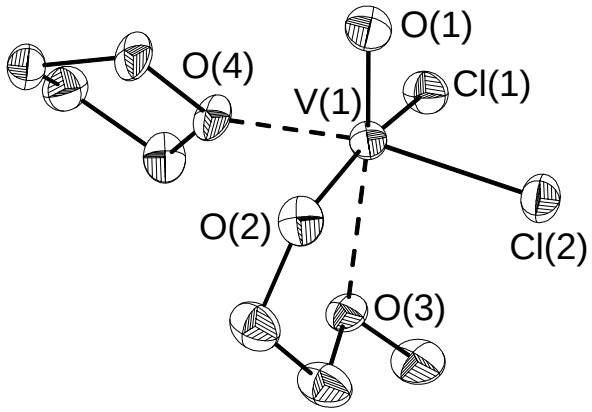

Fig. 2.7. Molecular structure of the Λ-form of **6**. Thermal ellipsoids are drawn at 50% probability level. Hydrogen atoms are omitted for clarity.

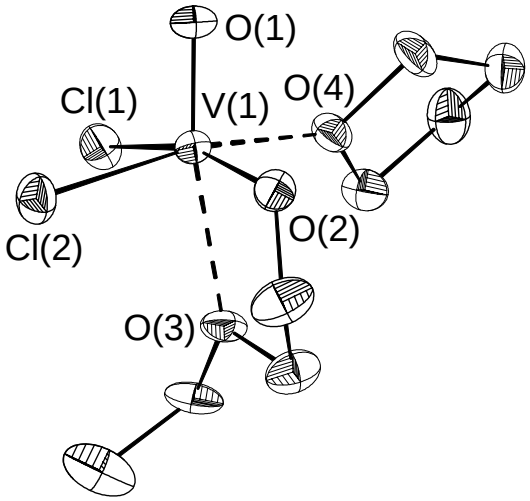

Fig. 2.8. Molecular structure of the Δ-form of **7**. Thermal ellipsoids are drawn at 50% probability level. Hydrogen atoms are omitted for clarity.

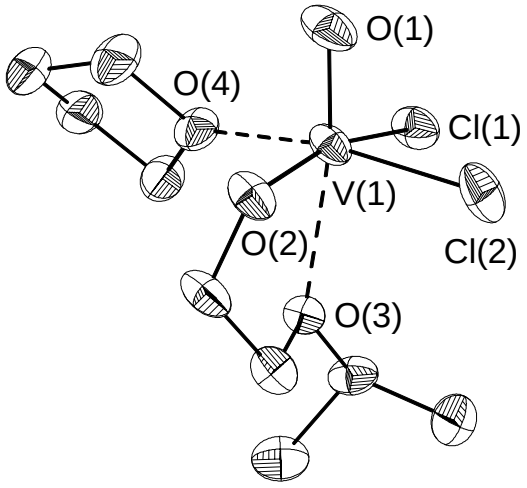

Fig. 2.9. Molecular structure of the Λ-form of **8**. Thermal ellipsoids are drawn at 50% probability level. Hydrogen atoms are omitted for clarity.

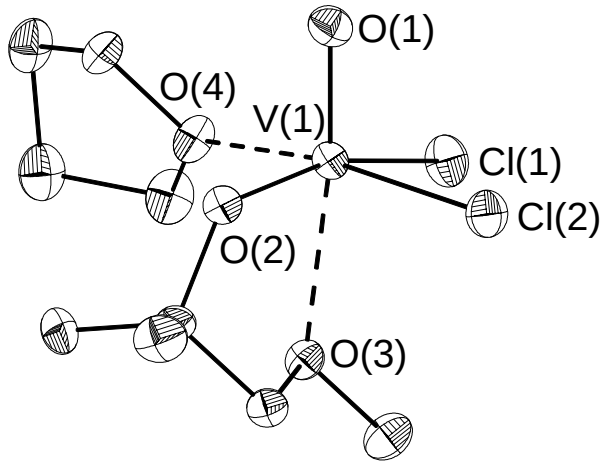

Fig. 2.10. Molecular structure of the Λ-form of **9**. Thermal ellipsoids are drawn at 50% probability level. Hydrogen atoms are omitted for clarity.

Table 2.7. Selected bond lengths (Å) and bond angles (°) for **6**–**9**.

	6	**7**	**8**	**9**
V(1)–O(1)	1.576(3)	1.579(4)	1.581(2)	1.581(3)
V(1)–O(2)	1.785(3)	1.788(4)	1.780(2)	1.777(2)
V(1)–O(3)	2.316(3)	2.288(4)	2.331(2)	2.348(3)
V(1)–O(4))	2.076(3)	2.093(4)	2.086(2)	2.103(3)
V(1)–Cl(1)	2.2906(14)	2.301(2)	2.3072(12)	2.3096(12)
V(1)–Cl(2)	2.2818(13)	2.2927(17)	2.2853(13)	2.2827(12)
O(2)–V(1)–O(4)	85.34(14)	89.65(19)	86.83(10)	87.78(11)
O(2)–V(1)–Cl(2)	95.32(11)	91.81(16)	94.60(9)	95.05(9)
O(4)–V(1)–Cl(2)	167.97(10)	167.66(13)	168.40(6)	169.37(8)
O(2)–V(1)–Cl(1)	158.51(12)	161.24(16)	160.87(7)	158.78(9)
O(4)–V(1)–Cl(1)	84.01(10)	85.06(13)	84.87(7)	82.94(8)
Cl(2)–V(1)–Cl(1)	91.33(5)	89.68(8)	90.23(4)	90.92(4)
O(1)–V(1)–O(3)	173.22(14)	169.5(2)	170.79(11)	173.03(12)

2.2.3 Reaction of $[VOCl_2(OCH_2CH_2OCH_3)]_2$ with Metal Alkyls and PPh_3

Alkylation of $[VOCl_2(OCH_2CH_2OCH_3)]_2$

$[VOCl_2(OCH_2CH_2OR)]_2$, falling into the scope of mixed vanadate chloride $[VOCl_2OR]$, bears two chloro ligands around each vanadium atom with the possibility of nucleophilic substitution such as alkylation. In view of this fact neopentyl lithium, benzyl Grignard reagent, trimethylsilymethyl Grignard reagent, and potassium phenylacetylene were chosen for alkylation of $[VOCl_2(OCH_2CH_2OCH_3)]_2$. These alkyl groups contain no β-hydrogen, thus the

possibility of complex decomposition *via* β-hydrogen elimination, which to a large extent is responsible for the kinetic lability of organometallic complexes, is excluded.

Reaction of $[VOCl_2(OCH_2CH_2OCH_3)]_2$ with 2 equiv of neopentyl lithium at –78 °C afforded an orange solution, which on warming to room temperature turned *via* green to dark blue, indicating the formation of vanadium(IV) species. $[VOCl(OCH_2CH_2OCH_3)]_2$ was isolated on purification. Alkylation of $[VOCl_2(OCH_2CH_2OCH_3)]_2$ with 2 equiv of potassium phenylacetylene at –78 °C gave rise to an orange solution. Similarly, this solution turned green on warming to room temperature, revealing the reduction of pentavalent vanadium to tetravalent. The reaction of $[VOCl_2(OCH_2CH_2OCH_3)]_2$ with benzyl Grignard reagent at –78 °C resulted in a brown solution, which turned gradually *via* green to dark brown on warming to room temperature. This color change presumably indicated the vanadium(IV) center was further reduced to vanadium(III) species. Attempts to isolate this species for characterization were unsuccessful. In the case of alkylation with trimethylsilymethyl Grignard reagent under the same conditions, however, light yellow needles of $[VO(CH_2SiMe_3)_3]$ were isolated in spite of some vanadium(V) being reduced. This complex was first synthesized from $[V(CH_2SiMe_3)_4]$ *via* rather complex hydrolysis and oxidation processes.[112] The ^{1}H-NMR spectrum of $[VO(CH_2SiMe_3)_3]$ shows two resonances at 0.09 and 1.79 ppm, corresponding to C*H*$_3$ and C*H*$_2$, respectively. These two signals were reported to show up at 0.15 and 1.80 ppm in the literature, respectively.[113] Both signals are very broad due to unresolved coupling to ^{51}V (I = 7/2, 100%). Using less than 2 equiv of trimethylsilymethyl Grignard reagent is preferable to approach $[VO(CH_2SiMe_3)_3]$. Extensive reduction of vanadium(V) was observed when more alkylation reagent was employed.

Reaction of $[VOCl(OCH_2CH_2OCH_3)]_2$ with PPh_3

Since $[VOCl_2(OCH_2CH_2OCH_3)]_2$ reacts with Lewis base THF giving rise to the solvate, the similar reaction is of considerable interest in case of PPh_3. With the aim to probe the effect of the donor ligand PPh_3 on the chloride bridges and to obtain a neutral phosphine coordinated monomeric $[VOCl_2(OCH_2CH_2OCH_3)(PPh_3)]$, the reaction of $[VOCl_2(OCH_2CH_2OCH_3)]_2$ with PPh_3 was carried out.

It has been found that the vanadium atom was reduced and alkoxo group abstraction from the vanadium took place, while phosphine was oxidized to phosphine oxide and appeared as ligand in the final vanadium(IV) product $[VOCl_2(O{=}PPh_3)_2]\cdot CH_2Cl_2$. The supposed and observed reactions between the dimeric complex and PPh_3 are given in Scheme 2.5.

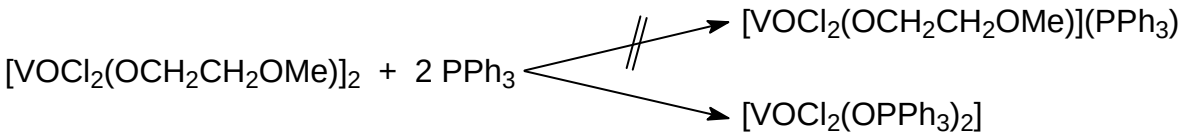

Scheme 2.5. Supposed and actual reactions of $[VOCl_2(OCH_2CH_2OCH_3)]_2$ with PPh_3.

The reaction of $[VOCl_2(OCH_2CH_2OCH_3)]_2$ with PPh_3 in the ratio of 1:2 in toluene at –78 °C gave rise to a dark red solution, which on standing at –30 °C overnight gave a lemon crystalline solid. ^{1}H-NMR indicated that this species is triphenylphosphine oxide. On storage at –30 °C for several weeks, the solution turned green and green crystals of $[VOCl_2(OPPh_3)_2]\cdot CH_2Cl_2$ suitable for X-ray diffraction separated. This complex is a known compound and fully characterized.[114] The formation of $[VOCl_2(OPPh_3)_2]$ indicated that the vanadium(V) center was reduced by PPh_3. This finding does not agree with what was reported by Cotton[57] and Henderson,[58] wherein the formation of a vanadium(III) species with phosphine ligands or both phosphine and phosphine oxide ligands was suggested. The V=O entity was cleaved in the reaction. $[VOCl_2(OPPh_3)_2]$ contains the VO^{2+} ion, which is a dominating entity in vanadium(IV) chemistry, and is stable enough to be isolated even in the presence of traces of moisture.[48]

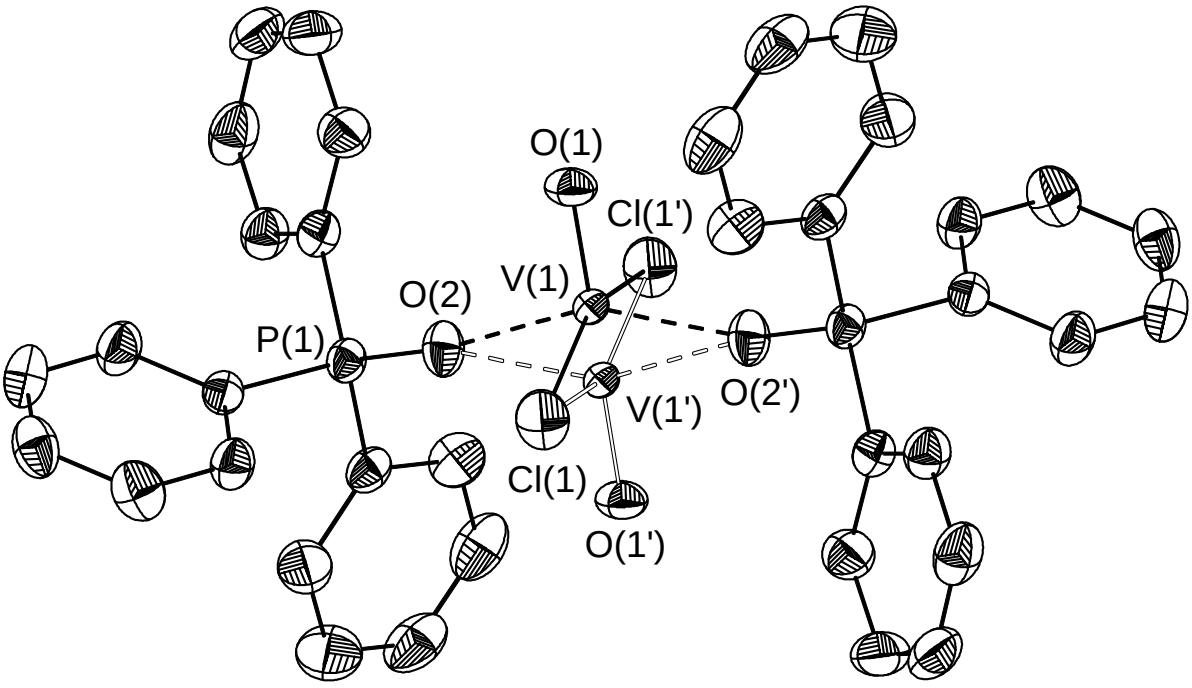

Fig. 2.11. Molecular structure of $[VOCl_2(O{=}PPh_3)_2]\cdot CH_2Cl_2$. Thermal ellipsoids are drawn at 50% probability level. Hydrogen atoms are omitted for clarity. Symmetry transformations used to generate equivalent atoms: ' –x+1, –y, –z+1.

Table 2.8. Selected bond lengths (Å) and bond angles (°) for $VOCl_2(O{=}PPh_3)_2{\cdot}CH_2Cl_2$.

V(1)–O(2)	1.9673(18)	V(1)–O(2')	1.9669(17)
V(1)–Cl(1)	2.3357(10)	V(1)–Cl(1')	2.2838(11)
V(1)–O(1)	1.575(3)		
O(1)–V(1)–O(2)	103.62(14)	O(1)–V(1)–O(2')	103.92(14)
O(1)–V(1)–Cl(1)	101.14(13)	O(1)–V(1)–Cl(1')	102.26(13)
O(2)–V(1)–Cl(1)	84.91(6)	O(2)–V(1)–Cl(1')	89.58(6)
O(2')–V(1)–Cl(1)	88.10(6)	O(2')–V(1)–Cl(1')	86.33(6)
Cl(1)–V(1)–Cl(1')	156.60(3)	O(2)–V(1)–O(2')	152.41(5)

The molecular structure of $[VOCl_2(OPPh_3)_2]{\cdot}CH_2Cl_2$ is shown in Fig. 2.11. Selected interatomic distances and bond angles are listed in Table 2.8. $[VOCl_2(OPPh_3)_2]$ crystallizes in monoclinic $P2_1/n$, with a CH_2Cl_2 molecule in the crystal lattice. This complex was reported to crystallize in monoclinic $P2_1/c$ space group.[114a] The position of the V=O moiety is highly disordered. The coordination geometry of vanadium is a square pyramid as revealed by the τ value of 0.07, which is considerably smaller than the literature τ value of 0.15. The oxygen atoms of the $O{=}PPh_3$ ligands and two chloride ligands form the basal plane, while the terminal oxo atom stands at the apex. The oxygen atoms and the chlorine ligands are arranged in *trans*-positions, respectively. The vanadium center deviates from the mean plane consisting of Cl_2O_2 in the direction of oxo group by 0.4684 Å. The V(1)–O(2) and V(1)–O(2') bonds have bond lengths of 1.9673(18) Å and 1.9669(17) Å, respectively, which are comparable to those reported (2.002(5) and 1.986(5) Å).[114a] The pair of V–Cl lengths do not differ significantly, the V(1)–Cl(1) and V(1)–Cl(1') being 2.3357(10) and 2.2838(11) Å, respectively. These distances are in accordance with those reported (2.312(3) and 2.304(3) Å, respectively). The V(1)–O(1) length of 1.575(3) Å is about 0.01 Å shorter than that reported. The Cl(1)–V–Cl(1') angle of 156.60(3)° is significantly shorter than that of 146.3(1)°. The difference in the O(2)–V–O(2') is merely 3°.

2.2.4 An Oxovanadium Alkoxide with a Tridentate Ligand

Synthesis and Spectroscopic Characterization

Alkoxy bridges appears as a dominant structural feature for oxovanadium alkoxides. They adopt variable coordination geometries depending on the nature of the ligands and the reacting conditions.[11,20,40,48] Chloride bridges are found after 1:1 reaction of $VOCl_3$ with bidentate ligands in $[VOCl_2(OCH_2CH_2OR)]_2$,[38,39] complexes **4** and **5**. In opposition, vanadate chloride **10** incorporating tridentate $[O,O,O]^-$ alkoxide ligand is mononuclear due to 2

intramolecular donor functions to saturate the coordination sphere around the Lewis acidic vanadium(V) center.

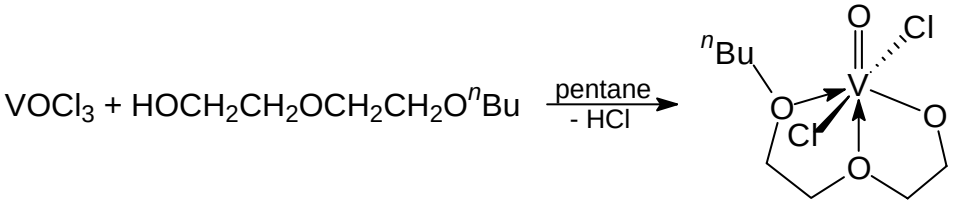

Scheme 2.6. Preparation of oxovanadium alkoxide **10** with tridentate ligand.

Complex **10** was synthesized by reaction of $VOCl_3$ with 1 equiv of $HOCH_2CH_2OCH_2CH_2O^nBu$ in pentane *via* HCl elimination (Scheme 2.6). The complex was isolated as brown powder. Orange single crystals suitable for X-ray diffraction were obtained from cold pentane mother solution. The ^{1}H-NMR spectrum displays broad resonances at 5.47, 4.28, and 4.13 ppm. The one at lowest field is ascribed to VOCH_2, while the other two are assigned to the remaining OCH_2 moieties. Three signals at 1.87, 1.45, and 0.93 ppm are due to the CH_2CH_2CH_3 moiety of the butyl group. ^{13}C-NMR shows the same order: the broad signal at 87 ppm arises from the VO*C*H_2 resonance, while the other O*C*H_2 moieties appear upfield. The IR spectrum presents the characteristic, strong, and sharp vibration band at 1029 cm^{-1} due to the V=O stretching frequency. The vibration bands at 646, 491, and 465 cm^{-1} are attributed to V–OR, asymmetrical and symmetrical Cl–V–Cl stretching vibrations, respectively. The mass spectrum does not support the mononuclear structure identified by X-ray diffraction. A fragment at an *m/z* of 526 related with loss of two chlorines from the dimer is observed. The ^{51}V-NMR spectrum in $CDCl_3$ shows two resonances at –300 ppm ($\nu_{1/2}$ = 399 Hz) and –346 ppm ($\nu_{1/2}$ = 270 Hz) in a ratio of 83:17. The downfield signal is ascribed to the dimeric species, while the upfield one corresponds to the monomeric species. The half widths support the designations as the downfield signal has broader half width of 399 Hz, while the upfield one has narrower half width of 270 Hz. This is in accordance with the findings that dimeric vanadates have larger molecular size and lower local symmetry hence broader half width.[115]

X-ray Crystallographic Study

Single crystals of complex **10** suitable for X-ray diffraction were obtained from cold pentane. It crystallizes in triclinic system, space group $P\bar{1}$. The molecular structure is shown in Fig. 2.12. Complex **10** contains two sets of crystallographically independent isomeric molecules in the unit cell depending on the different orientation of the pendant butyl group relative to the basal Cl_2O_2 plane. The two sets of molecules differ only marginally in their

coordination geometries around the vanadium center. The butyl group stands vertical to the plane consisting of Cl(1)–O(2)–Cl(2)–O(4) and parallel to the plane consisting of O(6)–Cl(4)–O(8)–Cl(3) in these two molecules. Selected bond lengths and bond angles are given in Table 2.9.

Table 2.9 Selected bond lengths (Å) and bond angles (°) for **10**.

V(1)–O(1)	1.591(2)	V(2)–O(5)	1.591(2)
V(1)–O(2)	1.787(2)	V(2)–O(6)	1.795(2)
V(1)–O(3)	2.203(2)	V(2)–O(7)	2.189(2)
V(1)–O(4)	2.113(2)	V(2)–O(8)	2.082(2)
V(1)–Cl(1)	2.339(1)	V(2)–Cl(3)	2.3315(11)
V(1)–Cl(2)	2.3178(10)	V(2)–Cl(4)	2.3347(11)
O(1)–V(1)–O(3)	179.01(11)	O(5)–V(2)–O(7)	178.21(11)
O(2)–V(1)–O(4)	153.10(10)	O(6)–V(2)–O(8)	153.49(10)
O(2)–V(1)–Cl(2)	95.10(9)	O(6)–V(2)–Cl(3)	92.80(9)
O(4)–V(1)–Cl(2)	85.26(7)	O(8)–V(2)–Cl(3)	82.80(7)
O(2)–V(1)–Cl(1)	93.34(9)	O(6)–V(2)–Cl(4)	94.70(9)
O(4)–V(1)–Cl(1)	81.50(7)	O(8)–V(2)–Cl(4)	84.72(7)
Cl(2)–V(1)–Cl(1)	164.78(4)	Cl(3)–V(2)–Cl(4)	165.02(4)

The tridentate [*O,O,O*] ligand bisects Cl–V–Cl angle and is arranged meridional around the central vanadium. The vanadium atoms have a nearly ideal octahedral coordination, wherein the oxo ligand and one ether oxygen are arranged in the *trans*-positions and the angles of O(1)–V(1)–O(3) and O(5)–V(2)–O(7) are 179.01(11) and 178.21(11)°, respectively. Two *trans*-orientated terminal chloro ligands are arranged in the equatorial plane, together with the alkoxo and the second ether donor atom, to complete the octahedral coordination geometry. The vanadium atoms displace only slightly from the equatorial planes toward the terminal oxo ligands (0.0192 Å for V(1), 0.0086 Å for V(2)), while they are in an almost perfect coplanar configuration with the four oxygen atoms, as demonstrated by the sums of the O–V–O angles around the vanadium center (359.5° and 356.8° for V(1) and V(2), respectively). The V=O bond lengths of 1.591(2) Å for both molecules are slightly longer than those in complex **1**, which has a similar coordination sphere around the vanadium center. The V–Cl bond distances between 2.3178(10) and 2.339(1) Å are well comparable to those in complex **1**. The V–O bond *trans* to the terminal oxo ligand is shortened compared to those found for **4** and **5** ligated with bidentate alkoxyalkoxides due to the tridentate ligand system.

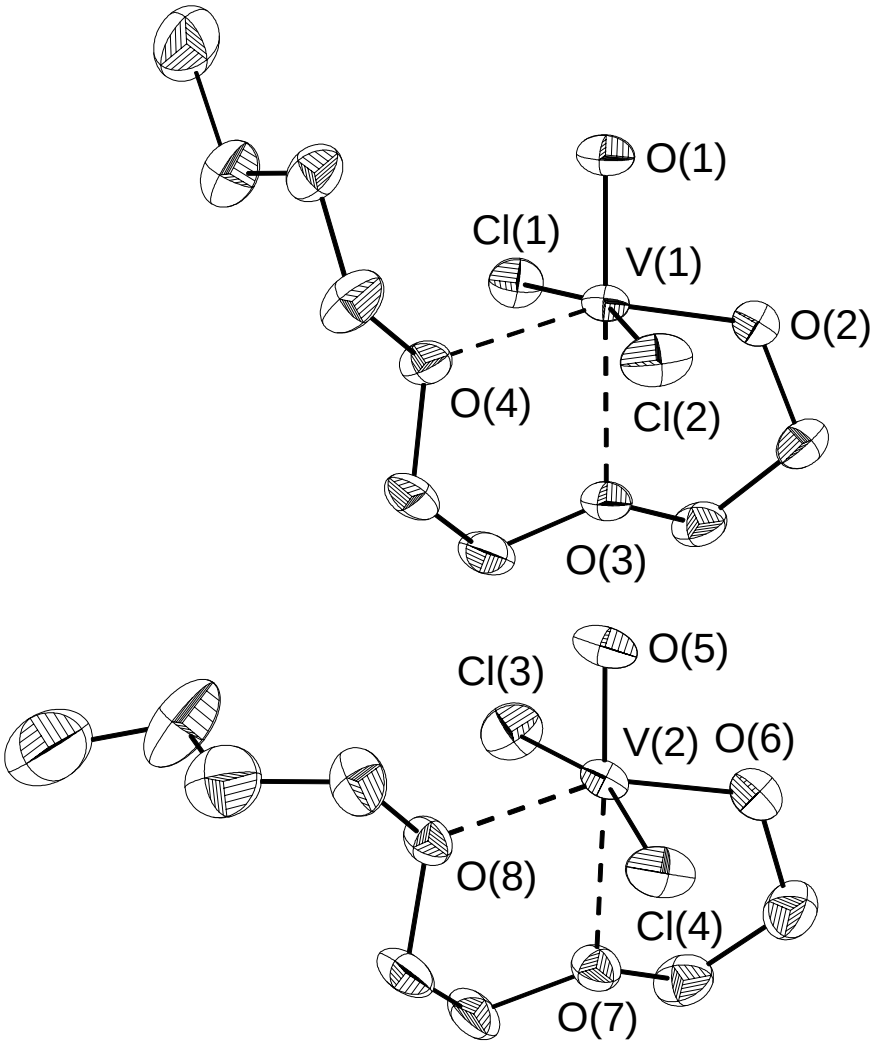

Fig. 2.12. Molecular structures of **10**. Thermal ellipsoids are drawn at 50% probability level. Hydrogen atoms are omitted for clarity.

2.2.5 Oxovanadium Alkoxides with Two Tetrahydrofurfuroxo Ligands

The use of the tetrahydrofurfuroxo ligand (thffo) for the synthesis of vanadium alkoxides was first reported by Sobota *et al.*, where they synthesized $[V_2(\mu,\eta^2\text{-thffo})_2Cl_2O_2]$ and investigated its ethylene polymerization activity.[96] Based on the successful synthesis of $[VOCl_2\{\eta^2\text{-}OCH_2\text{-}(cyclo\text{-}C_4H_7O)\}]_2$ (**5**), complexes **11** and **12** with 2 equiv tetrahydrofurfuroxo ligands were prepared and characterized (Scheme 2.7).

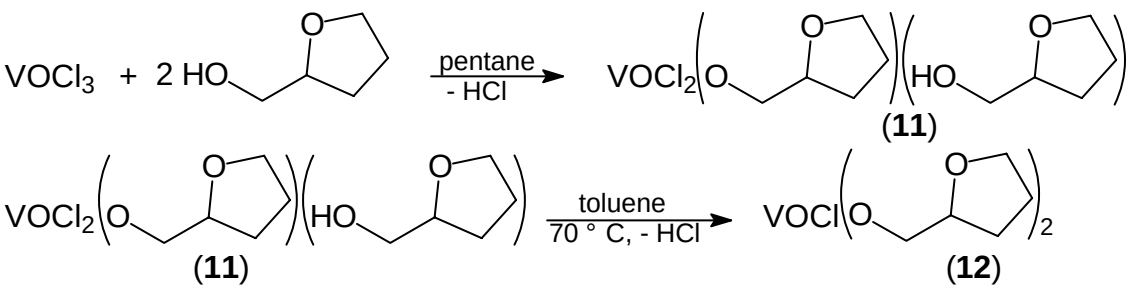

Scheme 2.7. Preparation of complexes **11** and **12**.

Reaction of $VOCl_3$ and 2 equiv of tetrahydrofurfuryl alcohol (Hthffo) in pentane at ambient temperature afforded [$VOCl_2$(thffo)(Hthffo)] (**11**) as orange powder, which is insoluble in pentane, sparingly soluble in diethyl ether and toluene, moderately in dichloromethane and hot toluene, well soluble in THF. Under reduced pressure at 70 °C in toluene, **11** loses 1 equiv of HCl to afford a brown solution, from which **12** separated as a brown solid. Complex **11** is stable at room temperature both in the solid state and in solution for several days without color change. Complex **12** is stable in the solid state like **11**, however, it decomposes in THF or dichloromethane solution after a period of several weeks to afford [VOCl{μ,η^2-OCH_2-(*cyclo*-C_4H_7O)}]$_2$.[96]

The ^{1}H-NMR of complex **11** displays a very broad signal at 6.27 ppm presumably due to the alcoholic hydrogen. The other signals of **11** appear at the analogous positions to **12**. There might be fast transformation between the two [OCH_2(*cyclo*-C_4H_7O)] ligands in different coordination fashions for complex **11**, therefore the designation of the signals in the ^{1}H-NMR spectrum is impossible and all signals show up as broad lines. ^{13}C-NMR signal due to the VO*C*H_2 is not observed in the ^{13}C-NMR spectrum for **11**, whereas the signal shows up at lowest field of 85.8 ppm for **12**. The ^{51}V-NMR spectra of **11** and **12** present chemical shifts at –345 and –333 ppm, respectively, around 100 ppm upfield from that of **5**. The dichloro vanadate [$VOCl_2${η^2-OCH_2(*cyclo*-C_4H_7O)}]$_2$ (**5**), [$VOCl_2${$HOCH_2$(*cyclo*-C_4H_7O)}{OCH_2-(*cyclo*-C_4H_7O)}] (**11**) and monochloro vanadate [VOCl{OCH_2(*cyclo*-$C_4H_7O)_2$}] (**12**) decompose to afford the same reduction species [VOCl{OCH_2(*cyclo*-C_4H_7O)}]$_2$ instead of the formation of [VO{OCH_2(*cyclo*-C_4H_7O)}$_2$]$_2$. The similar reaction was described by Funk, where both [$VOCl_2$(acac)] and [VOCl(acac)$_2$] decompose to afford [VO(acac)$_2$].[14]

2.2.6 An Oxovanadium Trisalkoxide

Synthesis and Spectroscopic Characterization

The reaction of 3 equiv lithium alkoxide—prepared *in situ* from the corresponding alkoxyethanol and ^{n}BuLi in a 1:1 ratio in pentane—with 1 equiv of $VOCl_3$, followed by reaction over 3 days gave **13** as light yellow liquid in good yield (Scheme 2.8).

$$VOCl_3 + 3\ LiOCMe_2CH_2OMe \xrightarrow[-\ 3\ LiCl]{pentane} VO(OCMe_2CH_2OMe)_3$$

Scheme 2.8. Synthesis of oxovanadium trisalkoxide **13**.

Complex **13** is colorless and subject to decomposition at room temperature with the color turning green. This compound was characterized by ^{1}H-, ^{13}C-, ^{51}V-NMR, IR spectroscopy, and MS spectrometry. The ^{1}H spectrum of complex **13** in C_6D_6 shows three signals at 3.33, 3.17,

and 1.52 ppm in the ratio of 2:3:6. They are ascribed to the OC*H*$_2$, OC*H*$_3$, and C(C*H*$_3$)$_2$ moieties, respectively. The ^{13}C-NMR spectrum of the title compound recorded in C_6D_6 exhibited two signals at 85.4 and 85.1 ppm, which are assigned to the quaternary carbons of different rotamers.[11,25] The signals at 81.0, 58.9, 27.0 ppm are due to *C*H$_2$, O*C*H$_3$, and OC(*C*H$_3$)$_2$, respectively. The IR spectrum for **13** contains a sharp and strong absorption due to V=O stretching vibration at 977 cm^{-1} in CS_2, the same signal appears at 980 cm^{-1} in Nujol, which is quite low for a vanadate. On the other hand, these values are within the scope of the vibrations between 960 cm^{-1} and 1007 cm^{-1} found for [VO(O^{t}Bu)$_3$]. The absorption at 664 cm^{-1} in CS_2 and 667 cm^{-1} in Nujol is ascribed to the V–OR stretching frequency. The mass spectrum for complex **13** presents peaks at *m*/*z* 649, 546, 443, and 273, which are assigned to $V_2O_2[OC(CH_3)_2CH_2OCH_3]_5$, $V_2O_2[OC(CH_3)_2CH_2OCH_3]_4$, $V_2O_2[OC(CH_3)_2CH_2O$-$CH_3]_3$, and $VO[OC(CH_3)_2CH_2OCH_3]_2$ moieties, respectively. The intensities of the bimetallic fragments are below 0.1% and the base fragment is $VO[OC(CH_3)_2CH_2OCH_3]_2$. The observation of bimetallic fragments suggested the existence of a dimer or oligomer with respect to disproportionation reactions in the gas phase. The cryoscopic measurements give a molecular weight of 362, which corresponds to the monomeric structure. In the literature, the cryoscopic measurement performed by Lachowicz and Thiele suggested that oxovanadium alkoxides with highly hindered ligands (R = ^{t}Bu, ^{t}Am) are monomeric, while those with primary or secondary groups (R = Et, ^{n}Pr, ^{n}Bu, ^{i}Bu) are dimeric or oligomeric.[27]

^{51}V-NMR spectroscopy affords valuable information on oxovanadium(V) trisalkoxides with respect to the exchange processes between monomers and oligomers since these compounds are usually liquids and their solid state structures are not known (Table 2.10). Only a few oxovanadium trisalkoxides have been structurally characterized. The coordination geometry about the vanadium atom can be described as an octahedron in $[VO(OCH_3)_3]_\infty$[33,34] or a trigonal-bipyramid in $[VO(OCH_2CH_2Cl)_3]_2$[11] and $[VO(cyclo\text{-}C_5H_9O)_3]_2$,[30] or very exceptionally, a tetrahedron in [VO(O^{t}Bu)$_3$].[34] In accordance with ^{51}V-NMR data, oxovanadium alkoxides usually form dimers and/or oligomers in solution. The presence of associated species depends on temperature, solvent, concentration, type and size of the R group.[10,24] The ^{51}V-NMR signal of $[VO(OR)_3]$ compounds usually shifts upfield with increase of electronegativity and steric hindrance of the R groups. The more bulky R group leads to stronger shielding of the vanadium nucleus. As shown in Table 2.10, the shielding of the vanadium nucleus increases in the order $[VO(OMe)_3] < [VO(OEt)_3] < [VO(O^iPr)_3] < [VO(O^tBu)_3]$. In the case of ether-functionalized alkoxides, this trend is well reproduced: the main ^{51}V-NMR signal of **13** (–647 ppm) appears 70 ppm upfield from that of $[VO\{OCH(CH_3)CH_2OCH_3\}_3]$[13]

(–575 ppm), and is comparable to those of [VO(O^iPr)$_3$] (–634.5 ppm for low concentration, –627.7 ppm for high concentration), [VO(O^tBu)$_3$] (–681.4 or –672.4 ppm), and [VO(O^tAm)$_3$] (–683.7 ppm). This result is reasonable because the $CH_3OCH_2C(CH_3)_2OH$ ligand is a tertiary alcohol.

Table 2.10. ^{51}V-NMR Chemical Shifts and Oligomerization Shifts Δδ for [VO(OR)$_3$].

R	$\delta(^{51}V)_{low}$[a] ppm	$\delta(^{51}V)_{high}$[a] ppm	Δδ[b] ppm L mol^{-1}	concn. range mmol L^{-1}	ref.
Me	–598.2	–547.5	99	12–520	11
Et	–605.4	–573.0	57	19–770	11
CH_2CH_2Cl	–608.6	–585.8	54	18–310	11
CH_2CCl_3	–628	[c]	[c]	100	11
CH_2CH_2F	–595	[c]	[c]	100	11
^{n}Pr	–603.7	–587.2	33	12–390	11
^{i}Pr	–634.5	–627.7	13	10–480	11
^{s}Bu	–600	[c]	[c]	100	11
^{i}Bu	[c]	–597[d]	[c]	[c]	29
^{t}Bu	–681.4	–681.0	1	0.5–460	11
^{t}Bu	[c]	–672.4[d]	[c]	[c]	34
^{t}Am	[c]	–683.7[e]	[c]	[c]	116
cyclo-C_5H_9	–623	–616	71	1–100	30
$CH(CH_3)CH_2OCH_3$		–574.8[e]	<1	[c]	13
$C(CH_3)_2CH_2OCH_3$ (**13**)	[c]	–647[d]	[c]	[c]	this work

[a] Relative to $VOCl_3$. The first entry is for low concentration; the second is for high concentration. The spectra were recorded in pentane, unless noted otherwise.
[b] δ(high concn.) – δ(low concn.), determined at room temperature for the concentration range indicated and extrapolated for an overall concentration gradient of 1 mol L^{-1}.
[c] Not determined.
[d] Solution in $CDCl_3$.
[e] Pure sample.

Based on the structural similarity between the ligands $CH_3OCH_2C(CH_3)_2OH$ and ^{t}BuOH, it can be assumed that complex **13** exists as monomer in solution. Thus, the signal at –647 ppm can be reasonably assigned to monomeric [VO{$OC(CH_3)_2CH_2OCH_3$}$_3$], while the two minor low-field signals at –584 and –595 ppm may correspond to two different oligomers.

Generally, $\Delta\delta(^{51}V)$ for oxovanadium alkoxides containing small R groups ($\Delta(\delta^{51}V)$ = 99 ppm L mol^{-1} for [VO(OCH_3)$_3$]$_n$) is higher than for those with bulky R ligands, which are less able to associate ($\Delta\delta(^{51}V)$ = 33, 13, and 1 ppm L mol^{-1} for [VO(O^nPr)$_3$], [VO(O^iPr)$_3$], and [VO(O^tBu)$_3$], respectively). The chemical shift difference $\Delta\delta(^{51}V)$ between the pure sample

and the most diluted one for $[VO\{OCH(CH_3)CH_2OCH_3\}_3]$ in the parent alcohol was less than 1 ppm, which demonstrated the absence of a second species during the course of the dilution. Though concentration dependence of the chemical shift of **13** was not carried out, it is reasonable to infer that monomeric $[VO\{OC(CH_3)_2CCH_2OCH_3\}_3]$ exists as the predominant component in solution. The significantly narrower half-width of complex **13** (18 Hz) compared with $[VO\{OCH(CH_3)CH_2OCH_3\}_3]$ (146 Hz) is another potent evidence for this view. The broadening of the half-width can be attributed to oligomerization or dimerization, which leads to an increase in molecular size and a decrease in local symmetry.[13,115] Both effects increase the relaxation rate *via* the molecular correlation time and the field gradient and hence the line width. The two minor signals at –584 (<1%) and –595 (<1%) ppm with broader half widths than the main signal are ascribed to a very small amount of dimeric and/or oligomeric species.

2.3 Oxovanadium(IV) Complexes

2.3.1 An Oxovanadum(IV) Dichloride with Benzophenone as Ligand

The vanadium chemistry of glycol and ditertiary glycols has been developed in the context of interaction of vanadates with phosphatases.[11,20,40,43] Selective cleavage of ditertiary glycols under mild conditions has been performed with $VO(acac)_2$ as catalyst.[117] In addition, the species derived from vanadium and catechols have attracted the attention of solution and structural chemists.[118] Despite of the reaction diversity of vanadium with diols, the reaction between $VOCl_3$ and tetraphenyl glycol has been surprisingly unexplored. Different from the reaction of $VOCl_3$ with $Me_3SiOCH_2CH_2OSiMe_3$,[20] $HOC(CH_3)_2C(CH_3)_2OH$,[40] and those reported by Rehder,[11] the C–C bond was cleaved and vanadium was reduced to afford $[VOCl_2(O{=}CPh_2)_2]$ (Scheme 2.9).

Treatment of $HOC(C_6H_5)_2C(C_6H_5)_2OH$ with 1 equiv of $VOCl_3$ led to a dark green mixture immediately, from which dark green crystals of $[VOCl_2(O{=}CPh_2)_2]$ (**14**) were isolated. Besides $[VOCl_2(O{=}CPh_2)_2]$, a gray green powder was obtained. This material is insoluble in hydrocarbons and dichloromethane, however, it is readily soluble in acetone, THF or methanol. Based on these properties and the reaction stoichiometry, it was ascribed to $VOCl_2$. Complex **14** was also prepared by reaction of $[VOCl_2(THF)_2]$ with 2 equiv of benzophenone in CH_2Cl_2. This complex is green crystals with melting point of 157 °C. It readily dissolves in CH_2Cl_2 and THF but is only sparingly soluble in toluene and pentane. The vibrations arising from V=O and V–Cl were found at 1016 and 368 cm^{-1}, respectively. Mass spectrometry gave

the fragment corresponding the ligand $OCPh_2$. Fig. 2.13 presents the molecular structure for **14**, selected bond lengths and bond angles are listed in Table 2.11.

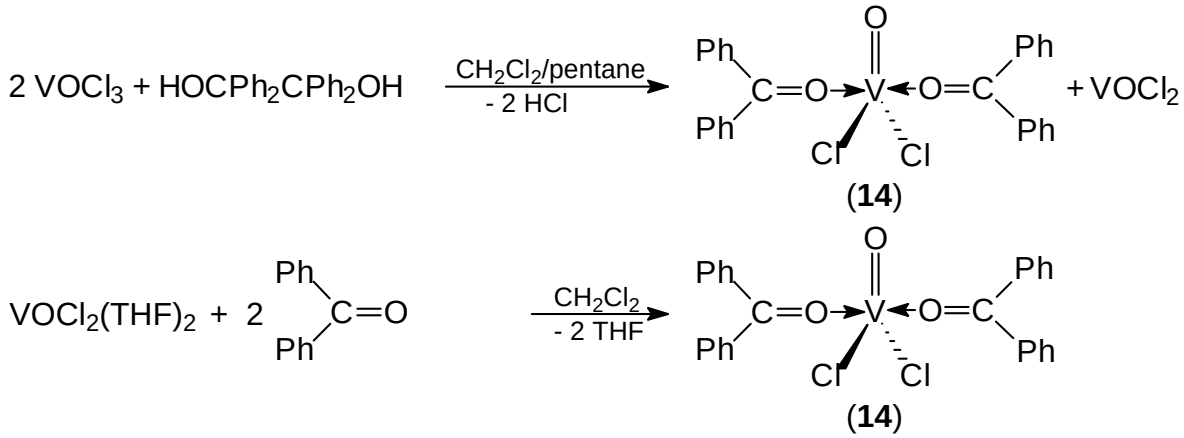

Scheme 2.9. Preparation of ketone coordinated oxovanadium(IV) dichloride **14**.

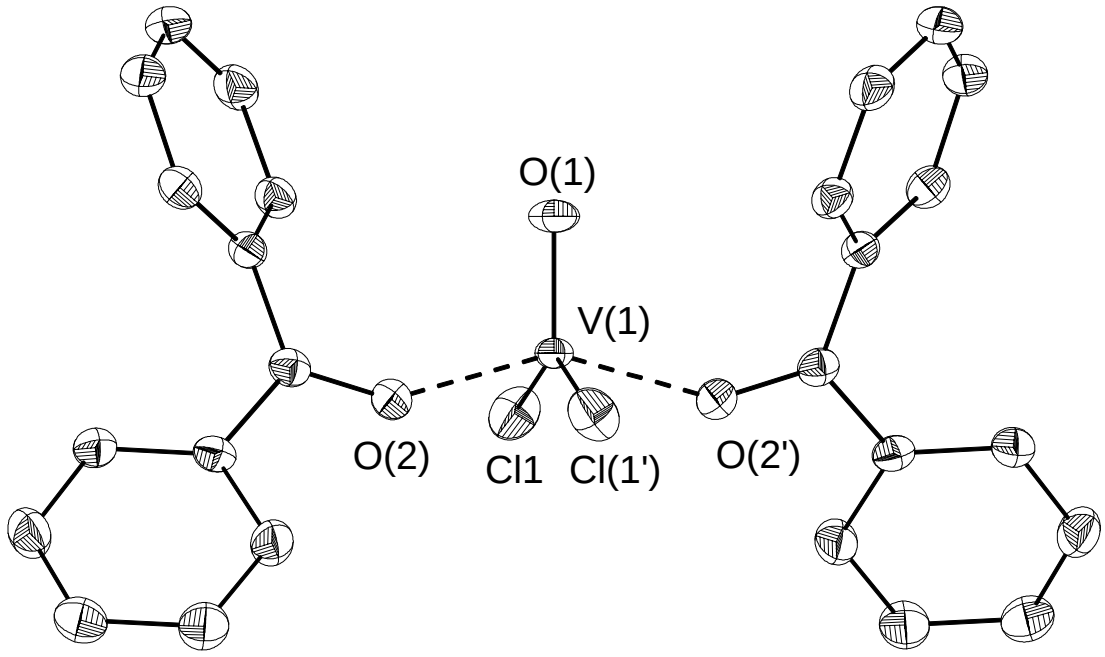

Fig. 2.13. A view of molecular structure of **14**. Thermal ellipsoids are drawn at 50% probability level. Hydrogen atoms are omitted for clarity. Symmetry transformations used to generate equivalent atoms: ' –x, y, –z+1/2.

Table 2.11. Selected bond lengths (Å) and bond angles (°) for complex **14**.

V(1)–O(1)	1.572(4)	V(1)–O(2)	1.999(3)
V(1)–Cl(1)	2.3105(11)		
O(1)–V(1)–Cl(1)	107.53(3)	O(1)–V(1)–O(2)	105.28(8)
O(2)–V(1)–Cl(1)	86.34(9)	O(2)–V(1)–Cl(1')	84.55(9)
O(2)–V(1)–O(2')	149.43(16)	Cl(1)–V(1)–Cl(1')	144.93(7)

Complex **14** crystallizes in monoclinic system, space group *C*2/*c*. The vanadium atom in **14** is in a square pyramidal environment ($\tau = 0.08$) with the terminal oxo group in the apex. Two

chlorine atoms and the benzophenone oxygen atoms are situated in *trans*-orientation in the basal plane. The 2-fold axis goes through the V=O bond and bisects the Cl(1)–V(1)–Cl(1') and O(2)–V(1)–O(2') angles. The Cl(1)–V(1)–Cl(1') angle of 144.93(7) °is comparable to that of 146.3(1) in $[VOCl_2(O=PPh_3)_2]$,[114a] while about 12° smaller than that in $[VOCl_2(O=PPh_3)_2]\cdot CH_2Cl_2$. The V=O bond distance of 1.572(4) Å is well comparable to that of 1.575(3) Å in $[VOCl_2(O=PPh_3)_2]\cdot CH_2Cl_2$. The V–Cl bond distance of 2.3105(11) Å is consistent with the average V–Cl bond distance of 2.308 Å in $[VOCl_2(O=PPh_3)_2]$.[114a] The V–O(2) bond length of 1.999(3) Å is good accordance with the corresponding average bond length of 1.994 Å in $[VOCl_2(O=PPh_3)_2]$.[114a]

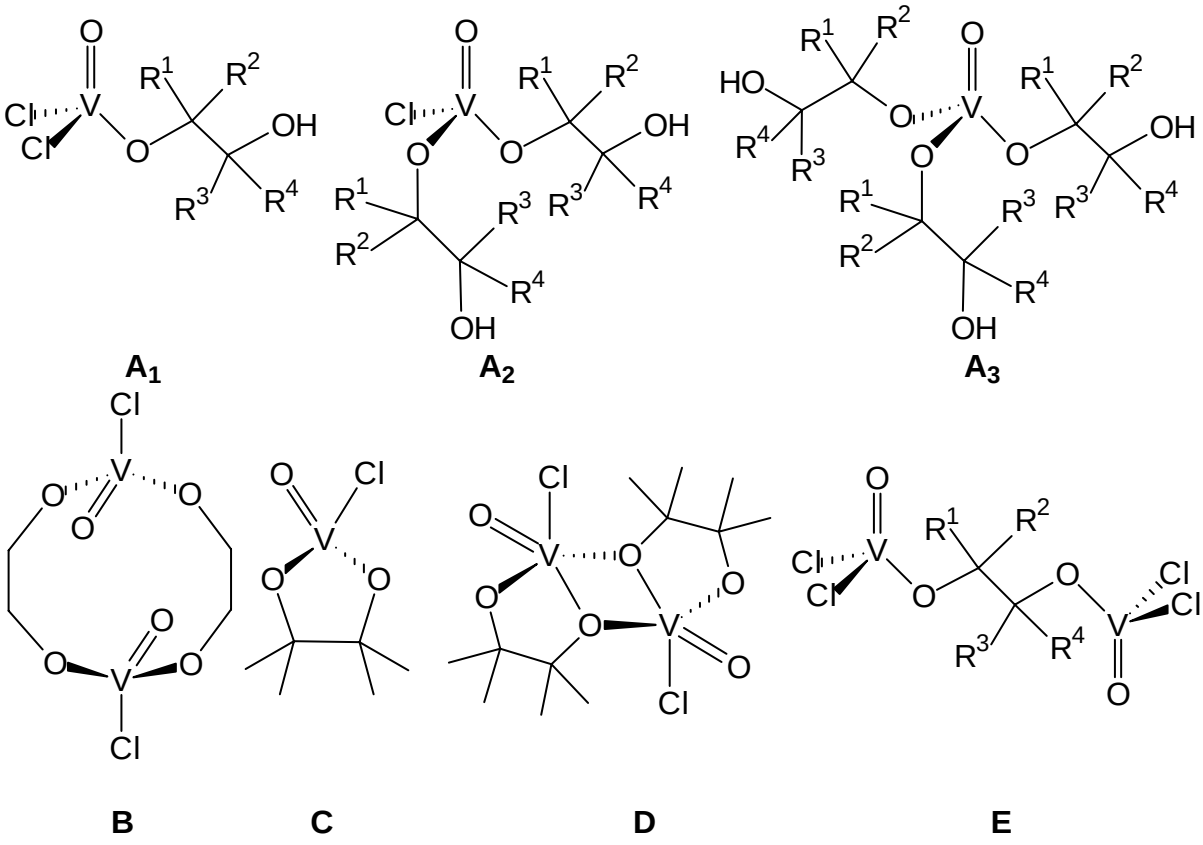

Scheme 2.10. Structural diversity of complexes derived from reaction of $VOCl_3$ with α-diols.[11,20,40]

As is shown in Scheme 2.10, the coordination pattern between $VOCl_3$ and α-diols is rather complex, depending on the reaction conditions, stoichiometry, and the nature of the diol, five possible compounds may form as shown in Scheme 2.10. The initial aim for the reaction of $VOCl_3$ with ditertiary glycol was to synthesize complexes in the form of B or D, where similar structures have been characterized by X-ray diffraction by Crans.[20,40] Thus, the substituent on the α-carbon dominates the reaction mode drastically and might be a key factor for different products.

2.3.2 An Alkoxyalkoxo Chloro Oxovanadium(IV) Complex

Synthesis and Spectroscopic Characterization

$[VOCl(OC(CH_3)_2CH_2OCH_3)]_2$ (**15**) was prepared either by decomposition reaction from the corresponding vanadium(V) complex **4**, or more readily by reaction of $VOCl_3$ with 3 equiv of the corresponding alcohol in CH_2Cl_2, followed by decomposition in the presence of the UV radiation (Scheme 2.11). For the first the entry, the Cl_2 evolved during the course of the decomposition was passed through a starch/KI solution and turned the solution dark blue overnight.

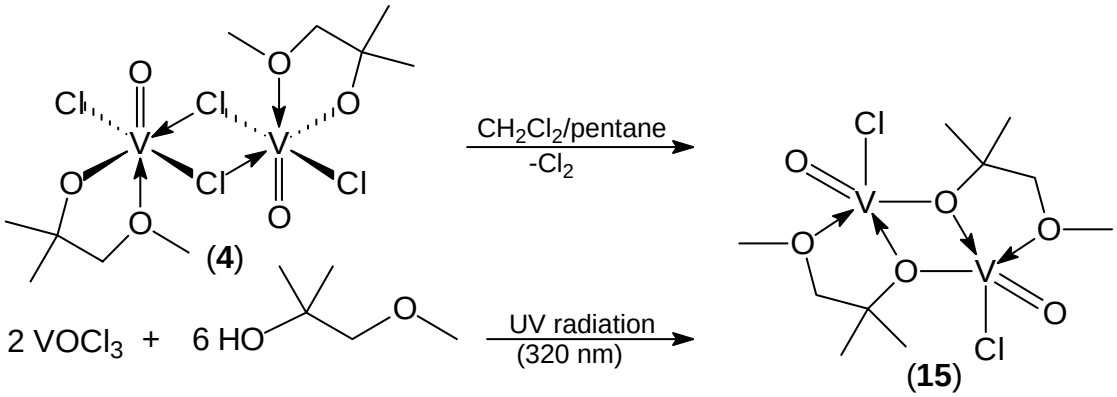

Scheme 2.11. Preparation of alkoxyalkoxo chloro oxovanadium(IV) complex (**15**).

Correlating well with the oxidation state, complex **15** is dark blue, both in the solid state and in solution. The crystals melt at 90 °C. It is insoluble in pentane, slightly soluble in toluene, and readily soluble in CH_2Cl_2 and polar solvents such as THF as blue solution. At room temperature a $HOC(CH_3)_2CH_2OCH_3$ solution of **15** was stable without substitution of the chloro ligand through alkoxylation. However, liberation of HCl was detected under reflux, indicating the occurrence of substitution reaction. The resulting viscous oil was dark blue probably in accordance with $[VO\{O(CH_3)_2CH_2OCH_3\}_2]_n$.

In the IR spectrum the intensive and sharp band at 1000 cm^{-1} is attributed to the V=O stretching frequency. The band at 682 cm^{-1} is assigned to V–OR vibration, while the peak at 390 cm^{-1} is due to the V–Cl stretching frequency. The molecular ion of **15** is detected in mass spectrometry indicating that it is much more stable than the pentavalent derivative **4**. Mass spectrometric data exhibit a signal at an *m/z* of 410 corresponding to the dimeric feature of the complex. The ESR spectrum of complex **15** in THF at 20 °C consists of eight principal lines (^{51}V, *I = 7/2*). The g_i and A_i are 1.9708 and 110 G, respectively, and are consistent with the values found for $[VOCl(thffo)]_2$,[96] which indicates the interaction between the metal centers is negligible.

X-ray Crystallographic Study of **15**

Complex **15** crystallizes in triclinic space group $P\bar{1}$. Two crystallographically independent molecules were found in the unit cell. The molecular structures are presented in Fig. 2.14. Selected bond lengths and bond angles are listed in Table 2.12.

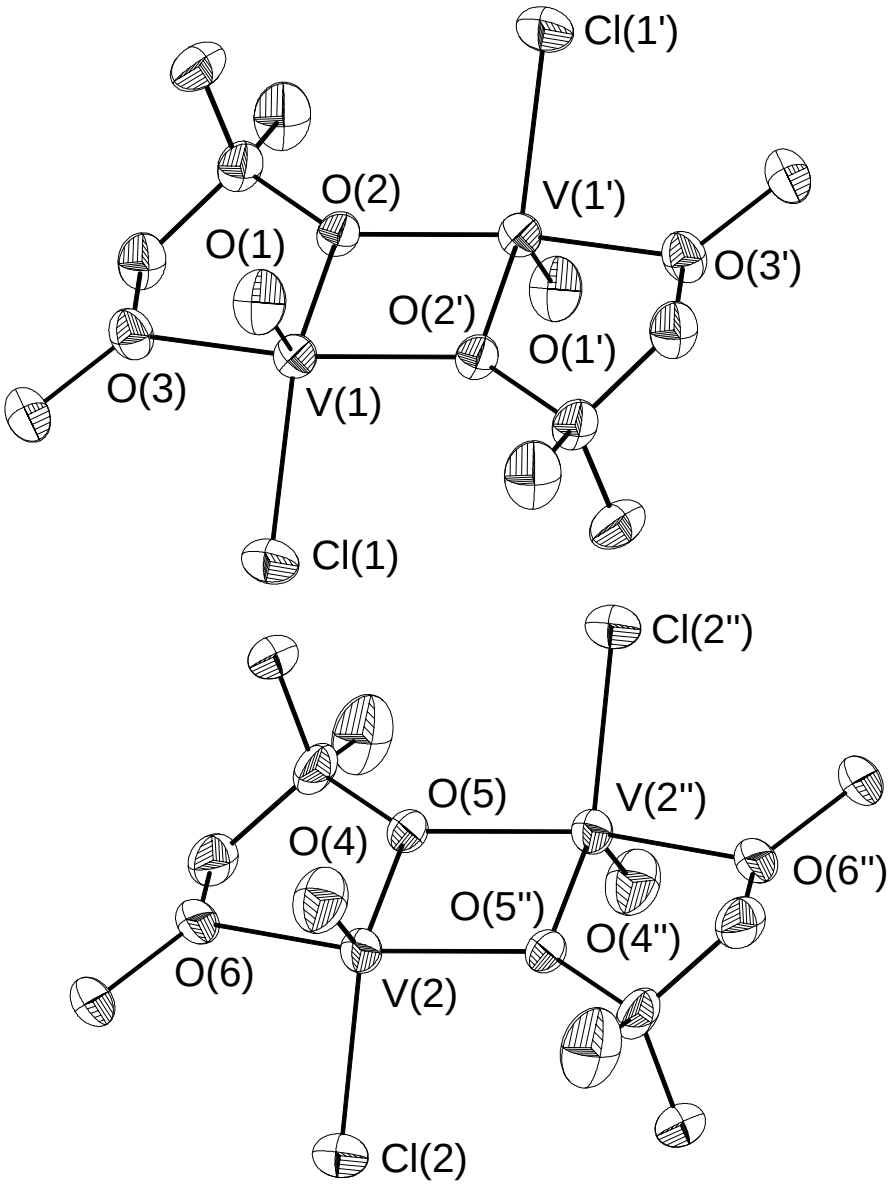

Fig. 2.14. Molecular structures of **15**. Thermal ellipsoids are drawn at 50% probability level. Hydrogen atoms are omitted for clarity. Symmetry transformations used to generate equivalent atoms: ' –x+2, –y, –z; '' –x+1, –y–1, –z+1.

Both molecules are dinuclear with the two independent $[VOCl\{OC(CH_3)_2CH_2OCH_3\}]$ moieties jointed by bridging alkoxide oxygens and symmetrical about a crystallographic inversion center. Thus, the oxo groups, the chloro ligands, and the alkoxyalkoxide ligands are arranged in an *anti*-orientation. A complex with similar arrangement of the ligands is found for $[VOCl\{OC(CH_3)_2C(CH_3)_2O\}]_2$,[40] while *syn*-oriented oxo groups are found for

$[VOCl\{OCH(CH_3)CH_2OCH_3\}]_2$, [119] $[VOCl\{OCH_2(cyclo\text{-}C_4H_7O)\}]_2$, [96] and oxovanadium pyrazolylcyclohexanolate.[45] The dinuclear molecules adopt a chair-like configuration. The vanadium atom in **15** is in a distorted square-pyramidal array (τ = 0.22 and 0.36 for V(1) and V(2), respectively) and the vanadium atoms deviate from the basal planes by 0.6233 Å for V(1) and 0.6301 Å for V(2). The bond geometries between V, Cl, and O are close to those in $[VOCl\{OCH(CH_3)CH_2OCH_3\}]_2$ and $[VOCl\{OCH_2(cyclo\text{-}C_4H_7O)\}]_2$. The distances of the two pairs of V–O in the V–O–V–O parallelogram are slightly different (1.954(2) Å, 1.978(2) Å for **15a**; 1.950(2) Å, 1.984(2) Å for **15b**). The V...V distances are 3.0944(10) and 3.1022(12) Å for **15a** and **15b**, respectively, which are slightly longer than that of 3.070(1) Å found in complex $[VOCl\{OCH_2(cyclo\text{-}C_4H_7O)\}]_2$ [96] and that of 3.084(3) Å in complex $[VOCl\{OC(CH_3)CH_2OCH_3\}]_2$ [119] and exclude V–V bonding interaction.

Table 2.12. Selected interatomic distances (Å) and bond angles (°) for **15**.

V(1)–O(1)	1.593(3)	V(2)–O(4)	1.607(3)
V(1)–O(2)	1.954(2)	V(2)–O(5)	1.950(2)
V(1)–O(2')	1.978(2)	V(2)–O(5")	1.984(2)
V(1)–O(3)	2.075(2)	V(2)–O(6)	2.073(2)
V(1)–Cl(1)	2.2849(11)	V(2)–Cl(2)	2.2761(11)
V(1)...V(1')	3.0944(10)	V(2)...V(2")	3.1022(12)
O(1)–V(1)–O(2)	114.24(13)	O(4)–V(2)–O(5)	117.01(15)
O(1)–V(1)–O(2')	105.11(12)	O(4)–V(2)–O(5")	103.65(13)
O(2)–V(1)–O(2')	76.17(10)	O(5)–V(2)–O(5")	75.93(10)
O(1)–V(1)–O(3)	100.67(12)	O(4)–V(2)–O(6)	97.97(14)
O(2)–V(1)–O(3)	77.82(9)	O(5)–V(2)–O(6)	78.48(10)
O(2')–V(1)–O(3)	149.05(10)	O(5")–V(2)–O(6)	151.98(11)
O(1)–V(1)–Cl(1)	109.96(11)	O(4)–V(2)–Cl(2)	112.26(13)
O(2)–V(1)–Cl(1)	135.65(8)	O(5)–V(2)–Cl(2)	130.58(8)
O(2')–V(1)–Cl(1)	96.01(7)	O(5")–V(2)–Cl(2)	96.54(7)
O(3)–V(1)–Cl(1)	90.95(8)	O(6)–V(2)–Cl(2)	91.45(8)
V(1)–O(2)–V(1')	103.83(10)	V(2)–O(5)–V(2")	104.07(10)

2.4 Acetonitrile Solvates of Oxovanadium Complexes

2.4.1 Syntheses and Spectroscopic Characterization

Neutral CH_3CN containing oxovanadium(V) complex $[VOCl_2(OCH_2CH_2OCH_3)(CH_3CN)]$ (**16**) and oxovanadium(IV) complexes $[VOCl_2(HOCH_2CH_2OR)(CH_3CN)]$ (R = Me, (**17**); Et,

(**18**)), and [$VOCl_2${$HOCH_2$(*cyclo*-C_4H_7O)}(CH_3CN)] (**19**) have been synthesized (Scheme 2.12) and structurally characterized. The reaction of $VOCl_3$ and 1 equiv of $HOCH_2CH_2OCH_3$ in pentane followed by treatment with the same amount of CH_3CN afforded [$VOCl_2(OCH_2CH_2OCH_3)(CH_3CN)$] (**16**) as red crystalline solid. It is not soluble in pentane and toluene while it is soluble in CH_2Cl_2 and CH_3CN. Complex **16** melts at 57 °C.

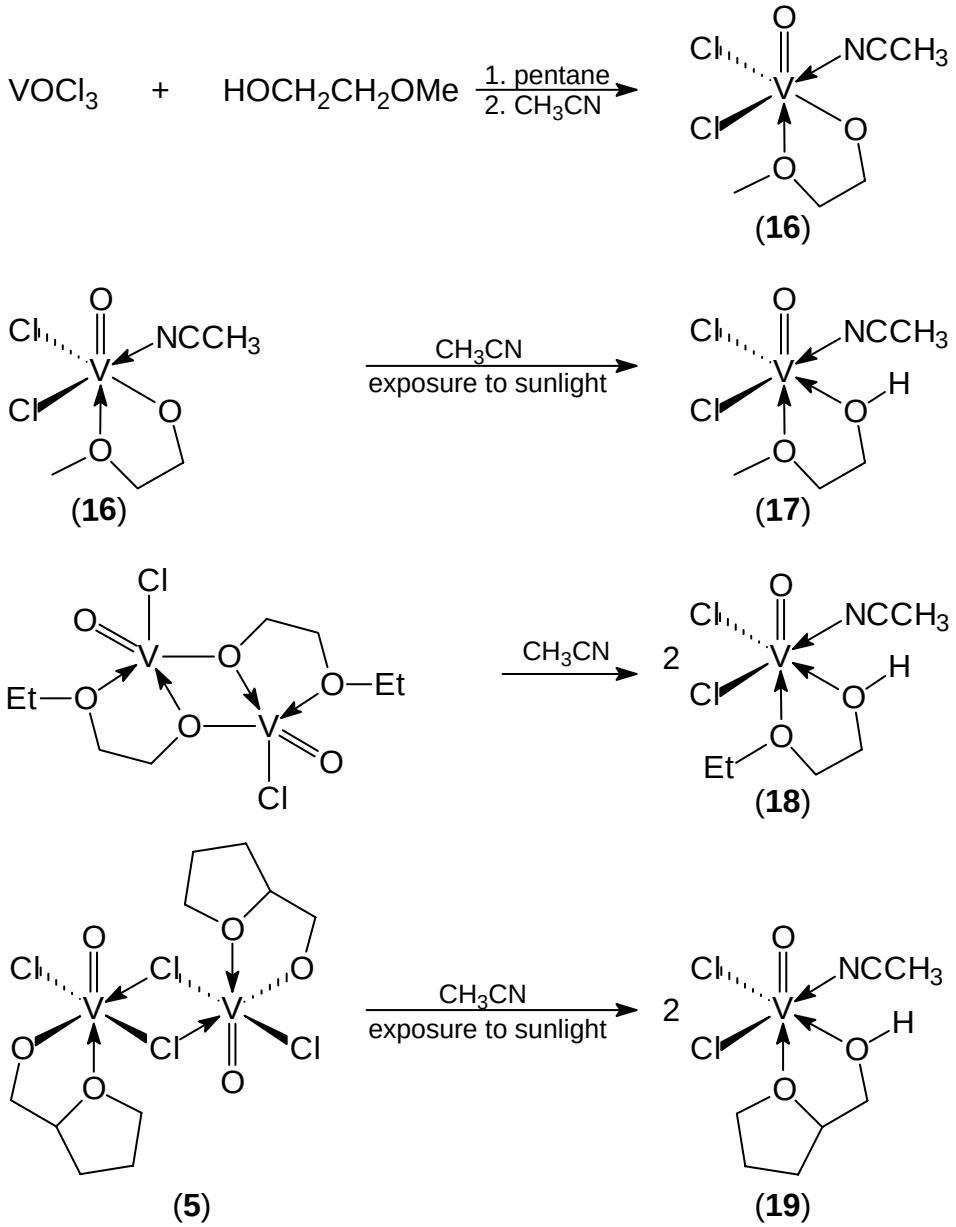

Scheme 2.12. Acetonitrile coordinated oxovanadium complexes **16**–**19**.

The ^{1}H-NMR of **16** in $CDCl_3$ displays four signals at 5.57, 3.90, 3.50, and 2.20 ppm. The three signals at lower field correspond to VOCH_2, CH_2OCH$_3$, and CH$_2$OCH_3 in the alcoholate moiety. The signal arising from CH_3 in CH_3CN centers at 2.20 ppm and is dramatically broadened owing to unresolved coupling to ^{14}N. The mass spectrum gives a fragment with an *m*/*z* value of 50 as base peak corresponding to CH_3Cl, which has also been found by matrix

isolation on heating $[VOCl_2(OCH_3)]$.[18] Single crystals of **16** suitable for X-ray crystal structure determination were obtained from a CH_3CN solution at –30 °C. The IR spectrum in Nujol mull gives two sharp and strong absorption bands at 2319 and 2292 cm^{-1}, which are due to the C≡N vibrations. The sharp and strong band at 1027 cm^{-1} is designated to V=O stretching frequency, while the V=O absorption bands for $[VOCl_3(CH_3CN)]$ and $[VOCl_3(CH_3CN)_2]$ display at 1016 and 992 cm^{-1}, respectively.[120] The absorption at 614 and 463 cm^{-1} are attributed to the V–OR and V–Cl vibrations, respectively.

Dissolution of **16** in CH_3CN, followed by exposure to sunlight under nitrogen for several days gave rise to a blue solution, from which blue crystals of $[VOCl_2(HOCH_2CH_2OCH_3)(CH_3CN)]$ (**17**) separated on storage at 0 °C for several weeks. Complex **17** was also obtained by exposure of an CH_3CN solution of $[VOCl_2(OCH_2CH_2OCH_3)]_2$[38] to sunlight, wherein $[VOCl_2(OCH_2CH_2OCH_3)]_2$ was prepared by reaction of $VOCl_3$ with $CH_3OCH_2CH_2OLi$.

Light blue powder of $[VOCl(OCH_2CH_2OC_2H_5)]_2$ obtained from the decomposition of the corresponding vanadium(V) complex, was dissolved in CH_3CN to result in a blue solution, from which $[VOCl_2(HOCH_2CH_2OC_2H_5)(CH_3CN)]$ (**18**) separated at –30 °C. When **18** is dissolved in CH_3CN and all solvent is removed in vacuum $[VOCl(OCH_2CH_2OC_2H_5)]_2$ is obtained. However, drastically exothermic reaction took place when HCl was bubbled through an CH_3CN solution of $[VOCl_2(OCH_2CH_2OC_2H_5)]_2$. The consequent vanadium(V) species in the dark red solution was stable and no appreciable color change was observed on exposure to UV radiation for over two weeks. This indicates the formation of $[VOCl_3(OCH_2CH_2OC_2H_5)]^-$, a much more reduction resistant anionic species than the neutral $[VOCl_2(OCH_2CH_2OC_2H_5)]_2$, which is reduced overnight on exposure to UV radiation. $[VOCl_2\{HOCH_2(cyclo\text{-}C_4H_7O)\}]$ (**19**) was synthesized analogously to **17** and **18**. Dissolution of **5** in CH_3CN, followed by exposure to sunlight for several weeks resulted in a blue solution, from which blue crystals of **19** suitable for X-ray diffraction were isolated on cooling to 0 °C.

Complexes **17**–**19** melt at 125, 132, and 122 °C, respectively. The melting points are much higher than those of complexes **6**–**9**, and **16**. The ^{1}H-NMR spectrum of complex **17** in CD_3CN exhibits only broad signals as this complex is paramagnetic. Nevertheless, resonances that are attributed to the HOCH_2, CH_2OMe, CH_3CN, and OCH_3 protons are observed at 4.50, 3.02, 1.74, and 0.73 ppm, respectively. IR spectra of complexes **17**–**19** in Nujol mull display a broad absorption band at 3093, 3134, and 3088 cm^{-1} arising from O–H vibration. Two signals at around 2320 and 2290 cm^{-1} that are attributed to the C≡N stretching vibrations are observed for all complexes. The V=O stretching frequency is observed at 1026, 1025, 1028 cm^{-1} for **17**–**19**, respectively. These values are consistent with those for the

oxovanadium(V) complexes **6–9**. The V–Cl stretching vibrations of complexes **17–19** display at 328, 335, and 324 cm^{-1}, respectively, which are at significantly lower compared with those of complexes **6–9**, and **16**. Mass spectra data for complexes **17–19** do not exhibit the molecular ions but $[VOCl(OR)]_2^+$. ESR spectra of **17** and **18** in CH_3CN, **19** in THF present the typical eight lines for mononuclear VO^{2+} species. The g_i values are 1.97, 1.98, and 1.97, while the A_i values are 109, 107, and 111 G, respectively.

The reaction between $VOCl_3$ and ROH has been found to depend significantly on the solvent.[38,39,119] $[VOCl_n(OR)_{3-n}]_x$ are formed in CCl_4, whereas $[VOCl_n(OR)_{3-n}(CH_3CN)_2]$ and anionic alkoxy chloro complexes are formed in CH_3CN.[121] Pentavalent vanadium compounds are generally considered to be one-electron oxidants, which utilize the V(V)/V(IV) couple. The species formed from V_2O_5 dissolved in hydrochloric acid are moderately strong oxidizing agents, which is confirmed by the evolution of chlorine and production of vanadium(IV) derivatives.[122,123] Decomposition of dimeric chloride bridged $[VOCl_2\{OC(CH_3)_2CH_2O\text{-}CH_3\}]_2$ (**4**) and $[VOCl_2\{OCH_2$*cyclo*$\text{-}(C_4H_7O)\}]_2$ (**5**) in the solid state or in nonpolar solvents gave $[VOCl\{OC(CH_3)_2CH_2OCH_3\}]_2$ (**15**) and $[VOCl\{OCH_2($*cyclo*$\text{-}C_4H_7O)\}]_2$, respectively, while the decomposition of $[VOCl\{OCH_2($*cyclo*$\text{-}C_4H_7O)\}_2]$ (**12**) in the solid state or in nonpolar solvents also gave $[VOCl\{OCH_2($*cyclo*$\text{-}C_4H_7O)\}]_2$. This indicates that chloro oxovanadium alkoxides can oxidize the chloro ligand as well as alkoxide ligand they hold.[14] The oxidation of the chloro ligand by the pentavalent atom has been proven for decomposition of complex **4** to give complex **15**.

With the clarity of this fact, the formation of **17–19** is easier to understand: pentavalent vanadium was reduced *via* one-electron oxidation of the chloro ligand, the monomeric complex was achieved by CH_3CN coordination. Complexes **17–19** are insoluble in pentane and toluene, but soluble in CH_2Cl_2 and CH_3CN. They are stable at room temperature under nitrogen. When exposed to air, they turn into blue sticky oils within a few minutes.

2.4.2 X-ray Crystallographic Studies

Molecular structures of **16–19** as well as the dimeric structures formed by intermolecular hydrogen bonds for **17–19** are presented in Fig. 2.16 to 2.24. Selected bond distances and bond angles are listed in Table 2.13 and 2.14. Molecules **16–19** crystallize as racemic mixtures with two molecules of each enantiomer in the unit cell. Molecular structure of complexes **17** and **19b** are shown in the Λ-form, while complexes **18**, and **19a** are shown in the Δ-form.

The vanadium(V) complex **16** crystallizes in orthorhombic space group $P2_12_12_1$, while **17–19** crystallize in monoclinic space group $P2_1/c$. The vanadium atoms are in a distorted octahedral

coordination in **16–19**: consisting of three oxygen atoms, two chlorine atoms, and one CH_3CN. The central vanadium atom deviates from the mean coordination plane O(2)–Cl(1)–Cl(2)–N(1) by 0.215, 0.232, and 0.165 Å for **16**, **17**, and **18**, respectively. For **19**, the vanadium atom, the chloro ligand, and the oxo group are found to be disordered, providing two molecular configurations, marked as **19a** and **19b** (a:b = 69%:31%), respectively. The vanadium atoms deviate from the coordination plane O(2)–N(1)–Cl(1a)–Cl(2a) and N(1)–O(3)–Cl(2b)–Cl(1b) by 0.0807 and 0.0379 Å for **19a** and **19b**, respectively. The sum of angles formed by these four atoms are 356.43°, 356.66°, 356.02°, 354.92°, and 353.99° for **16**, **17**, **18**, **19a**, and **19b**, respectively, defining a distorted plane. For complexes **16–18**, the O(1), O(2), O(3), Cl(2) atoms define an almost perfect plane as evidenced by the sum of the angles around the vanadium centers of 359.39°, 359.73°, 359.80°, for complexes **16**, **17**, and **18**. The vanadium deviates from the mean plane by 0.1175, 0.00694, and 0.0620 Å for **16–18**, respectively.

Table 2.13. Selected bond lengths (Å) and bond angles (°) for **16–18**.

	16	**17**	**18**
V(1)–O(1)	1.5823(18)	1.583(3)	1.6045(11)
V(1)–O(2)	1.7821(17)	2.081(3)	2.0959(11)
V(1)–O(3)	2.3234(16)	2.263(3)	2.2680(11)
V(1)–Cl(1)	2.2952(7)	2.3789(12)	2.3273(5)
V(1)–Cl(2)	2.2985(7)	2.3183(12)	2.3875(4)
O(2)...Cl(1')		3.031	3.048
V(1)–N(1)	2.142(2)	2.119(4)	2.1336(14)
O(1)–V(1)–O(2)	99.03(9)	94.51(14)	93.89(6)
O(2)–V(1)–Cl(1)	91.84(6)	89.83(8)	88.85(3)
O(1)–V(1)–Cl(2)	99.81(7)	103.38(11)	103.77(5)
O(1)–V(1)–O(3)	168.52(9)	167.16(13)	166.52(5)
N(1)–V(1)–Cl(1)	168.91(7)	167.68(10)	166.93(4)
O(2)–V(1)–Cl(2)	160.35(6)	161.53(10)	162.09(4)
O(2)–V(1)–O(3)	76.29(7)	73.16(11)	73.55(4)
Cl(2)–V(1)–O(3)	84.16(5)	88.68(8)	88.59(3)

As expected for **16–18** the bond distances of **16** are significantly different from those of the vanadium(IV) complexes: the $V–O_{alcoholate}$ is 1.7821(17) Å, while the corresponding $V–O_{alcohol}$ distances are 2.081(3), 2.0959(11), 2.043(3), and 2.021(5) Å for **16–19**, respectively. Moreover, the two V–Cl bond lengths in **16** are only slightly different and considerably shortened compared to those without involvement in hydrogen bonds for **17–19**. The V–N

distance of 2.142(2) Å in complex **16** is slightly longer than those of 2.119(4) and 2.1336(14) Å in **17**, **18**, and those between 2.098(2) and 2.124(5) Å in vanadium(V) complexes [$VOCl_3$(N≡CR)] (R = Me, Ph, Bz).[52,53] The V–N bond lengths in **19a** and **19b** are significantly different. The one of 2.193(4) Å in **19a** is rather longer than those in **16**–**18**, while the one in **19b** is of 2.013(6) Å and is considerably shorter than those in **16**–**19a**.

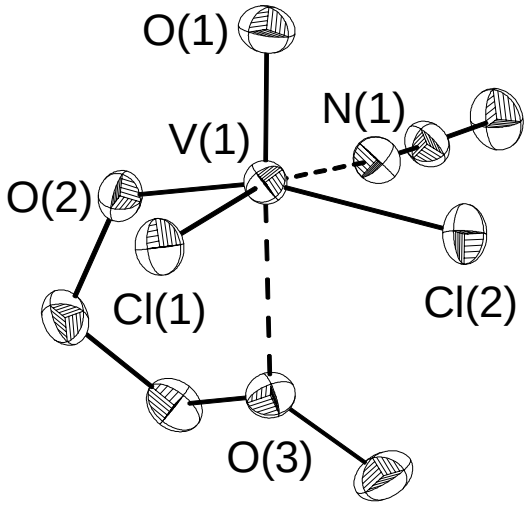

Fig. 2.15. Molecular structure of Λ-form of **16**. Thermal ellipsoids are drawn at 50% probability level. Hydrogen atoms are omitted for clarity.

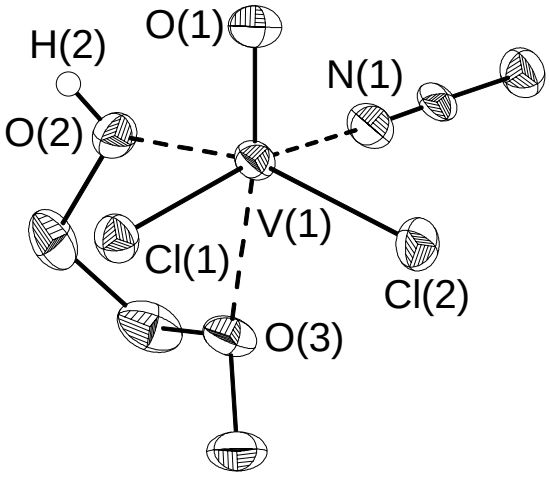

Fig. 2.16. Molecular structure of Λ-form of **17**. Hydrogen atoms are omitted for clarity except for the hydroxy hydrogen.

Intermolecular hydrogen bonding is involved in complexes **17**–**19**. The bonds consist of the alcoholic atom O(2) of one molecule and one chlorine atom of the other enantiomer. The internuclear O(2)…Cl(1') distances are 3.031, 3.048, 3.029, and 3.018 Å for **17**, **18**, **19a**, and **19b**, respectively. The V–Cl bond lengths where Cl is involved in hydrogen bonding is 0.06–0.08 Å longer than for the other Cl, indicating the weakening of the former bond due to H…Cl interaction. The angles of O–H…Cl are nearly linear, being 176.23, 172.82, 175.97, and 175.94°, respectively.

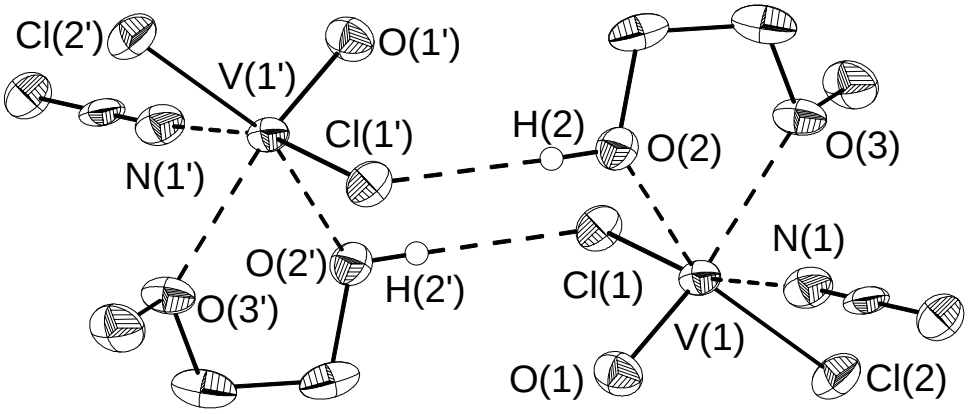

Fig. 2.17. Intermolecular hydrogen bonding between the Δ- and Λ-form of molecules in **17**. Symmetry transformations used to generate equivalent atoms: ' –x, 1–y, –z.

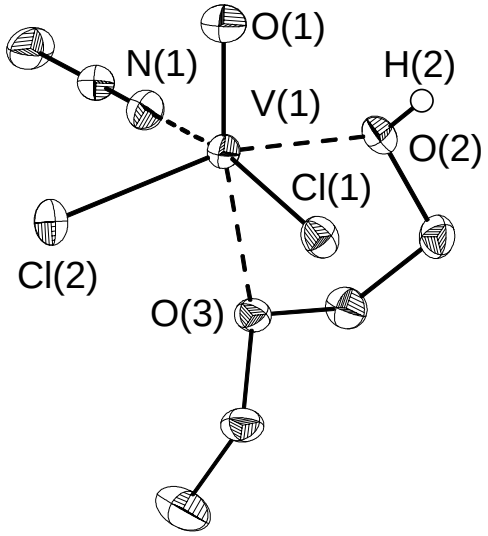

Fig. 2.18. Molecular structure of Δ-form of **18**. Hydrogen atoms are omitted for clarity except for hydroxy hydrogen.

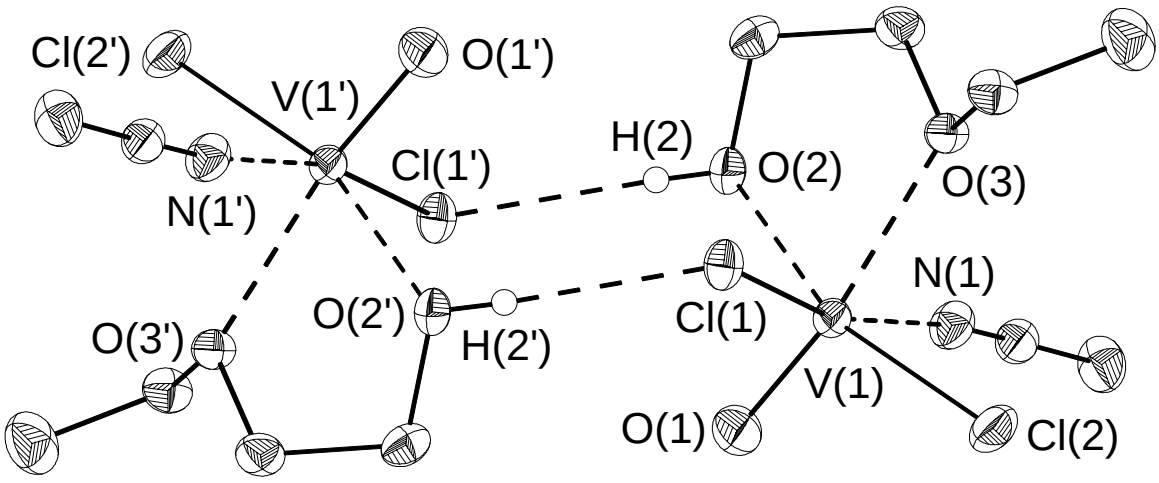

Fig. 2.19. Intermolecular hydrogen bonding between the Δ- and Λ-form of molecules in **18**. Symmetry transformations used to generate equivalent atoms: ' –x+1,–y+1,–z+1.

Table 2.14. Selected interatomic distances (Å) and bond lengths (°) for **19**.

19a		**19b**	
V(1a)–O(1a)	1.586(7)	V(1b)–O(1b)	1.577(13)
V(1a)–N(1)	2.193(4)	V(1b)–N(1)	2.013(6)
V(1a)–Cl(1a)	2.304(3)	V(1b)–Cl(1b)	2.309(7)
V(1a)–O(2)	2.043(3)	V(1b)–O(2)	2.314(5)
V(1a)–O(3)	2.265(3)	V(1b)–O(3)	2.021(5)
V(1a)–Cl(2a)	2.378(5)	V(1b)–Cl(2b)	2.390(12)
O(2)...Cl(2a')	3.029(7)	O(2)...Cl(2b')	3.018(16)
O(1a)–V(1a)–O(3)	167.0(3)	O(1b)–V(1b)–O(2)	168.08(60)
Cl(1a)–V(1a)–Cl(2a)	90.94(19)	Cl(1b)–V(1b)–Cl(2b)	89.4(5)
O(2)–V(1)–Cl(1)	160.26(15)	O(3)–V(1b)–Cl(1b)	158.2(3)
O(2)–V(1)–N(1)	84.36(13)	N(1)–V(1b)–Cl(1b)	84.5(2)
N(1)–V(1a)–Cl(1a)	88.79(12)	N(1)–V(1b)–O(3)	89.1(2)
N(1)–V(1a)–Cl(2a)	164.6(3)	N(1)–V(1b)–Cl(2b)	163.5(5)
O(2)–V(1)–Cl(2)	90.82(19)	O(3)–V(1b)–Cl(2b)	91.0(5)

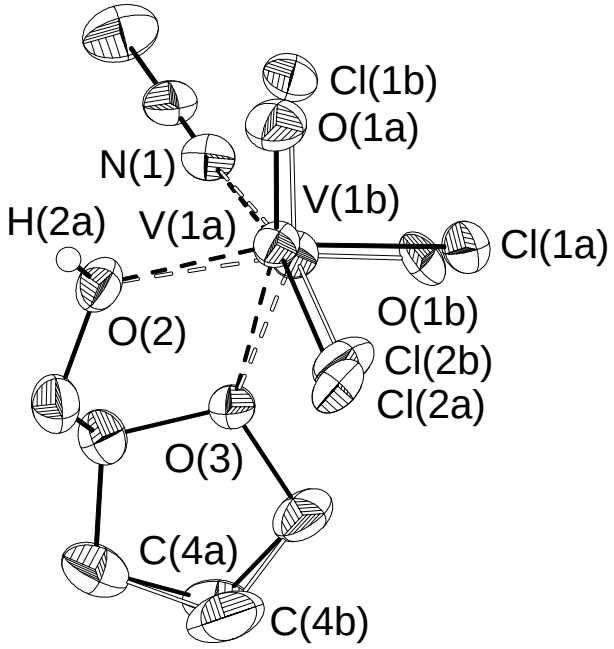

Fig. 2.20. Molecular structure of Λ-form of **19**, the second positions of the disordered atoms are denoted in dashed lines. Hydrogen atoms are omitted for clarity expect for hydroxy hydrogen.

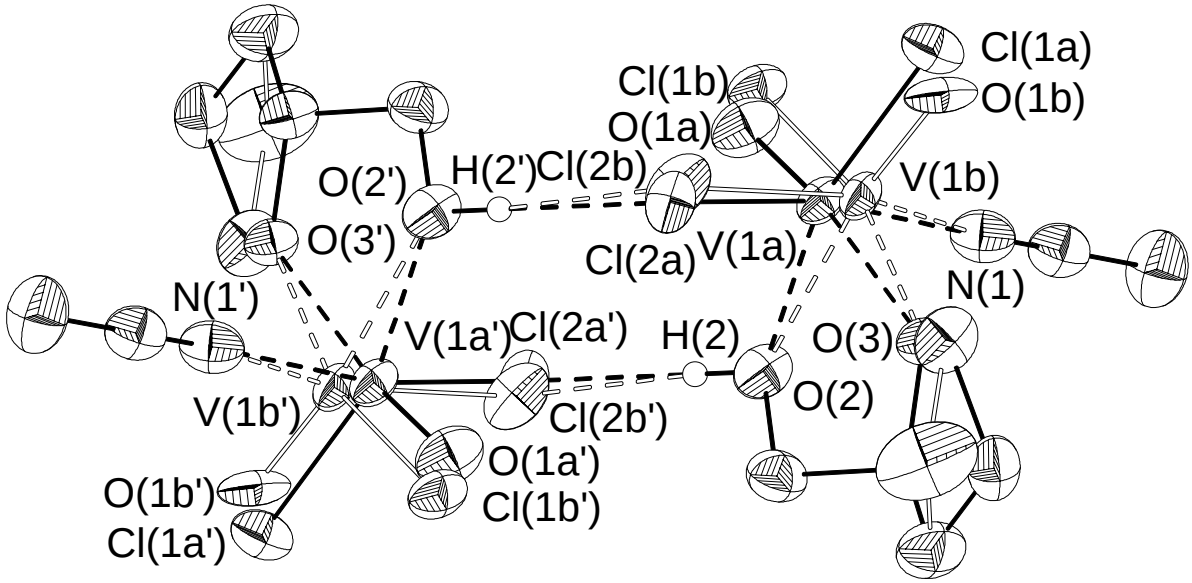

Fig. 2.21. Intermolecular hydrogen bonding between the Λ- and Δ-form of molecules in **19**, the second positions of the disordered atoms are denoted in dashed lines. Symmetry transformations used to generate equivalent atoms: ' 1–x, 1–y, –z.

2.5 Catalytic Studies

2.5.1 Ethylene Polymerization

Homogeneous ethylene polymerization was performed readily in toluene by using $[VOCl_2(OCH_2CH_2OCH_3)]_2$ in combination with either MAO or DEAC as cocatalyst and MTCA as promoter. Mixing catalyst precursor and cocatalyst in toluene resulted in the formation of a clear pink solution showing good activity for polymerization. Selected results of ethylene polymerization are listed in Table 2.15.

Table 2.15. Ethylene polymerization results with $[VOCl_2(OCH_2CH_2OCH_3)]_2$.

Entry	Cocatalyst	$[V]_0$ mmol L^{-1}	[Al]/[V] *n*/*n*	Activity kg PE (mol[V])$^{-1}$ h^{-1} bar^{-1}	M_w kg mol^{-1}	M_n kg mol^{-1}	M_w/M_n
1[a]	MAO	0.2	80	100	954	87	11.0
2[b]	MAO	0.1	100	6	1084	119	9.9
3[b]	MAO	0.02	400	300	1414	168	8.4
4[b]	MAO	0.02	1000	15	1169	155	8.5
5[d]	MAO	0.02	400	3	[c]	[c]	[c]
6[b]	DEAC	0.1	20	320	696	110	6.3
7[b]	DEAC	0.1	100	560	586	60	8.9
8[b][d]	DEAC	0.1	100	360	390	34	11.4

[a] Schlenk tube; *p*(ethylene) = 1 bar, 30 min at 22 °C; solvent: toluene; Al/MTCA = 1:2.5.
[b] Glass autoclave; *p*(ethylene) = 2 bar, 30 min at 30 °C; solvent: toluene; Al/MTCA = 1:1.
[c] Entry 5 contained a substantial amount of insoluble material resulting in very poor data detection.
[d] Precatalyst: $VOCl_3$; Glass autoclave; *p*(ethylene) = 2 bar, 30 min at 30 °C; solvent: toluene; Al/MTCA = 1:1.25.

At atmospheric pressure and room temperature $[VOCl_2(OCH_2CH_2OCH_3)]_2$ shows moderate activity (100 kg PE (mol[V])$^{-1}$ h^{-1} bar^{-1}) for ethylene polymerization with MAO as cocatalyst and MTCA as promoter. In contrast to $VOCl_3$, $[VOCl_2(OCH_2CH_2OCH_3)]_2$ is more efficient and displays an activity of 560 kg PE (mol[V])$^{-1}$ h^{-1} bar^{-1} for ethylene polymerization in combination with DEAC, while $VOCl_3$ shows an activity of 360 kg PE (mol[V])$^{-1}$ h^{-1} bar^{-1} at the same conditions. The best Al/V for MAO was found to be 400 to give the highest activity of 300 kg PE (mol[V])$^{-1}$ h^{-1} bar^{-1}, while with other Al/V ratios, the activities are rather low. As known,[8,38] DEAC was proven to be a more effective cocatalyst than MAO: at a Al/V ratio of 100, the activity of the $[VOCl_2(OCH_2CH_2OCH_3)]_2$/DEAC system is two orders of magnitude higher than that of the $[VOCl_2(OCH_2CH_2OCH_3)]_2$/MAO system (560 and 6 kg PE (mol[V])$^{-1}$ h^{-1} bar^{-1} for DEAC and MAO as cocatalysts, respectively). The activities are enhanced with increasing Al/V ratio in the range between 20 and 100 (entries 6 and 7).

As reported in the literature,[8] one of the problems of vanadium catalyzed polymerization is the fast deactivation due to the reduction of the active species to inactive vanadium(II) species. To overcome this disadvantage, polychloro MTCA capable of continuously oxidizing V(II) to active V(III) was employed during the polymerization. Polymerization with the ratio of DEAC/MTCA 1:1 achieved very good activity for both $[VOCl_2(OCH_2CH_2OCH_3)]_2$ and $VOCl_3$ based catalysis, and the polymerization proceeds vigorously over a period of 30 min. In sharp contrast, while polymerization without addition of MTCA, though with very high initial activities, stopped quickly and gave only negligible polymerization productivities. On the other hand, since MTCA acts only as promoter, the ratio of Al/MTCA 1:1 is high enough to sustain the catalysis. The polymers produced from $[VOCl_2(OCH_2CH_2OCH_3)]_2$ with either MAO or DEAC as cocatalyst have very high M_w values, especially those from $[VOCl_2(OCH_2CH_2OCH_3)]_2$/MAO, showing M_w to be of 10^6 magnitude.

2.5.2 1-Hexene Oligomerization

The 1-hexene oligomerization catalyzed by different vanadates was performed over a period of 24 h in a Schlenk flask with DEAC as cocatalyst at 22 °C. The ratio of V:DEAC:MTCA was 1:100:100. The results of 1-hexene oligomerization are listed in Table 2.16. Under the same conditions the activity is independent from the nuclearity of the precatalyst employed. On the other hand, the performance of the *iso*-propyl derivative stands out from the complexes investigated. Oligomerization rather than polymerization took place since oils were the only isolated products. The molecular mass and polydispersity of the oligomers were determined by using GPC and calibrated against polystyrene standards. The hexene oligomers

show molecular masses around 400 g mol^{-1} and polydispersities around 1.5, but the oligomers obtained by this procedure fall nearly out of the calibrated range of the GPC.

Table 2.16. 1-Hexene oligomerization with vanadium(V) complexes.[a]

Entry	Precatalyst	Yield g
1a	$VOCl_3$	0.34
1b		0.38
2a	$[VOCl_2(OCH_2CH_2OMe)]_2$	0.35
2b		0.34
3a	$[VOCl_2(OCH_2CH_2OEt)]_2$	0.56
3b		0.54
4a	$[VOCl_2(OCH_2CH_2O^iPr)]_2$	3.06
4b		3.51
5a	$[VOCl_2\{OCH_2$*cyclo*$-(C_4H_7O)\}]_2$ (**5**)	0.50
5b		0.41
6a	$[VOCl_2(OCH_2CH_2O^iPr)(THF)]$ (**11**)	0.55
6b		0.55
7a	$[VOCl_2(OCH_2CH_2O^iPr)(THF)]$ (**12**)	0.46
7b		0.47
8a	$[VOCl_2(OCH_2CH_2OPh)]$	0.31
8b		0.42

[a] 20 mL of 1-hexene were employed for each entry.

2.5.3 Styrene Oligomerization and 1-Decene Oligomerization

The catalytic activities of $[VOCl_2(OCH_2CH_2OCH_3)]_2$ and $[VOCl_2(OCH_2CH_2OPh)]$ for the oligomerization of styrene and 1-decene were examined. Oligomerization studies were conducted employing a catalyst prepared by adding the vanadium compound to a toluene solution of MAO as the cocatalyst and MTCA as promotor. Results are listed in Table 2.17 and Table 2.18).

Table 2.17. Oligomerization of styrene with $[VOCl_2(OCH_2CH_2OCH_3)]_2$.[a]

T °C	Yield (%)	M_w g mol^{-1}	M_n g mol^{-1}	M_w/M_n
20	99.6	2900	1200	2.3
40	85.3	3000	1500	2.0
50	71.1	2700	1600	1.7

[a] Reaction conditions: V catalyst/styrene/MAO/MTCA = 1:520:40:40, 20 h; solvent: toluene.

The M_w of the oligostyrene products ranges between 2700 and 3000 with the polydispersity around 2. Temperature dependence for the styrene oligomerization with the dimeric complex

as catalyst was tested. The catalytic activity decreases with rising temperatures and is highest at room temperature for styrene oligomerization. Under the same conditions the activity for 1-decene oligomerization is only 10% of that for styrene oligomerization for the catalyst used.

Table 2.17. Activity (kg (mol [V])$^{-1}$ h^{-1}) of olefin conversions with vanadium(V) compounds.[a]

Precatalyst	Styrene	1-Decene
$[VOCl_2(OCH_2CH_2OCH_3)]_2$	27.7	2.5
$[VOCl_2(OCH_2CH_2OPh)]$	27.9	2.7

[a] Reaction conditions: styrene: 26 mmol, 1-decene: 16 mmol; V catalyst/MAO/MTCA = 1:40:40, 1.5 h at 23 °C; solvent: toluene.

2.5.4 Cyclooctene Epoxidation

The epoxidation reaction of cyclooctene with TBHP in the presence of $VOCl_2(OR)$ was studied. Adding TBHP to a cold CH_2Cl_2 solution of $VOCl_2(OR)$ resulted in a dark red solution, and this color change is attributed to the formation of the red oxoperoxovanadium(V) ion. While fading of the red to light yellow corresponds to the appearance of a $[VO(O_2)_2]^-$ complex.[6b] Adding cyclooctene to this solution and refluxing of the solution over 24 h followed by destruction of excess TBHP and vanadium catalyst and removal of the volatiles gave cyclooctene oxide in 50–71% yield.

3 Experimental Section

3.1 General Remarks

All experimental manipulations were carried out in an oxygen free dry nitrogen atmosphere using standard Schlenk glassware and techniques unless otherwise noted. The handling of air and moisture sensitive materials and the preparation of samples for spectral measurements were carried out inside a glove box or on Schlenk lines. Since vanadium(V) compounds are usually light-sensitive, direct sunlight was kept out during preparation and the products were stored in the dark. The glassware was flame-dried in vacuum, cooled to ambient temperature, and flushed with nitrogen three times before use.

Melting points were determined in vacuum in sealed capillaries on a BSGT Heiligenberg Apotec II apparatus. Numerical values were uncorrected.

NMR spectra (**^{1}H, ^{13}C, ^{51}V**) ($CDCl_3$, C_6D_6 or C_7D_8 solutions) were recorded at ambient temperature on a Bruker ARX 200 or ARX 400 spectrometer. ^{13}C-NMR spectra were recorded proton decoupled. All chemical shifts are reported in ppm relative to the ^{1}H and ^{13}C residue of the deuterated solvents. In case of ^{51}V-NMR, $VOCl_3$-$CDCl_3$ (2:1) was used as external standard.

IR spectra were recorded using a Nicolet Magna IR spectrometer 750 as Nujol mulls or solutions in CS_2 on KRS-5 or KBr plates. Intensities were abbreviated as follows: vs (very strong), s (strong), m (medium), w (weak), and vw (very weak).

Mass spectra were obtained on a Varian MAT 311 A spectrometer using electron impact ionization (EI, 70 eV). Only characteristic fragments containing the isotopes of the highest abundance are given.

Elemental analyses were performed on a Perkin-Elmer Series II CHNS/O Analyzer 2400 or on a Thermo Finnigan CHNS-Analyzer Flash EA 112.

ESR spectra were obtained using a Bruker ER 200D-SRC spectrometer and the signals were referred to the signal of diphenylpicrylhydrazyl (DPPH, g = 2.0037).

Cryoscopic Measurement was performed by using a Beckmann thermometer. Benzene was used as cryscopic solvent.

X-ray structure determinations were collected on a Siemens SMART CCD diffractometer (graphite monochromated Mo-Kα radiation, λ = 0.71073 Å) with area-detector by use of ω scans. The structures were solved by direct methods using SHELXS-97[124] and refined on F^2 using all reflections with SHELXL-97.[125] All non-hydrogen atoms were refined anisotropically. The hydrogen atoms were placed in calculated positions and assigned an isotropic

displacement parameter of 0.08 $Å^2$. SADABS[126] was used to perform area-detector scaling and absorption corrections. The figures were produced using DIAMOND.[127] Crystal data for all compounds related to data collection, structure solution, and refinement are summarized in the appendix.

GPC data of styrene and 1-hexene oligomers were obtained on a Waters model 150 LC/GPC in THF solvent running at ambient temperature and were calibrated using polystyrene standards. GPC measurements of polyethylene samples were carried out by high temperature GPC at 140 °C, using 1,2,4-trichlorobenzene as solvent and narrow polystyrene standard sample as reference. The measurements were performed with a PL-GPC210 with 4 PL-Gel Mixed A columns, with triple detection: RALLS detector (Precision Detector, PD2040 at 800 nm), H502 viscometer (Viscotek), refractive detector and DM400 datamanager (Viscotek).

3.2 Materials

Toluene, hexane, and pentane were distilled under nitrogen from dark purple solutions of sodium benzophenone ketyl containing tetraethylene glycol dimethyl ether prior to use. THF was treated in the same way but without using tetraethylene glycol dimethyl ether. CH_3CN was distilled twice over $LiAlH_4$ followed by distillation over 4 Å molecular sieves and stored under nitrogen. CH_2Cl_2 was distilled from CaH_2 followed by two fold distillation from 4 Å molecular sieves prior to use. CS_2 used for IR measurements was dried with CaH_2 and distilled under nitrogen.[128] $VOCl_3$ (99%, Aldrich) was used as purchased without purification. Cyclooctene (95%, FERAK Berlin), 1-decene (94%, Aldrich), 1-hexene (97%, Aldrich), styrene (99%, Aldrich) were distilled from CaH_2 followed by drying with 4 Å molecular sieves and stored under nitrogen. Ethylene gas (99.995%, Messer Griesheim) was passed through an Oxiclear gas purifier before being passed into the polymerization autoclave. TBHP (5.0–6.0 M in decane or nonane, water <4%, Aldrich) was dried over 3 Å molecular sieves, titrated and handled according to the literature method.[129] DEAC (97%, Strem) was used as toluene solution. MAO (10% wt. in toluene, Aldrich) was employed as received. MTCA (99%, Aldrich) was dried over 4 Å molecular sieves prior to use. $CDCl_3$ was distilled from CaH_2 followed by twofold distillation from 4 Å molecular sieves prior to use. C_6D_6 and C_7D_8 were distilled under nitrogen from dark purple solutions of sodium benzophenone ketyl. $VOCl_2 \cdot 2THF$[130] and $[VOCl_2(OCH_2CH_2OR)]_2$ (R = Me, Et, ^{i}Pr)[39] were synthesized according to literature methods. CH_3ONa and C_2H_5ONa were prepared quantitatively by reaction of sodium with excess of the corresponding alcohol. $[VOCl(OCH_2CH_2OEt)]_2$ and $[VOCl_2(OCH_2CH_2OPh)]$ were provided by Dr. E. C. E. Rosenthal.

3.3 Syntheses of Complexes

3.3.1 $[VOCl_2(OCH_3)(HOCH_3)_2]$ (1)

Dropwise addition of $VOCl_3$ (1.5 mL, 15.6 mmol) at ambient temperature to a solution of CH_3OH (1.9 mL, 46.8 mmol) in pentane (150 mL) gave rise to a brown solution with liberation of HCl, after which the reaction was allowed to proceed for another 2 h until no HCl was evolved. The solution was decanted from dark red oily residue (1.74 g). Orange crystals (0.20 g) were obtained after storing the mother solution at 0 °C for several days. The dark red oil was dissolved in 200 mL of pentane, from which orange crystals (0.63 g) were obtained within several days of storing at 0 °C. Single crystals suitable for X-ray structure determination were obtained on cooling the mother solution to –30 °C for several weeks.

Yield: 0.83 g (3.6 mmol, 23%).

M.p.: 20 °C.

^{1}H-NMR (400 MHz, $CDCl_3$): δ = 5.19 (s_{br}, 9H, C*H*$_3$).

^{1}H-NMR (400 MHz, C_6D_6): δ = 4.57 (s_{br}, 9H, C*H*$_3$).

^{13}C-NMR (100.64 MHz, $CDCl_3$): δ = 76.2 (*C*H$_3$).

^{51}V-NMR (105.19 MHz, $CDCl_3$): δ = –443.

IR (KBr, CS_2): ν = 3560 w (O–H), 1148 w (V–O–C), 1052 vs (C–O), 1025 vs (V=O), 926 vw, 912 vw, 859 vw, 681 s, 668 s (V–OR), 633 s (V–OR), 583 w, 491 vs (V–Cl), 455 s (V–Cl), 440 m cm^{-1}.

MS (102 °C): *m/z* (%) = 167 (20) $[VOCl_2(OCH_2)]^+$, 132 (69) $[VOCl(OCH_2)]^+$, 102 (26) $[VO(OCH_2)]^+$, 86 (11) $[VCl]^+$, 67 (35) $[VO]^+$, 36 (100) $[HCl]^+$.

Anal. Calc. for $C_3H_{11}Cl_2O_4V$ (232.96): C 15.47, H 4.76. Found: C 15.00, H 4.13.

3.3.2 $[VOCl(\mu\text{-}OCH_3)(OCH_3)]_2$ (2)

$VOCl_3$ (1.5 mL, 15.6 mmol) was added dropwise at ambient temperature to a suspension of CH_3ONa (1.69 g, 31.2 mmol) in pentane (200 mL). The reaction mixture changed from light orange to dark red and was vigorously stirred overnight before filtration to remove NaCl precipitate. Concentration of the filtrate to circa 100 mL and cooling to –78 °C for several weeks yielded orange crystalline complex. The mother solution was concentrated to remove all volatile species. Single crystals were obtained from the residue at 0 °C within several months.

Yield: 1.15 g (3.5 mmol, 45%).

M.p.: 63 °C.

^{1}H-NMR (400 MHz, $CDCl_3$): δ = 5.21 (s, 12H, C*H*$_3$).

^{13}C-NMR (100.64 MHz, $CDCl_3$): δ = 76.2 (CH_3).

^{51}V-NMR (105.19 MHz, $CDCl_3$): δ = –436 ($\nu_{1/2}$ = 2300 Hz), –388 ($\nu_{1/2}$ = 800 Hz).

IR (KBr, CS_2): ν = 1149 w (V–O–C), 1054 vs (C–O), 1017 vs (V=O), 999 m, 855 vw, 807 vw, 681 s, 668 m (V–OR), 632 s (V–OR), 592 w, 492 m, 455 s (V–Cl) cm^{-1}.

MS (38 °C): *m/z* (%) = 164 (5) $[VOCl(OCH_3)_2]^+$, 163 (30) $[VOCl(OCH_3)(OCH_2)]^+$, 134 (28) $[V(OH)Cl(OCH_3)]^+$, 133 (23) $[VOCl(OCH_3)]^+$, 132 (14) $[VOCl(OCH_2)]^+$, 128 (100) $[VO(OCH_3)(OCH_2)]^+$, 97 (48) $[VO(OCH_2)]^+$, 67 (28) $[VO]^+$, 51 (4) $[V]^+$, 36 (13) $[HCl]^+$.

Anal. Calc. for $C_4H_{12}Cl_2O_6V_2$ (328.92): C 14.60, H 3.68. Found: C 14.81, H 3.58.

3.3.3 [{VOCl(μ-OC$_2$H$_5$)(OC$_2$H$_5$)}$_2$(μ-THF)] (3)

$VOCl_3$ (1.6 mL, 16.6 mmol) was added at ambient temperature to a suspension of C_2H_5ONa (2.25 g, 33.1 mmol) in THF (100 mL) with the color changing from yellow to colorless and eventually to red. The reaction mixture was stirred overnight, after which 100 mL of pentane was added to let NaCl precipitate. NaCl was filtered off and the filtrate was concentrated slowly in vacuum to remove the solvents yielding an orange liquid. Orange single crystals suitable for X-ray structural determination were obtained by storing the mother solution at –78 °C for several months.

Yield: 1.92 g (4.2 mmol, 50%).

^{1}H-NMR (200 MHz, $CDCl_3$): δ = 5.48 (s_{br}, 8H, VOCH_2), 3.90 (s_{br}, 12H, CH_2OCH_2), 1.90 (s_{br}, 12H, CH_2CH_2 in THF), 1.51 (s_{br}, 12H, CH_3).

^{13}C-NMR (50.32 MHz, $CDCl_3$): δ = 86.2 ($VOCH_2$), 69.8 (*C*-2-THF), 25.3 (*C*-3-THF), 17.6 (CH_3).

^{51}V-NMR (105.19 MHz, $CDCl_3$): δ = –303.

IR (KBr, CS_2): ν = 1140 w (V–O–C), 1087 m (C–O), 1069 m (C–O), 1030 s, 1014 s (V=O), 919 m, 868 m, 803 vw, 669 w (V–OR), 492 m, 465 m (V–Cl) cm^{-1}.

MS (119 °C): *m/z* (%) = 192 (0.1) $[VOCl(OC_2H_5)_2]^+$, 191 (0.4) $[C_4H_9ClO_3V]^+$, 177 (10) $[VOCl(OC_2H_5)(OCH_2)]^+$, 167 (9) $[VOCl_2(OCH_2)]^+$, 149 (7) $[C_2H_7ClO_2V]^+$, 132 (3) $[VOCl(OCH_2)]^+$, 72 (37) $[C_4H_8O]^+$, 42 (100) $[C_3H_6]^+$, 36 (53) $[HCl]^+$.

Anal. Calc. for $C_{12}H_{28}Cl_2O_7V_2$ (457.13): C 31.53, H 6.17. Found: C 30.28, H 5.62. The elemental analysis data agrees with the composition of $VOCl(OC_2H_5)_2 \cdot 0.4THF$. (Anal. Calc.: C 30.37, H 6.01).

3.3.4 [VO(μ-Cl)Cl(η^2-OC(CH$_3$)$_2$CH$_2$OCH$_3$)]$_2$ (4)

To a $HOC(CH_3)_2CH_2OCH_3$ (2.14 g, 20.5 mmol) solution in pentane (150 mL) was added slowly a pentane solution (50 mL) of $VOCl_3$ (2.0 mL, 20.9 mmol) at ambient temperature.

The solution turned from yellow to red. Orange microcrystals formed immediately. The reaction mixture was stirred for 2 h and heated with a warm water bath to remove HCl. The solution was decanted and stored at 0 °C overnight. Orange crystals were isolated by decantation.

Yield: 3.40 g (7.1 mmol, 69%).

M.p.: 48 °C.

^{1}H-NMR (200 MHz, C_6D_6): δ = 2.99 (s, 3H, OC*H*$_3$), 2.86 (s, 2H, OC*H*$_2$), 1.09 (s, 6H, C(C*H*$_3$)$_2$).

^{1}H-NMR (200 MHz, $CDCl_3$): δ = 3.65 (s, 2H, OC*H*$_2$), 3.50 (s, 3H, OC*H*$_3$), 1.61 (s, 6H, C(C*H*$_3$)$_2$).

^{13}C-NMR (100.64 MHz, $CDCl_3$): δ = 99.7 (*C*(Me)$_2$), 79.4 (*C*H$_2$OMe), 59.4 (O*C*H$_3$), 25.6 (C(*C*H$_3$)$_2$).

^{51}V-NMR (105.19 MHz, $CDCl_3$): (concentrated solution) δ = –270 ($\nu_{1/2}$ = 130 Hz, 88%), –282 ($\nu_{1/2}$ = 26 Hz, 11%), –317 ($\nu_{1/2}$ = 27 Hz, 1%).

^{51}V-NMR (105.19 MHz, $CDCl_3$): (dilute solution) δ = –273 ($\nu_{1/2}$ = 120 Hz, 96%), –281 (60 Hz, 4%).

HT ^{51}V-NMR (105.19 MHz, C_7D_8):

T = 23 °C: δ = –268 ($\nu_{1/2}$ = 114 Hz, 96%), –280 ($\nu_{1/2}$ = 84 Hz, 4%).

T = 37 °C: δ = –276 ($\nu_{1/2}$ = 135 Hz, 82%), –278 ($\nu_{1/2}$ = 117 Hz, 17%), –316 ($\nu_{1/2}$ = 33 Hz, 1%).

T = 47 °C: δ = –277 ($\nu_{1/2}$ = 111 Hz, 39%), –280 ($\nu_{1/2}$ = 200 Hz, 56%), –316 ($\nu_{1/2}$ = 85 Hz, 5%).

T = 57 °C: δ = –276 ($\nu_{1/2}$ = 129 Hz, 88%), –282 ($\nu_{1/2}$ = 27 Hz, 5%), –315 ($\nu_{1/2}$ = 44 Hz, 7%).

IR (KBr, Nujol mull): ν = 1234 m, 1195 m, 1143 s (V–O–C), 1074 s (C–O), 1026 s (V=O), 998 vs, 988 vs, 944 s, 932 s, 919 s, 890 s (C–O–C), 812 s, 773 m, 653 m (V–OR), 487 w (V–Cl), 436 w (V–Cl–V) cm^{-1}.

IR (KBr, CS_2): ν = 1186 m, 1160 m 1142 vs, 1117 s (V–O–C), 1097 m, 1023 vs (V=O), 1006 vs, 996 s, 948 vs (C–O–C), 913 s, 819 m, 660 m (V–OR), 552 w, 497 s, 475 vs (V–Cl), 453 vs, 431 s (V–Cl–V) cm^{-1}.

MS (22 °C): *m/z* (%) = 410 (4) [M – 2 Cl]$^+$, 395 (17), [M – 2 Cl – CH_3]$^+$, 381 (3) [M – 2 Cl – C_2H_5]$^+$, 365 (6) [M – 2 Cl – OC_2H_5]$^+$, 352 (4) [M – 2 Cl – OC_3H_6]$^+$, 338 (12) [M – 2 Cl – OC_4H_8]$^+$, 324 (7) [M – 2 Cl – OC_5H_{10}]$^+$, 307 (5) [M – 2 Cl – $OC(CH_3)_2CH_2OCH_3$]$^+$, 258 (14) [$VO(OC(CH_3)_2CH_2OCH_3)(OC(CH_3)CH_2OCH_3)$]$^+$, 225 (60) [$VOCl_2(OC(CH_3)CH_2OCH_3)$]$^+$, 210 (14) [$VOCl_2(OC_4H_9)$]$^+$, 195 (45) [$VOCl_2(OC_3H_6)$]$^+$, 177 (19) [$VOCl(OH)OC_3H_6$]$^+$, 160 (100) [$VOCl(OC_3H_6)$]$^+$.

Anal. Calc. for $C_{10}H_{22}Cl_4O_6V_2$ (481.96): C 24.92, H 4.60. Found: C 25.05, H 4.58.

3.3.5 $[VO(\mu\text{-}Cl)Cl\{\eta^2\text{-}OCH_2cyclo\text{-}(C_4H_7O)\}]_2$ (5)

To a pentane solution (400 mL) of $VOCl_3$ (1.0 mL, 10.4 mmol) was slowly added $HOCH_2cyclo$-(C_4H_7O) (1.0 mL, 10.4 mmol) at room temperature. Red powder formed immediately with the liberation of HCl. The reaction was allowed to proceed for 3 h, after which the solution was evacuated to remove the HCl evolved. The solution was filtered and cooled to 0 °C, while the red powder was dried in vacuum and collected. Red crystals suitable for X-ray diffraction were obtained in several days and were combined with the red powder.

Yield: 1.43 g (6.0 mmol, 58%).

M.p.: 73 °C.

^{1}H-NMR (400 MHz, C_6D_6): δ = 4.78 (s_{br}, 2H, VOC*H*$_2$), 3.78 (s_{br}, 2H, C*H*$_2$OCH), 3.49 (s_{br}, 1H, OC*H*), 1.38 (s_{br}, 1H, CH_2CH_2CHO), 1.24 (s_{br}, 2H, CH_2CH_2CHO), 0.96 (s_{br}, 1H, CH_2CH_2CHO).

^{1}H-NMR (400 MHz, $CDCl_3$): δ = 5.63 (s_{br}, 2H, VOC*H*$_2$), 4.53 (s_{br}, 1H, C*H*O), 4.21 (s_{br}, 1H, C*H*$_2$OCH), 4.02 (s_{br}, 1H, C*H*$_2$OCH), 2.12 (s_{br}, 3H, CH_2CH_2CH + CH_2CH_2CH), 1.86 (s_{br}, 2H, CH_2CH_2CH).

^{13}C-NMR (100.64 MHz, C_6D_6): δ = 93.5 (O*C*H$_2$CHO), 80.2 (*C*H), 70.6 (CHO*C*H$_2$), 27.0 ($OCH_2CH_2CH_2CH$), 25.8 (OCH_2CH_2).

^{51}V-NMR (105.19 MHz, $CDCl_3$): δ = –247.

IR (KBr, Nujol mull): ν = 1247 w, 1223 m, 1175 m, 1130 m (V–O–C), 1084 w, 1035 s (C–O), 1021 s (V=O), 984 vs, 966 vs, 935 vs (C–O–C), 918 vs (C–O–C), 865 s, 849 s, 803 s, 692 w, 637 s (V–OR), 539 w, 523 w, 460 w (V–Cl), 431 w (V–Cl–V) cm^{-1}.

MS (243 °C): *m/z* (%) = 406 (30) $[M - 2\ Cl]^+$, 376 (5) $[M - 2\ Cl - HCHO]^+$, 370 (6) $[M - 2\ Cl - HCl]^+$, 340 (5) $[M - 2\ Cl - HCHO - HCl]^+$, 306 (5) $[V_2O_2Cl_2(Hthffo)]^+$, 286 (15) $[V_2O_2Cl_2(C_5H_6O)]^+$, 269 (50) $[VO(thffo)_2]^+$, 85 (76) $[CH_2C_4H_7O]^+$, 71 (52) $[CH_2CHOCH_2CH_2]^+$, 36 (100) $[HCl]^+$.

Anal. Calc. for $C_{10}H_{18}Cl_4O_6V_2$ (477.93): C 25.13, H 3.80. Found: C 25.22, H 3.79.

3.3.6 $[VOCl_2(\eta^2\text{-}OCH_2CH_2OCH_3)(THF)]$ (6)

$[VOCl_2(OCH_2CH_2OCH_3)]_2$ (1.00 g, 2.3 mmol) was dissolved in 20 mL of toluene at room temperature. To this solution was added THF (0.8 mL, 10.0 mmol). The resulting dark red solution was allowed to stand at 0 °C. Red crystals suitable for X-ray structure determination were obtained within several days.

Yield: 0.92 g (3.2 mmol, 70%).

M.p.: 76 °C.

^{1}H-NMR (400 MHz, $CDCl_3$): δ = 5.37 (s_{br}, 2H, VOCH_2), 4.04 (s_{br}, 4H, CH_2-2-THF), 3.98 (t, $^{3}J_{HH}$ = 5.0 Hz, 2H, CH_2OMe), 3.59 (s, 3H, CH_3), 1.95 (m, 4H, CH_2-3-THF).

^{13}C-NMR (50.32 MHz, $CDCl_3$): δ = 83.3 (VO*C*H_2), 73.7 (*C*H_2-2-THF), 71.9 (*C*H_2OMe), 59.7(*C*H_3), 24.9 (*C*H_2-3-THF).

^{51}V-NMR (105.19 MHz, $CDCl_3$) δ = –266 ($\nu_{1/2}$ = 424 Hz, >99%), –301 (<1%).

IR (KBr, CS_2): ν = 1231 vw, 1195 vw, 1127 m (V–O–C), 1104 vw, 1091 w, 1047 s (C–O), 1024 vs (V=O), 996 s, 914 m, 893 m (C–O–C), 867 m (C–O–C), 706 m, 606 vw (V–OR), 484 w (V–Cl), 458 vw, 438 vw cm^{-1}.

MS (222 °C): *m/z* (%) = 354 (61) $[VOCl(OCH_2CH_2OMe)]_2^+$, 319 (6) $[V_2O_2Cl(OCH_2CH_2OMe)_2]^+$, 279 (14) $[V_2O_2Cl_2(OCH_2CH_2OMe)]^+$, 260 (16) $[V_2O_2Cl(OCH_2CH_2OMe)_2 - C_3H_7O]^+$, 249 (2) $[M - 2\ Cl]^+$, 217 (95) $[VO(OCH_2CH_2OMe)_2]^+$, 212 (1) $[M - THF]^+$, 142 (10) $[M - 2Cl - THF]^+$, 59 (100) $[C_3H_7O]^+$.

Anal. Calc. for $C_7H_{15}Cl_2O_4V$ (285.04): C 29.50, H 5.30. Found: C 29.38, H 5.52.

3.3.7 $[VOCl_2(\eta^2\text{-}OCH_2CH_2OC_2H_5)(THF)]$ (7)

$[VOCl_2(OCH_2CH_2OC_2H_5)]_2$ (1.00 g, 2.2 mmol) was dissolved in 3.0 mL of THF giving rise to a dark red solution accompanied by release of heat. To this solution were added immediately 10 mL of pentane. Red crystalline product formed immediately. After decantation red crystals were obtained.

Yield: 1.12 g (3.7 mmol, 85%).

M.p.: 61 °C.

^{1}H-NMR (200 MHz, $CDCl_3$): δ = 5.49 (s_{br}, 2H, VOCH_2), 3.98 (s_{br}, 4H, CH_2-2-THF), 3.92 (t, $^{3}J_{HH}$ = 4.4 Hz, 2H, CH_2OEt), 3.77 (q, $^{3}J_{HH}$ = 6.9 Hz, 2H, CH_2CH$_3$), 1.91 (s_{br}, 4H, CH_2-3-THF), 1.22 (t, $^{3}J_{HH}$ = 6.9 Hz, 3H, CH_3).

^{13}C-NMR (50.32 MHz, $CDCl_3$): δ = 87.6 (VO*C*H_2), 72.0 (*C*-2-THF), 69.2 (*C*H_2OEt), 67.4 (*C*H_2CH$_3$), 25.3 (*C*-3-THF), 14.2 (*C*H_3).

^{51}V-NMR (105.19 MHz, $CDCl_3$): δ = –262 (96%), –341 (4%).

HT ^{51}V-NMR (105.19 MHz, C_7D_8):

T = 23 °C: δ = –261 ($\nu_{1/2}$ = 450 Hz, 93%), –341 ($\nu_{1/2}$ = 330 Hz , 7%).

T = 38 °C: δ = –267 ($\nu_{1/2}$ = 500 Hz, 94%), –341 ($\nu_{1/2}$ = 600 Hz , 6%).

T = 49 °C: δ = –270 ($\nu_{1/2}$ = 580 Hz, 97%), –341 ($\nu_{1/2}$ =1000 Hz , 3%).

T = 60 °C: δ = –272 ($\nu_{1/2}$ = 640 Hz).

IR (KBr, CS_2): ν = 1297 vw, 1255 vw, 1229 vw, 1173 vw, 1125 m (V–O–C), 1069 m, 1049 vs (C–O), 1025 vs (V=O), 1005 m, 919 m (C–O–C), 880 w (C–O–C), 793 vw, 667 w (V–OR), 528 vw, 484 m (V–Cl), 436 w cm^{-1}.

MS (222 °C): *m/z* (%) = 382 (24) $[VOCl(OCH_2CH_2OEt)]_2^+$, 274 (21) $[V_2O_3Cl(OCH_2CH_2OEt)]^+$, 245 (37) $[VO(OCH_2CH_2OEt)_2]^+$, 156 (2) $[VO(OCH_2CH_2OEt)]^+$, 59 (100) $[C_3H_7O]^+$.

Anal. Calc. for $C_8H_{17}Cl_2O_4V$ (299.06): C 32.13, H 5.73. Found: C 31.72, H 5.55.

3.3.8 $[VOCl_2\{\eta^2\text{-}OCH_2CH_2OCH(CH_3)_2\}(THF)]$ (8)

$[VOCl_2\{OCH_2CH_2OCH(CH_3)_2\}]_2$ (1.18 g, 2.4 mmol) was dissolved in 6 mL of THF at room temperature leading to a dark red solution, which was treated with 46 mL of pentane and stored at –30 °C. Red crystals formed from the solution overnight and were isolated below 0 °C.

Yield: 1.15 g (3.7 mmol, 75%).

M.p.: 19 °C.

^{1}H-NMR (400 MHz, $CDCl_3$): δ = 5.73 (s_{br}, 2H, VOCH_2), 3.92 (m, 4H, CH_2-2-THF), 3.80 (t, $^3J_{HH}$ = 3.9 Hz, 2H, CH_2OCH), 3.76 (sept, $^3J_{HH}$ = 6.1 Hz, 1H, C*H*), 1.89 (s_{br}, 4H, CH_2-3-THF), 1.16 (d, $^3J_{HH}$ = 6.1 Hz, 6H, CH_3).

^{13}C-NMR (100.64 MHz, $CDCl_3$): δ = 92.2 (VO*C*H_2), 72.3 (*C*H), 70.3 (*C*H_2-2-THF), 66.6 (*C*H_2O^{i}Pr), 25.3 (*C*H_2-3-THF), 21.4 (*C*H_3).

^{51}V-NMR (105.19 MHz, $CDCl_3$): δ = –279 (99%), –343 (1%).

IR (KBr, CS_2): ν = 1368 m, 1332 m, 1261 w, 1229 w, 1147 m, 1128 s (V–O–C), 1104 m, 1068 s, 1046 vs (C–O), 1025 vs (V=O), 964 m, 922 s (C–O–C), 871 m, 802 w, 774 vw, 668 m (V–OR), 607 vw, 529 w, 482 s (V–Cl), 437 m cm^{-1}.

MS (80 °C): *m/z* (%) = 290 (3) $[VOCl(OCH_2CH_2O^iPr)(OH)]^+$, 248 (5) $[VOCl(OCH_2CH_2O^iPr)(C_3H_7)]^+$, 227 (1) [M – 2 Cl – Me]$^+$, 225 (1) [M – THF – Me]$^+$, 206 (13) $[VOCl(HOCH_2CH_2O^iPr)]^+$, 205 (3) $[VOCl(OCH_2CH_2O^iPr)]^+$, 200 (3) [M – 2 Cl – C_3H_6]$^+$, 170 (6) [M – 2 Cl – THF]$^+$, 73 (29) $[C_4H_9O]^+$, 70 (1) [M – 2 Cl – THF – C_3H_6]$^+$, 43 (100) $[^iPr]^+$.

Anal. Calc. for $C_9H_{19}Cl_2O_4V$ (313.09): C 34.53, H 6.12. Found: C 34.49, H 5.80.

3.3.9 $[VOCl_2(\eta^2\text{-}OC(CH_3)_2CH_2OCH_3)(THF)]$ (9)

$[VOCl_2(OC(CH_3)_2CH_2OCH_3)]_2$ (0.90 g, 1.9 mmol) was dissolved in 9.0 mL of THF under vigorous shaking at room temperature giving rise to a dark red solution. Treatment of this solution with 20 mL of pentane led to formation of red crystals immediately, which were isolated by decantation and the solution was stored at –30 °C overnight. Orange crystals suitable for X-ray diffraction were obtained within several weeks.

Yield: 1.12 g (3.6 mmol, 94%).

M.p.: 53 °C.

^{1}H-NMR (200 MHz, $CDCl_3$): δ = 3.92 (m, 4H, C*H*$_2$-2-THF), 3.74 (s, 2H, C*H*$_2$OCH$_3$), 3.53 (s, 3H, OC*H*$_3$), 1.88 (m, 4H, C*H*$_2$-3-THF), 1.46 (s, 6H, C(C*H*$_3$)$_2$).

^{13}C-NMR (50.32 MHz, $CDCl_3$): δ = 97.2 (VO*C*), 80.0 (*C*H$_2$OCH$_3$), 71.0 (C*H*$_2$-2-THF) , 59.8 (O*C*H$_3$), 25.5 (C(*C*H$_3$)$_2$), 25.3 (*C*H$_2$-3-THF).

^{51}V-NMR (105.19 MHz, $CDCl_3$): δ = –270 ($\nu_{1/2}$ = 150 Hz, 99%), –342 (1%).

IR (KBr, CS_2): ν = 1365 w, 1273 vw, 1233 vw, 1186 w, 1160 w, 1142 m, 1117 m (V–O–C), 1097 w, 1070 m (C–O), 1023 vs (V=O), 1006 m, 948 vs (C–O–C), 914 m (C–O–C), 874 w, 819 w, 659 vw (V–OR), 646 vw, 498 m, 475 m (V–Cl), 453 m, 430 m cm^{-1}.

MS (26 °C): *m/z* (%) = 410 (2) $[VOCl\{OC(CH_3)_2CH_2OMe\}]_2^+$, 395 (8) $[V_2O_2Cl_2\{OC(CH_3)_2CH_2OMe\}_2 - CH_3]^+$, 365 (3) $[V_2O_2Cl_2\{OC(CH_3)_2CH_2OMe\}_2 - CH_3 - CH_2O]^+$, 277 (1) $[M - Cl]^+$, 242 (1) $[M - 2\ Cl]^+$, 227 (4) $[M - 2\ Cl - Me]^+$, 225 (5), $[M - THF - Me]^+$, 205 (1) $[M - Cl - THF]^+$, 190 (3) $[M - Cl - THF - Me]^+$, 177 (3) $[M - Cl - THF - C_2H_4]^+$, 170 (2) $[M - 2\ Cl - THF]^+$, 160 (13) $[M - Cl - THF - CH_2OCH_3]^+$, 155 (2) $[M - 2\ Cl - THF - Me]^+$, 42 (100) $[C_2H_2O]^+$.

Anal. Calc. for $C_9H_{19}Cl_2O_4V$ (313.09): C 34.53, H 6.12. Found: C 34.77, H 5.93.

3.3.10 Alkylation of $[VOCl_2(OCH_2CH_2OCH_3)]_2$

1. Reaction of $[VOCl_2(OCH_2CH_2OCH_3)]2$ with neo-pentyl lithium:

A toluene solution (50 mL) containing $[VOCl_2(OCH_2CH_2OCH_3)]_2$ (1.46 g, 3.4 mmol) was cooled to –78 °C, to which $C_5H_{11}Li$ (0.57 g, 7.3 mmol) was added. The reaction mixture was warmed gradually to ambient temperature, while the color turned from orange, then green to finally blue. The mixture was stirred at room temperature overnight. Filtration of the reaction mixture gave a colorless solution and a blue residue. The latter was readily soluble in CH_2Cl_2, from which blue crystals of $[VOCl(OCH_2CH_2OCH_3)]_2$ were isolated after concentration.

2. Reaction of $[VOCl_2(OCH_2CH_2OCH_3)]2$ with phenylethynyl potassium:

To a THF solution (100 mL) of $[VOCl_2(OCH_2CH_2OCH_3)]_2$ (1.40 g, 3.3 mmol) was added PhC≡CK (1.85 g, 13.2 mmol) at –78 °C. On warming to ambient temperature the reaction mixture turned from dark red to green and was stirred for 3 h before filtration. Removal of the solvent in vacuum at 0 °C and addition of toluene (150 mL) gave a brown solution with a small amount of dark precipitate. ^{51}V-NMR of the brown solution showed no signal between +1500 and –500 ppm.

3. Reaction of $[VOCl_2(OCH_2CH_2OCH_3)]_2$ with trimethylsilylmethyl Grignard reagent:

$(CH_3)_3SiCH_2MgCl$ (3.5 mmol) in diethyl ether (1.0 M, 3.5 mL) was pumped to remove the solvent and treated with 50 mL of toluene and $[VOCl_2(OCH_2CH_2OCH_3)]_2$ (0.73 g, 1.7 mmol) at ambient temperature. The brown solution turned to green immediately. The reaction mixture was allowed to react overnight. Removal of all solvent followed by addition of 30 mL of CH_2Cl_2 and filtration of the mixture gave rise to a light green solution. After standing at –30 °C for several days light yellow crystalline $VO(OCH_2SiMe_3)_3$ was obtained.

Yield: 0.22 g (0.7 mmol, 60% based on Grignard reagent).

^{1}H-NMR (200 MHz, $CDCl_3$): δ = 1.79 (s_{br}, $\nu_{1/2}$ = 190 Hz, 6H, C*H*$_2$), 0.09 (s, 27H, C*H*$_3$). [lit.,[113] ^{1}H-NMR (500.1 MHz, C_6D_6): δ = 1.80 ($\nu_{1/2}$ = 80 Hz, C*H*$_2$), 0.15 (C*H*$_3$)].

3.3.11 Reaction of $[VOCl_2(OCH_2CH_2OCH_3)]_2$ with PPh_3

To a solution of $[VOCl_2(OCH_2CH_2OCH_3)]_2$ (0.24 g, 0.6 mmol) in toluene (20 mL) was added PPh_3 (0.30 g, 1.1 mmol) at –78 °C with stirring for 3 h. The dark red solution was stored at –30 °C overnight with color change to lemon. Lemon needles formed. After standing at –30 °C for several weeks the lemon needles disappeared. The solution turned to dark green, and green crystals formed. Removal of all solvent and recrystallization from CH_2Cl_2 resulted in light green crystals of $VOCl_2(O{=}PPh_3)_2{\cdot}CH_2Cl_2$, which were characterized by X-ray diffraction. Upon pumping off the lattice solvent in vacuum green powder was obtained.

Yield: 0.17 g (0.3 mmol, 47% based on PPh_3).

M.p.: >290 °C (from CH_2Cl_2; lit.,[131] 276 °C, from CH_2Cl_2/CH_3CN; lit.,[132] 255 °C (decomposition), from C_2H_5OH/C_6H_6).

Anal. Calc. for $C_{36}H_{30}Cl_2O_3P_2V$ (694.43): C 62.27, H 4.35. Found: C 61.03, H 4.56. The elemental analysis data agrees with the composition of $VOCl_2(O{=}PPh_3)_2{\cdot}0.2CH_2Cl_2$. (Anal. Calc.: C 61.11, H 4.31).

3.3.12 $[VOCl_2(\eta^3\text{-}OCH_2CH_2OCH_2CH_2OC_4H_9)]$ (10)

A pentane solution (200 mL) containing $HOCH_2CH_2OCH_2CH_2OC_4H_9$ (1.8 mL, 10.4 mmol) was treated dropwise with $VOCl_3$ (1.0 mL, 10.4 mmol). Yellow powder formed immediately with liberation of HCl. The reaction mixture was stirred for 2 h before heating with a warm water bath to remove HCl. The solution was decanted, concentrated to circa 100 mL and stored at 0 °C, while the yellow powder was collected and dried in vacuum. Orange crystals (0.28 g) suitable for X-ray crystal structure determination were obtained from the mother solution within several days. The two portions of product were combined.

Yield: 2.51 g (8.4 mmol, 80%)

M.p.: 82 °C.

(Assignment of the carbon atoms: $O^{1}CH_2{}^{2}CH_2O^{3}CH_2{}^{4}CH_2O^{5}CH_2{}^{6}CH_2{}^{7}CH_2{}^{8}CH_3$).

^{1}H-NMR (400 MHz, $CDCl_3$): δ = 5.47 (s_{br}, 2H, $^{1}CH_2$), 4.28 (s_{br}, 2H, CH_2), 4.13 (s_{br}, 6H, CH_2), 1.87 (s_{br}, 2H, $^{6}CH_2$), 1.45 (s_{br}, 2H, $^{7}CH_2$), 0.93 (s_{br}, 3H, $^{8}CH_3$).

^{13}C-NMR (100.64 MHz, $CDCl_3$) δ = 87.1 ($^{1}CH_2$), 79.4 (CH_2), 73.9 (CH_2), 69.9 (CH_2), 68.1 (CH_2), 30.0 ($^{6}CH_2$), 18.5 ($^{7}CH_2$), 13.4 ($^{8}CH_3$).

^{51}V-NMR (105.19 MHz, $CDCl_3$): δ = –300 ($\nu_{1/2}$ = 399 Hz, 83%), –346 ($\nu_{1/2}$ = 128 Hz, 17%).

IR (KBr, CS_2): ν = 1298 vw, 1261 w, 1245 w, 1233 vw, 1111 vs (V–O–C), 1091 m, 1058 s (C–O), 1029 vs (V=O), 1012 s, 997 m, 986 vs (C–O–C), 954 w, 943 m, 933 w, 917 w, 901 m, 893 m, 822 vw, 807 vw, 796 vw, 741 m, 646 s (V–OR), 491 vw, 465 vw (V–Cl) cm^{-1}.

MS (242 °C): *m/z* (%) = 526 (1) $[2\ M - 2\ Cl]^+$, 482 (1) $[2\ M - 2\ Cl - C_2H_4O]^+$, 447 (1) $[2\ M - 3\ Cl - C_2H_4O]^+$, 418 (2) $[2\ M - 2\ Cl - C_2H_4O - C_2H_5]^+$, 263 (11) $[VOCl(OCH_2CH_2OBu)]^+$, 228 (59) $[VO(OCH_2CH_2OBu)]^+$, 207 (10) $[C_4H_9ClO_4V]^+$, 184 (24) $[VO(OCH_2CH_2OBu)]^+$, 36 (100) $[HCl]^+$.

Anal. Calc. for $C_8H_{17}Cl_2O_4V$ (299.06): C 32.13, H 5.73. Found: C 32.15, H 5.58.

3.3.13 [$VOCl_2${OCH_2*cyclo*-(C_4H_7O)}{$HOCH_2$*cyclo*-(C_4H_7O)}] (11)

To a solution of $HOCH_2$*cyclo*-(C_4H_7O) (2.3 mL, 22.7 mmol) in pentane (400 mL) was added dropwise $VOCl_3$ (1.0 mL, 10.4 mmol) at room temperature. Orange powder formed immediately. The mixture was stirred for 2 h before heating with a warm water bath to remove HCl. The orange powder was isolated and washed with pentane (2 · 20 mL).

Yield: 3.23 g (9.5 mmol, 91%).

M.p.: 95 °C.

^{1}H-NMR (400 MHz, $CDCl_3$): δ = 6.27 (s_{br}, 1H, O*H*), 4.90 (s_{br}, 4H, VOCH_2), 4.53 (s_{br}, 2H, C*H*), 4.23 (s_{br}, 2H, CH_2OCH), 4.04 (s_{br}, 2H, CH_2OCH), 2.08 (s_{br}, 6H, one H of CH_2CH_2CH + CH_2CH_2CH), 1.74 (s_{br}, 2H, one H of CH_2CH_2CH).

^{13}C-NMR (100.64 MHz, $CDCl_3$): δ = not found (VO*C*H_2), 80.2 (*C*H), 70.6 (CHO*C*H_2), 27.2 (CH*C*H_2CH_2), 25.9 (OCH_2CH_2).

^{51}V-NMR (105.19 MHz, $CDCl_3$): δ = –345 ($\nu_{1/2}$ = 1500 Hz).

IR (KBr, Nujol mull): ν = 3095 s (O–H), 2728 m, 2672 m, 1366 s, 1331 m, 1321 m, 1255 m, 1246 m, 1231 m, 1189 w, 1125 w (V–O–C), 1072 m (C–O), 1026 vs (V=O), 1004 s, 979 vs (C–O–C), 944 m, 934 s (C–O–C), 924 m, 890 w, 813 s, 710 s (V–OR), 588 vw, 503 w, 479 vw, 468 w (V–Cl), 424 vw cm^{-1}.

MS (224 °C): *m/z* (%) = 406 (53) $[VOCl(thffo)]_2^+$, 376 (9) $[V_2O_2Cl_2(thffo)_2 - CH_2O]^+$, 371 (7) $[V_2O_2Cl(thffo)_2]^+$, 370 (11) $[V_2O_2Cl_2(thffo)_2 - HCl]^+$, 340 (10) $[V_2O_2Cl_2(thffo)_2 - HCl -$

$CH_2O]^+$, 322 (5) $[V_2O_3Cl_2(Hthffo)]^+$, 306 (8) $[V_2O_2Cl_2(Hthffo)]$, 305 (7) $[V_2O_2Cl_2(thffo)_2]^+$, 286 (30) $[V_2O_3Cl(thffo)]^+$, 269 (74) $[VO(thffo)_2]^+$, 204 (4) $[VOCl(Hthffo)]^+$, 85 (100) $[C_5H_9O]^+$.

Anal. Calc. for $C_{10}H_{19}Cl_2O_5V$ (341.10): C, 35.21; H, 5.61%. Found: C, 35.44; H, 5.31%.

3.3.14 $[VOCl\{OCH_2$*cyclo*$-(C_4H_7O)\}_2]_2$ (12)

$VOCl_3$ (1.0 mL, 10.4 mmol) was added dropwise to a pentane solution (400 mL) containing $HOCH_2$*cyclo*$-(C_4H_7O)$ (2.2 mL, 21.7 mmol) at room temperature. Orange powder formed immediately. The reaction mixture was stirred overnight. The colorless pentane solution was discarded, while the solid residue was dissolved in warm toluene (150 mL). Concentration of this solution under reduced pressure at 70 °C to 50 mL followed by cooling to –30 °C for several days gave the product as brown solid.

Yield: 0.70 g (1.1 mmol, 22%).

M.p.: 92 °C (decomposition).

^{1}H-NMR (400 MHz, $CDCl_3$): δ = 5.03 (s_{br}, 4H, VOCH_2), 4.37 (s_{br}, 2H, C*H*), 4.10 (s_{br}, 2H, CHOCH_2), 3.87 (s_{br}, 2H, CHOCH_2), 2.00 (s_{br}, 6H, CHCH_2CH_2), 1.73 (s_{br}, 2H, CHCH_2CH_2).

^{13}C-NMR (100.64 MHz, $CDCl_3$): δ = 85.8 (VO*C*H_2), 80.0 (*C*H), 69.6 (CHO*C*H_2), 27.1 (CH*C*H_2CH_2), 25.6 (OCH_2*C*H_2).

^{51}V-NMR (105.19 MHz, $CDCl_3$): δ = –333 ($\nu_{1/2}$ = 1600 Hz, ≥99%), –455 (≤1%).

IR (KBr, Nujol mull) ν = 1366 s, 1330 m, 1320 m, 1276 w, 1246 w, 1231 m, 1189 w, 1125 w (V–O–C), 1075 m (C–O), 1050 m (C–O), 1026 s (V=O), 979 vs (C–O–C), 933 s, 922 m, 873 w, 851 m (V–O–V), 813 m, 709 m (V–OR), 676 w, 587 w, 503 w, 467 w (V–Cl), 424 w cm^{-1}.

MS (183 °C): *m/z* (%) = 406 (47) $[VOCl(thffo)]_2^+$, 370 (7) $[V_2O_2Cl_2(thffo)_2 – HCl]^+$, 340 (9) $[V_2O_2Cl_2(thffo)_2 – HCl – CH_2O]^+$, 306 (7) $[V_2O_2Cl_2(Hthffo)]^+$, 286 (28) $[V_2O_3Cl(thffo)]^+$, 269 (66) $[VO(thffo)_2]^+$, 204 (4) $[VOCl(Hthffo)]^+$, 85 (100) $[C_5H_9O]^+$.

Anal. Calc. for $C_{20}H_{36}Cl_2O_{10}V_2$ (609.28): C 39.43, H 5.96. Found: C 39.44, H 5.76.

3.3.15 $[VO(OC(CH_3)_2CH_2OCH_3)_3]$ (13)

47.5 mmol of ^{n}BuLi (2.5 M in hexane, 19.0 mL) were added dropwise to a hexane solution (150 mL) of $HOC(CH_3)_2CH_2OCH_3$ (5.03 g, 48.3 mmol) at 0 °C. White lithium salt formed toward the end of the addition. The mixture was stirred for 1 h and treated with a $VOCl_3$ (1.5 mL, 15.6 mmol) solution in hexane (50 mL). White precipitate formed immediately and the reaction proceeded for 3 days. Filtration of the white solid and removal of the volatiles in

vacuum gave colorless oil quantitatively, which was further purified by distillation under reduced pressure. The main loss of the product is due to decomposition during distillation.

Yield: 4.16 g (11.0 mmol, 71%).

B.p.: 104 °C/5 · 10^{-3} mbar.

Molecular weight obtained from cryoscopic measurement: 362.

^{1}H-NMR (200 MHz, C_6D_6): δ = 3.33 (s, 6H, C*H*$_2$), 3.17 (s, 9H, OC*H*$_3$), 1.52 (s, 18H, C(C*H*$_3$)$_2$).

^{13}C-NMR (50.32 MHz, C_6D_6): δ = 85.4 (VO*C*), 85.1 (VO*C*), 81.0 (*C*H$_2$), 58.9 (OC*H*$_3$), 27.0 (C(*C*H$_3$)$_2$).

^{51}V-NMR (105.19 MHz, $CDCl_3$): δ = –584 (<1%, $\nu_{1/2}$ = 26 Hz), –595(<1%, $\nu_{1/2}$ = 31 Hz), –647 (>98%, $\nu_{1/2}$ = 18 Hz).

IR (KBr, CS_2): ν = 1181 m, 1134 s (V–O–C), 1115 s (V–O–C), 977 vs (V=O), 926 m (C–O–C), 876 vw, 856 vw, 825 m (V–O–V), 814 w, 798 m, 664 w (V–OR), 646 w (V–OR), 553 vw, 540 vw, 528 vw, 480 w cm^{-1}.

IR (KBr, Nujol) ν = 1183 m, 1139 s (V–O–C), 1117 s (V–O–C), 980 vs (V=O), 926 w (C–O–C), 825 w (V–O–V), 799 w, 783 w, 667 vw (V–OR), 647 vw, 541 vw, 479 vw cm^{-1}.

MS (51 °C): *m/z* (%) = 649 (0.02) $[V_2O_2(mmp)_5]^+$, 546 (0.03) $[VO(mmp)_2]_2^+$, 443 (0.07) $[V_2O_2(mmp)_3]^+$, 273 (100) $[VO(mmp)_2]^+$.

Anal. Calc. for $C_{30}H_{66}O_{14}V_2$ (376.36): C 47.87, H 8.84. Found: C 47.78, H 9.18.

3.3.16 $[VOCl_2(O{=}CPh_2)_2]$ (14)

Method 1: Treatment of $HOC(Ph_2)C(Ph_2)OH$ (1.93 g, 5.3 mmol) dissolved in CH_2Cl_2 (60 mL) with a pentane solution (20 mL) containing $VOCl_3$ (0.5 mL, 5.2 mmol) resulted in a dark green solution with the release of HCl. The mixture was allowed to react for 1 h before being heated with a warm water bath to remove HCl. After stirring overnight, the reaction mixture was filtered. The residue was readily soluble in acetone, while the filtrate was concentrated to about 25 mL and kept at –78 °C. Green crystals were obtained from a CH_2Cl_2/toluene (2:1) solution within several weeks.

Yield: 0.88 g (1.8 mmol, 34% based on $VOCl_3$).

Method 2: $VOCl_2$·2THF (1.55 g, 5.5 mmol) was mixed with benzophenone (2.00 g, 11.0 mmol), after which CH_2Cl_2 (20 mL) was added to this mixture giving a dark green solution. After stirring for 1 h the solvent was pumped off. 20 mL of CH_2Cl_2 were added to the residue followed by treatment with 20 mL of toluene. Dark green crystalline product formed immediately and was collected by filtration.

Yield: 1.86 g (3.7 mmol, 67%).

M.p.: 157 °C.

IR (KRS-5, Nujol mull): ν = 1667 m (C=O), 1615 m (Ph), 1590 m (Ph), 1581 m (Ph), 1571 m, 1551 m, 1331 s, 1317 s, 1277 s, 1074 w (V–O–C), 1030 w, 1016 m (V=O), 998 m, 993 m, 985 w, 957 w, 940 m, 924 w, 891 w, 858 w, 850 w, 810 w, 778 w, 772 m (Ph), 761 w, 700 s (Ph), 639 m, 617 vw, 602 w, 368 w (V–Cl), 314 w, 305 w, 289 w, 278 w cm^{-1}.

MS (118 °C) : *m/z* (%) = 243 (33) $[CPh_3]^+$, 182 (60) $[Ph_2C{=}O]^+$, 105 (100) $[PhC{=}O]^+$, 77 (42) $[Ph]^+$, 51 (9) $[V]^+$.

Anal. Calc. for $C_{26}H_{20}Cl_2O_3V$ (502.29): C 62.17, H 4.01. Found: C 66.63, H 5.03. The elemental analysis data agrees with the composition of $VOCl_2(O{=}CPh_2)_2{\cdot}C_7H_8$. (Anal. Calc.: C 66.68, H 4.75).

3.3.17 $[VOCl(\mu,\eta^2\text{-}OC(CH_3)_2CH_2OCH_3)]_2$ (15)

To a pentane solution (150 mL) containing $HOC(CH_3)_2CH_2OCH_3$ (5.0 mL, 42.8 mmol) was added dropwise a pentane solution (20 mL) of $VOCl_3$ (2.0 mL, 20.9 mmol) at room temperature. The resulting solution was stirred for 3 h and heated with a warm water bath to complete the elimination of HCl. The resulting solution was decanted and stored at 0 °C. The solution was concentrated to about 80 mL and stored at –30 °C for 2 months. Blue crystals were obtained. Removal of the volatiles and exposure of the dark brown residue to sunlight for 24 h led to decomposition to blue oil. The blue oil was dissolved in a 1:1 mixture of CH_2Cl_2 and pentane, from which crystals suitable for X-ray diffraction were obtained.

Yield 1.73 g (4.2 mmol, 40% based on vanadium)

M.p.: 90 °C.

IR (KRS-5, Nujol mull): ν = 1279 m, 1241 s, 1213 w, 1199 w, 1163 s, 1152 m (V–O–C), 1043 vs (C–O), 1000 vs (V=O), 950 m, 928 vs (C–O–C), 898 s (C–O–C), 806 s, 722 m, 682 s (V–OR), 604 w, 561 vw, 514 s, 471 s, 436 s, 390 s (V–Cl), 355 m, 337 m, 303 vw, 286 w, 279 w cm^{-1}.

MS (122 °C): *m/z* (%) = 410 (3) $[M]^+$, 395 (13) $[M - CH_3]^+$, 375 (1) $[M - Cl]^+$, 365 (5) $[M - C_2H_5O]^+$, 338 (10) $[M - C_4H_8O]^+$, 307 (4) $[V_2O_2Cl_2(mmp)]^+$, 288 (4) $[V_2O_3Cl(mmp)]^+$, 273 (2) $[VO(mmp)_2]^+$, 258 (12) $[VO(mmp)_2 - Me]^+$, 186 (3) $[VO_2(mmp)]^+$, 87 (100) $[C_5H_{11}O]^+$.

ESR (20 °C, THF): g_i = 1.9708, $A(^{51}V)$ = 11.04 mT.

Anal. Calc. for $C_{10}H_{22}Cl_2O_6V_2$ (411.07): C 29.22, H 5.39. Found: C 29.23, H 5.12.

3.3.18 $[VOCl_2(\eta^2\text{-}OCH_2CH_2OCH_3)(CH_3CN)]$ (16)

Addition of a pentane solution (10 mL) of $VOCl_3$ (0.5 mL, 5.2 mmol) to a pentane solution (200 mL) of $HOCH_2CH_2OCH_3$ (0.4 mL, 5.2 mmol) at room temperature gave rise to a brown

solution. The solution was stirred for 0.5 h followed by addition of CH_3CN (0.4 mL, 7.7 mmol). Red crystalline solid formed immediately. The mixture was stirred another 3 h and the red solid was isolated by filtration. Single crystals suitable for X-ray diffraction were obtained from a CH_3CN solution on storage at –30 °C for several days.

Yield: 0.91 g (3.6 mmol, 69%).

M.p.: 57 °C.

^{1}H-NMR (400 MHz, $CDCl_3$): δ = 5.57 (s_{br}, 2H, VOC*H*$_2$), 3.90 (s_{br}, 2H, C*H*$_2$OCH$_3$), 3.50 (s, 3H, OC*H*$_3$), 2.20 (s_{br}, 3H, C*H*$_3$CN).

^{13}C-NMR (50.32 MHz, $CDCl_3$): δ = 117.8 (*C*N), 88.8 (VO*C*H$_2$), 71.6 (*C*H$_2$OCH$_3$), 59.2 (O*C*H$_3$), 2.0 (*C*H$_3$).

^{51}V-NMR (105.19 MHz, $CDCl_3$): δ = –278 ($\nu_{1/2}$ = 450 Hz).

IR (KBr, Nujol mull): ν = 2319 s (C≡N), 2292 s (C≡N), 1366 s, 1345 s, 1262 s, 1227 s, 1159 m, 1105 s (V–O–C), 1074 s (C–O), 1027 s (V=O), 984 s, 946 s, 910 s (C–O–C), 827 s, 614 s (V–OR), 584 s, 463 m (V–Cl) cm^{-1}.

MS (201 °C): *m*/*z* (%) = 354 (8) $[VOCl(OCH_2CH_2OMe)]_2^+$, 217 (25) $[VO(OCH_2CH_2OMe)_2]^+$, 50 (100) $[CH_3Cl]^+$, 41 (10) $[CH_3CN]^+$, 36 (46) $[HCl]^+$.

Anal. Calc. for $C_5H_{10}Cl_2NO_3V$ (253.99): C 23.64, H 3.97, N 5.51. Found: C 24.02, H 4.15, N 5.84.

3.3.19 [VOCl$_2$(η^2-HOCH$_2$CH$_2$OCH$_3$)(CH$_3$CN)] (17)

$VOCl_2(OCH_2CH_2OCH_3)(CH_3CN)$ (0.70 g, 2.7 mmol) was dissolved in CH_3CN (15 mL), and the resultant red solution was exposed to sunlight at ambient temperature. The solution turned gradually into green within 8 h and blue after several days. Blue crystals suitable for X-ray diffraction were isolated after standing at 0 °C for 3 days.

Yield: 0.34 g (1.3 mmol, 49%).

M.p.: 125 °C.

^{1}H-NMR (400 MHz, CD_3CN): δ = 4.50 (s_{br}, 2H, HOC*H*$_2$), 3.02 (s_{br}, 2H, C*H*$_2$OMe), 1.74 (s, 3H, C*H*$_3$CN), 0.73 (s, 3H, OC*H*$_3$).

IR (KRS-5, Nujol mull): ν = 3093 s (O–H), 2317 m (C≡N), 2290 m (C≡N), 2249 w, 2049 w, 1966 w, 1265 m, 1236 s, 1192 m, 1156 m, 1118 m, 1075 s (C–O), 1026 s (V=O), 983 vs, 945 s (C–O–C), 897 s (C–O–C), 821 m, 772 w, 686 w, 608 w, 551 m, 442 m, 411 m, 328 s (V–Cl), 272 m cm^{-1}.

MS (142 °C): *m*/*z* (%) = 354 (11) $[VOCl(OCH_2CH_2OMe)]_2^+$, 269 (9) $[V_2O_2Cl(CH_3CN)(C_3H_7O)]^+$, 260 (4) $[V_2O_3Cl(OCH_2CH_2OMe)]^+$, 217 (29)

$[VO(OCH_2CH_2OMe)_2]^+$, 142 (2) $[VO(OCH_2CH_2OMe)]^+$, 76 (2) $[HOCH_2CH_2OMe]^+$, 59 (29) $[C_3H_7O]^+$, 41 (100) $[CH_3CN]^+$, 36 (70) $[HCl]^+$.

MS (221 °C): *m/z* (%) = 354 (59) $[VOCl(OCH_2CH_2OMe)]_2^+$, 318 (13) $[V_2O_2Cl_2(OCH_2CH_2OMe)_2 - HCl]^+$, 279 (13) $[V_2O_2Cl_2(OCH_2CH_2OMe)]^+$, 260 (12) $[V_2O_3Cl(OCH_2CH_2OMe)]^+$, 217 (85) $[VO(OCH_2CH_2OMe)_2]^+$, 142 (6) $[VO(OCH_2CH_2OMe)]^+$, 76 (3) $[HOCH_2CH_2OMe]^+$, 59 (100) $[C_3H_7O]^+$.

ESR (20 °C, CH_3CN): $g_i = 1.9727$, $A(^{51}V) = 10.94$ mT.

Anal. Calc. for $C_5H_{11}Cl_2NO_3V$ (255.00): C 23.55, H 4.35, N 5.49. Found: C 23.91, H 4.15, N 6.08.

3.3.20 $[VOCl_2(\eta^2\text{-}HOCH_2CH_2OC_2H_5)(CH_3CN)]$ (18)

$[VOCl(OCH_2CH_2OC_2H_5)]_2$ (0.32 g, 0.8 mmol) was dissolved in CH_3CN (50 mL) at room temperature giving a blue solution, which was concentrated to about 15 mL and stored at –30 °C for several days. Bright blue crystals suitable for X-ray diffraction were isolated. After decantation and concentration of the mother solution followed by standing at –30 °C for several days another portion of crystals was isolated.

Yield: 0.21 g (0.8 mmol, 50%).

M.p.: 132 °C.

IR (KRS-5, Nujol mull): ν = 3134 s (O–H), 2319 s (C≡N), 2293 s (C≡N), 2250 w, 1956 w, 1252 m, 1232 m, 1114 w (V–O–C), 1091 m (C–O), 1063 s (C–O), 1025 s (V=O), 1005 m, 981 vs, 943 m, 924 m (C–O–C), 895 s (C–O–C), 815 w, 785 s, 712 m, 594 m, 551 m, 491 m, 443 w, 413 m, 385 w, 335 vs (V–Cl) cm^{-1}.

MS (143 °C): *m/z* (%) = 382 (22) $[VOCl(OCH_2CH_2OEt)]_2^+$, 293 (7) $[V_2O_2Cl_2(OCH_2CH_2OEt)]^+$, 274 (13) $[V_2O_3Cl(OCH_2CH_2OEt)]^+$, 258 (5) $[V_2O_2Cl(OCH_2CH_2OEt)]^+$, 245 (29) $[VO(OCH_2CH_2OEt)_2]^+$, 156 (2) $[VO(OCH_2CH_2OEt)]^+$, 73 (24) $[C_4H_9O]^+$, 45 (35) $[C_2H_5O]^+$, 41 (82) $[CH_3CN]^+$, 36 (9) $[HCl]^+$.

MS (221 °C): *m/z* (%) = 382 (62) $[VOCl(OCH_2CH_2OEt)]_2^+$, 293 (23) $[V_2O_2Cl_2(OCH_2CH_2OEt)]^+$, 245 (100) $[VO(OCH_2CH_2OEt)_2]^+$, 156 (7) $[VO(OCH_2CH_2OEt)]^+$, 73 (69) $[C_4H_9O]^+$, 45 (75) $[C_2H_5O]^+$, 36 (9) $[HCl]^+$.

ESR (20 °C, CH_3CN): $g_i = 1.98$, $A(^{51}V) = 10.74$ mT.

Anal. Calc. for $C_6H_{13}Cl_2NO_3V$ (269.02): C 26.79, H 4.87, N 5.21. Found: C 26.63, H 4.61, N 5.29.

3.3.21 $[VOCl_2\{\eta^2\text{-}HOCH_2(cyclo\text{-}C_4H_7O)\}(CH_3CN)]$ (19)

$[VOCl_2\{OCH_2(cyclo\text{-}C_4H_7O)\}]_2$ (0.50 g, 1.0 mmol) was dissolved in CH_3CN/toluene (2 mL/8 mL) at room temperature giving rise to a red solution, which was kept at –30 °C for several weeks without color change. When standing in sunlight for several weeks it turned into dark blue. Blue crystals were isolated.

Yield: 0.18 g (0.6 mmol, 32%).

M.p.: 122 °C.

IR: (KRS-5, Nujol mull) ν = 3088 s (O–H), 2315 s (C≡N), 2288 s (C≡N), 1619 w, 1272 m, 1239 m, 1226 m, 1137 w, 1096 w, 1047 s (C–O), 1028 s (V=O), 980 vs, 933 s (C–O–C), 923 s (C–O–C), 855 m, 812 s, 679 w, 645 w, 598 w, 565 vw, 516 w, 436 w, 413 m, 396 m, 365 m, 324 vs (V–Cl), 286 m cm^{-1}.

MS (179 °C) *m*/*z* (%) = 406 (37) $[VOCl(thffo)]_2^+$, 371 (16) $[V_2O_2Cl(thffo)]^+$, 340 (6) $[V_2O_2Cl_2(thffo)_2 - HCl - CH_2O]^+$, 269 (53) $[VO(thffo)_2]^+$, 85 (100) $[CH_2cyclo\text{-}(C_4H_7O)]^+$, 36 (56) $[HCl]^+$.

ESR (20 °C, THF): g_i = 1.9695, A(^{51}V) = 11.12 mT.

Anal. Calc. for $C_7H_{13}Cl_2NO_3V$ (281.03): C 29.92, H 4.66, N 4.98. Found: C 30.02, H 4.56, N 4.92.

3.4 Polymerization and Oligomerization

3.4.1 Ethylene Polymerization

The polymerization of ethylene was carried out either in a Schlenk tube or in a glass autoclave (1 L) equipped with a mechanical stirrer. For Schlenk tube polymerization, toluene (50 mL), MAO (0.8 mmol), vanadium catalyst, and MTCA (0.8 mmol) were stirred for 10 min. Afterwards ethylene was polymerized at room temperature at an ethylene pressure of 1 bar. For autoclave polymerization, toluene (200 mL), MAO, and MTCA were injected sequentially into the autoclave at 30 °C, and the mixture was stirred for 15 min. The vanadium precatalyst was then injected into the reactor and allowed to interact with MAO for 10 min. In the case of DEAC the cocatalyst solution was divided into two parts: one half was injected into the autoclave together with MTCA and the other half was used to activate the sample of precatalyst solution for 15 min prior to injection into the reactor. The ethylene pressure in the autoclave was kept at 2 bar during all polymerizations. Polymerizations were quenched with a 5% solution of HCl in ethanol (150 mL). The mixtures were poured into water (150 mL) and stirred for 30 min. The white precipitate was collected by filtration,

washed with ethanol, and dried at 60 °C to a constant weight. Molecular masses and polydispersities were determined by GPC.

Table 3.1. Ethylene polymerization results.

Entry	Cocatalyst	$[V]_0$ mmol L^{-1}	[Al]/[V] *n*/*n*	PE g	Activity kg PE (mol[V])$^{-1}$ h bar^{-1}	10^{-3} M_w g mol^{-1}	10^{-3} M_n g mol^{-1}	M_w/M_n
1[a], [e]	MAO	0.2	80	0.50	100	954	87	11.0
2[b], [e]	MAO	0.1	100	0.12	6	1084	119	9.9
3[b], [e]	MAO	0.02	400	1.80	300	1414	168	8.4
4[b], [e]	MAO	0.02	1000	0.06	15	1169	155	8.5
5[f], [g]	MAO	0.02	400	0.01	3	[c]	[c]	[c]
6[b], [e]	DEAC	0.1	100	11.12	560	586	60	8.9
7[b], [e]	DEAC	0.1	20	6.44	320	696	110	6.3
8[b], [f]	DEAC	0.1	100	7.10	360	390	34	11.4
9[d], [e]	DEAC	0.02	100	2.25	560	[h]	[h]	[h]

[a] Schlenk tube; *p*(ethylene) = 1 bar, 30 min at 22 °C; solvent: toluene; [Al]/[MTCA] = 1:2.5.
[b] Glass autoclave; *p*(ethylene) = 2 bar, 30 min at 30 °C; solvent: toluene; [Al]/[MTCA] = 1:1.
[c] Entry 5 contained a substantial amount of insoluble material resulting in very poor data detection.
[d] Glass autoclave; *p*(ethylene) = 2 bar, 30 min at 30 °C; solvent: toluene; [Al]/[MTCA] = 1:5.
[e] Precatalyst: $[VOCl_2(OCH_2CH_2OCH_3)]_2$.
[f] Precatalyst: $VOCl_3$.
[g] Glass autoclave; *p*(ethylene) = 2 bar, 30 min at 30 °C; solvent: toluene; [Al]/[MTCA] = 1:1.25.
[h] Not measured

3.4.2 1-Hexene Oligomerization

The oligomerization was performed over a period of 24 h in a 100 mL Schlenk flask with DEAC as cocatalyst at 22 °C. The vanadium catalyst (0.01 mmol, 0.01 M[V] in toluene) was stirred together with half of the DEAC (0.5 mmol, 2.5 mL, 0.2 M in toluene) for 15 min prior to injection into the oligomerization flask, which was charged with 20 mL of 1-hexene. The other half of the DEAC (0.5 mmol, 2.5 mL, 0.2 M in toluene) and MTCA (1 mmol, 0.13 mL) were injected into the autoclave under stirring. The oligomerization was quenched with 10 mL of a 1:1 mixture of dilute HCl and ethanol. This mixture was poured into a separating funnel charged with 100 mL of water. The water phase was extracted with diethyl ether (3 · 50 mL), the organic phase was further washed with 2 · 50 mL of water till neutral. The organic phases were combined and dried with Na_2SO_4 overnight. All solvents were evaporated by rotary evaporator. The remaining sticky oils were dried in vacuum (10^{-2} mbar) and characterized by GPC.

Table 3.2. 1-Hexene oligomerization with vanadium(V) complexes.[a]

Entry	Precatalyst	Yield g
1a	$VOCl_3$	0.34
1b		0.38
2a	$[VOCl_2(OCH_2CH_2OMe)]_2$	0.35
2b		0.34
3a	$[VOCl_2(OCH_2CH_2OEt)]_2$	0.56
3b		0.54
4a	$[VOCl_2(OCH_2CH_2O^iPr)]_2$	3.06
4b		3.51
5a	$[VOCl_2(thffo)]_2$ (**5**)	0.50
5b		0.41
6a	$[VOCl_2(OCH_2CH_2OEt)(THF)]$ (**7**)	0.55
6b		0.55
7a	$[VOCl_2[OCH_2CH_2O^iPr](THF)]$ (**8**)	0.46
7b		0.47
8a	$[VOCl_2(OCH_2CH_2OPh)]$	0.31
8b		0.42

[a] 20 mL of 1-hexene were employed for each entry.

3.4.3 Styrene and 1-Decene Oligomerization

Styrene and 1-decene polymerization reactions were performed in a 50-mL Schlenk flask and an external temperature-controlled bath on a Schlenk line. In a typical procedure, toluene (10 mL) and MAO (2 mmol) were loaded into the Schlenk flask. The vanadium compound (0.05 mmol based on vanadium atoms) was then added as a toluene solution (0.01 M) and the mixture was stirred at room temperature for 5 min. After the external bath temperature had been stabilized, MTCA (2 mmol) and the monomer (3 mL) were added with a syringe. The oligomerization was performed over a period of 20 h for styrene. The oligomerization was terminated by addition of acidic methanol (MeOH/HCl = 10:1; 3 mL). The product was precipitated into ethanol (200 mL), filtered off, and dried under vacuum. The molecular mass and the molecular mass distribution of oligostyrene were determined by GPC.

Table 3.3. Styrene oligomerization with $[VOCl_2(OCH_2CH_2OCH_3)]_2$.[a]

Entry	T °C	Yield g	Conversion (%)	M_w g mol^{-1}	M_n g mol^{-1}	M_w/M_n
1	23	2.72	99.6	2900	1200	2.3
2	40	2.33	85.3	3000	1500	2.0
3	50	1.94	71.1	2700	1600	1.7

[a] Reaction conditions: V catalyst/styrene/MAO/MTCA = 1:520:40:40.

The oligomerization of 1-decene with $[VOCl_2(OCH_2CH_2OMe)]_2$ and $[VOCl_2(OCH_2CH_2OPh)]$ resulted in 0.19 g and 0.20 g of oligmer over a period of 1.5 h at 23 °C, respectively.

3.5 Cyclooctene Epoxidation

3.5.1 Handling of TBHP

Assay of the TBHP solution is determined by iodometric titration. The concentration is 5.83 M. The following rules should be applied when handling solutions of TBHP: never add a strong acid or transition metal salts to high strength TBHP solutions, never work with pure TBHP and avoid using high strength solutions whenever possible. TBHP solutions should not be stored in glass bottles due to the slight danger of gas evolution.

3.5.2 Epoxidation Procedure

To a 100 mL Schlenk flask were added 1.5–2.0 g of 3 Å molecular sieves, 50 mL of CH_2Cl_2, and 0.1 mmol of vanadium catalyst (based on $VOCl_2(OR)$). The system was cooled with liquid nitrogen and TBHP (5.2 mL, 15.0 mmol) dried with 3 Å molecular sieve was layerd on the frozen solution. The system was allowed to warm to room temperature under stirring. The solution turned from brown into dark red and 1.10 g (10.0 mmol) of cyclooctene were added after 10 min. The system was allowed to warm to ambient temperature within 0.5 h with the solution turning into light yellow. The solution was refluxed under stirring for 24 h followed by addition of MnO_2 into the reaction system to destroy excess TBHP. The mixture was filtered and washed with water ($3 \cdot 100$ mL) till neutral. The organic phase was dried overnight with Na_2SO_4 and then filtered. After removal of the volatiles under reduced pressure, colorless liquids containing a mixture of cyclooctene, decane, and cyclooctene oxide were obtained.

Table 3.4. Cyclooctene oxidation studies in a vanadium/TBHP system.

Precatalyst	Output g	Calculated yield g	(%)	Conversion (%)
$[VOCl_2(OCH_2CH_2OMe)]_2$	1.65	0.74	45	59
$[VOCl_2(OCH_2CH_2OEt)]_2$	1.59	0.86	54	68
$[VOCl_2(OCH_2CH_2O^iPr)]_2$	1.80	0.86	48	69
$[VOCl_2(mmp)]_2$ (**4**)	1.68	0.89	53	71
$[VOCl_2(thffo)]$ (**5**)	1.72	0.67	39	50
$[VOCl_2(OCH_2CH_2OCH_2CH_2OBu)]$ (**10**)	1.77	0.86	48	68
$[VOCl_2(OCH_2CH_2OPh)]$	1.86	0.77	41	61

[V]:[TBHP]:[cyclooctene] = 1:150:100. 24 h at 40 °C; solvent: CH_2Cl_2.

The yields were calculated according to the relative intensities of the characteristic signals of the four components in ^{1}H-NMR. Thus, the characteristic resonance for C*H*C*H* (2H) in cyclooctene, CH_2 (2H) in CH_2Cl_2, C*H*C*H* (2H) in cyclooctene oxide, and CH_3 (6H) in nonane appears at 5.6 ppm, 5.3 ppm, 2.8 ppm, and 0.8–0.9 ppm, respectively. The results are listed in Table 3.4.

4 Summary and Outlook

In this work a series of novel oxovanadium complexes with alkoxide, ketone, and alcohol ligands has been synthesized and characterized by means of NMR (^{1}H, ^{13}C, ^{51}V), IR, MS and X-ray crystallography. Selected oxovanadium complexes with alkoxyalkoxide ligands were tested for olefin polymerization and epoxidation reactions.

Simple alkoxo complexes **1** and **2** were synthesized and structurally characterized (Scheme 4.1). It has been shown that different starting materials have a great influence on the final product. Complex **1** was obtained from the reaction of $VOCl_3$ with CH_3OH, while complex **2** was prepared from the reaction of $VOCl_3$ with CH_3ONa.

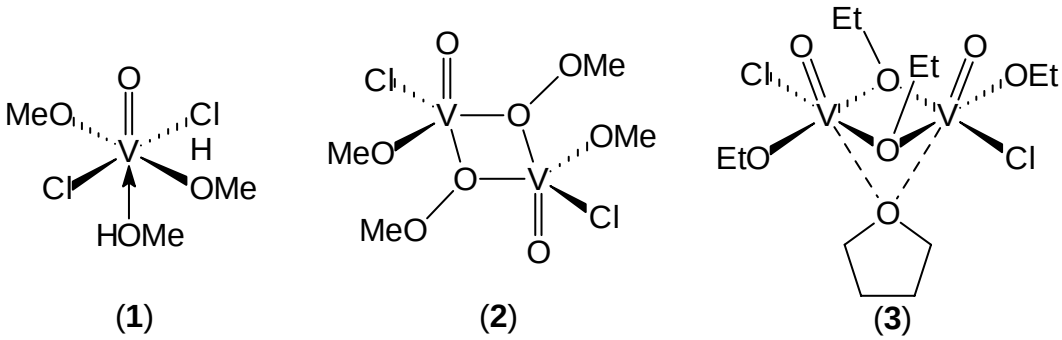

Scheme 4.1. Simple oxovanadium methoxides and ethoxide **1**–**3**.

Reaction of $VOCl_3$ with C_2H_5ONa in THF produced an unprecedented dinuclear alkoxo chloro vanadium(V) complex **3**, which represents the first structurally characterized example of a vanadium(V) alkoxide with *syn*-orientated oxo groups due to the weak coordination of the THF ligand to both vanadium atoms (Scheme 4.1).

Chloride bridged vanadium(V) complexes **4** and **5** have been synthesized from the reaction of $VOCl_3$ with the corresponding alcohols (Scheme 4.2). Complexes **4** and **5** show an enhanced thermal stability compared to the simple alkoxo chloro vanadium(V) complexes **1**–**3**.

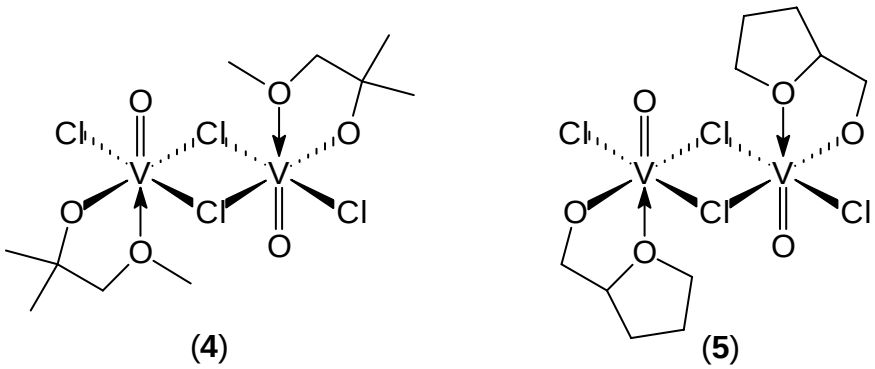

Scheme 4.2. Chloride bridged oxovanadium(V) complexes **4** and **5**.

A series of alkoxyalkoxo chloro vanadium(V) complexes were reacted with THF, PPh_3, and CH_3CN in order to study the reactivity of the chloro bridge in the presence of Lewis bases. Reactions of $[VOCl_2(OCH_2CH_2OR)]_2$ (R = Me, Et, ^{i}Pr) and **4** with THF produced monomeric solvates **6–9** (Scheme 4.3). This reaction is reversible as demonstrated by quantitative recovery of the dimeric complexes when removing the THF from **6–9** under vacuum.

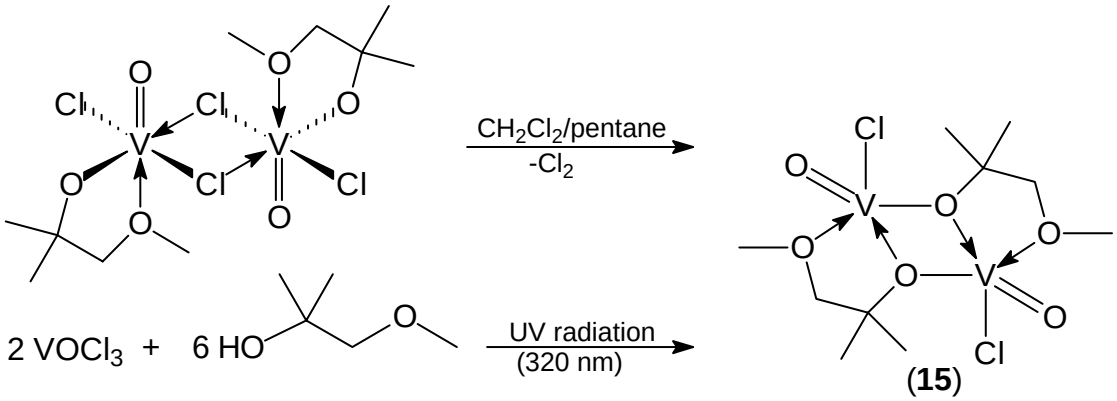

Scheme 4.3. Reaction of chloride bridged dimers with tetrahydrofuran.

Complex **10** containing a tridentate $[O,O,O]^-$ alkoxo ligand was synthesized and structurally characterized (Scheme 4.4). The alkoxo ligand in the monomeric complex adopts a meridional configuration in the solid state.

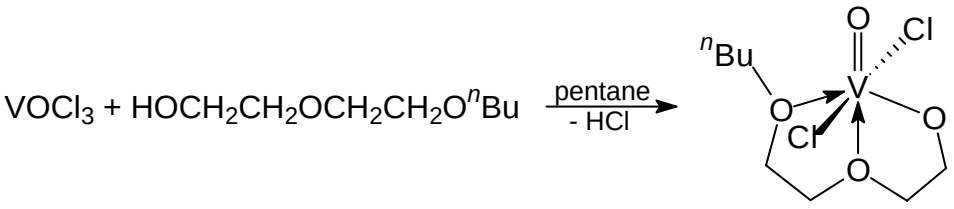

Scheme 4.4. Preparation of complex **10**.

Treatment of $VOCl_3$ with 2 equiv of $HOCH_2(cyclo\text{-}C_4H_7O)$ afforded $[VOCl_2(thffo)(Hthffo)]$ (**11**), which eliminates 1 equiv of HCl to produce $[VOCl(thffo)_2]$ (**12**) (Scheme 4.5). The dimeric chloride bridged complex **5** as well as **11** and **12** decompose to give vanadium(IV) complex $[VOCl\{\mu,\eta^2\text{-}OCH_2(cyclo\text{-}C_4H_7O)\}]_2$.

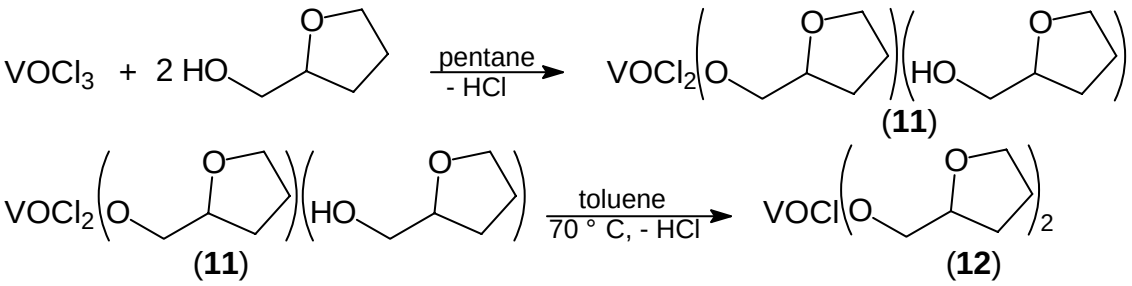

Scheme 4.5. Preparation of tetrahydrofurfuryl coordinated oxovanadium complexes **11–12**.

Oxovanadium trisalkoxide $[VO\{OC(CH_3)_2CH_2OCH_3\}_3]$ was prepared in good yield by reaction of $VOCl_3$ and the corresponding lithium alcoholate (Scheme 4.6). The solution species was probed by means of ^{51}V-NMR and MS. Both agree with a monomeric species of **13** in solution or in the gas phase.

$$VOCl_3 + 3\ LiOCMe_2CH_2OMe \xrightarrow[-\ 3\ LiCl]{pentane} VO(OCMe_2CH_2OMe)_3$$

Scheme 4.6. Preparation of oxovanadium trisalkoxide **13**.

Treatment of $HOC(Ph)_2C(Ph)_2OH$ with $VOCl_3$ led to cleavage of the C–C bond accompanied by reduction of the vanadium(V) center to vanadium(IV) (Scheme 4.7). A novel benzophenone coordinated complex $[VOCl_2(O{=}CPh_2)_2]$ (**14**) was isolated. This reaction is of interest in selective organic synthesis. Synthesis of **14** from $VOCl_2(THF)_2$ and benzophenone was also achieved.

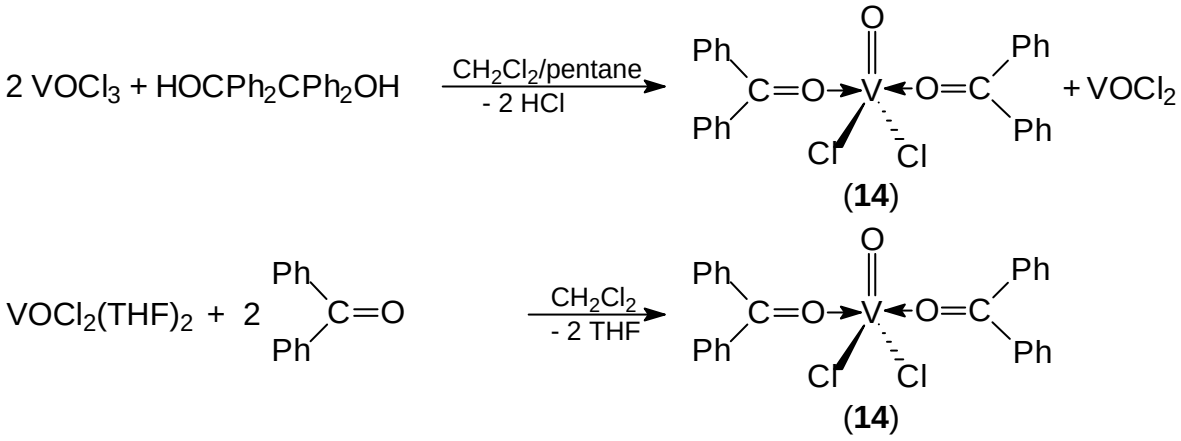

Scheme 4.7. Preparation of ketone coordinated oxovanadium(IV) dichloride **14**.

Reaction of $[VOCl_2(OCH_2CH_2OCH_3)]_2$ with PPh_3 in CH_2Cl_2 led to abstraction of the alkoxyalkoxo ligand from the vanadium center, while the vanadium(V) complex was reduced by PPh_3 to produce the neutral vanadium(IV) adduct $[VOCl_2(O{=}PPh_3)_2]\cdot CH_2Cl_2$ (Scheme 4.8).

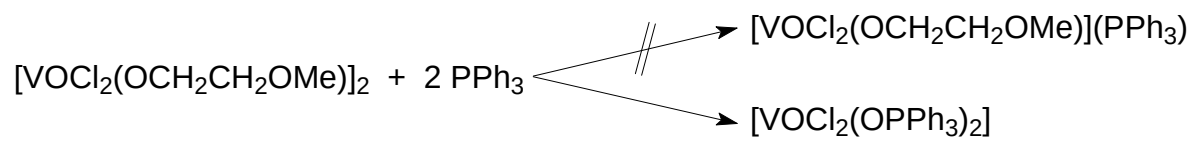

Scheme 4.8. Reactions of $[VOCl_2(OCH_2CH_2OMe)]_2$ with PPh_3.

Complex **4** was reduced both in solution and in the solid state giving rise to **15** (Scheme 4.9). The reaction occurs *via* chloride ligand oxidation with release of Cl_2. This complex is a dimer

with alkoxide bridges. An alternative way to **15** was the reaction of $VOCl_3$ with more than 2 equiv of alcohol under UV radiation.

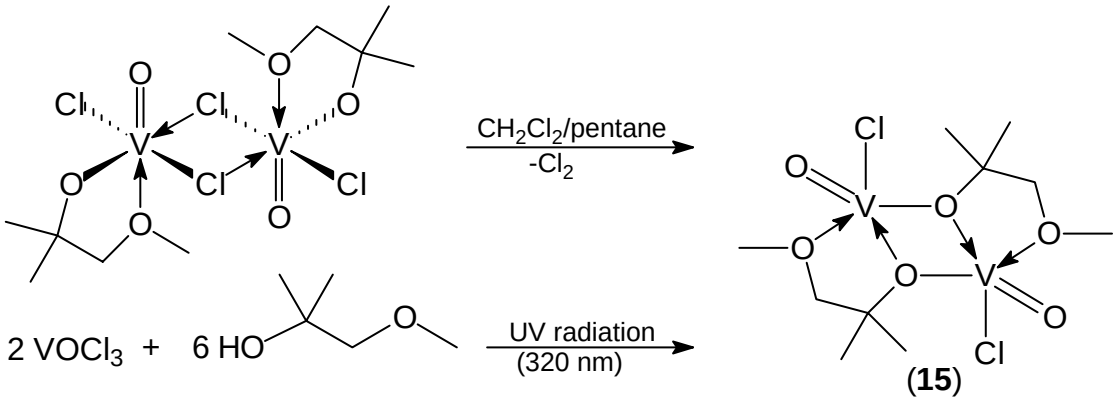

Scheme 4.9. Preparation of oxovanadium(V) alkoxide **15**.

CH_3CN reacted with $[VOCl_2(OCH_2CH_2OCH_3)]_2$ leading to cleavage of the chloro bridge and yielding monomeric $[VOCl_2(OCH_2CH_2OCH_3)(CH_3CN)]$ **16**, which was slowly reduced to vanadium(IV) complex **17** (Scheme 4.10). Similar to preparation of **17**, complexes **18** and **19** were synthesized by reduction of $[VOCl_2(OCH_2CH_2OC_2H_5)]_2$ and **5** in CH_3CN under UV radiation. Complexes **17**–**19** differ from **16** by the chelating ligand, which is an alcoholate in **16**, while it is an alcohol in **17**–**19**.

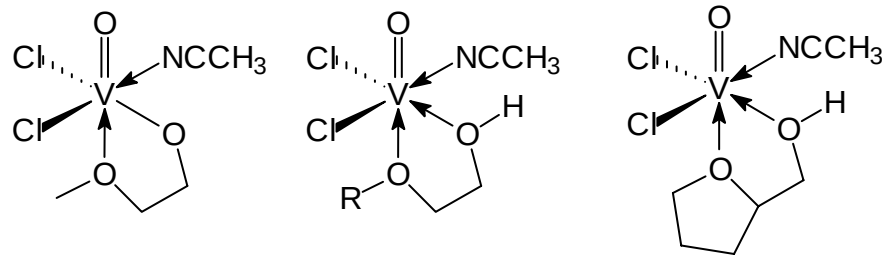

Scheme 4.10. Acetonitrile coordinated oxovanadium complexes **16**–**19**.

Dimeric complex $[VOCl_2(OCH_2CH_2OCH_3)]_2$ is a good catalyst precursor for olefin polymerization when activated with DEAC or MAO. It displayed a remarkably higher activity than a $VOCl_3$ based catalyst under the same conditions. The lifetime of the catalytic species sustained over 30 min in presence of MTCA. Without MTCA the polymerization was initiated with very high activity but resulted in a rather low overall productivity. The activity increases with enhancement of the Al:V ratio. The polymers presented high molecular weights and rather high polydispersities. Polymerization activated by MAO displayed much lower activities compared with that activated by DEAC. $[VOCl_2(OCH_2CH_2OCH_3)]_2$ catalyzed styrene and 1-decene oligomerization with MAO as cocatalyst and MTCA as promoter. The

activity for styrene oligomerization was ten times higher than that for 1-decene oligomerization. The 1-hexene oligomerization with different vanadium(V) complexes in combination with DEAC revealed that under the same conditions the activity is independent from the catalyst precursor used. Besides, the activity of $[VOCl_2(OCH_2CH_2O^iPr)]_2$ stands out from the other complexes.

Oxovanadium(V) complexes $[VOCl_2(OCH_2CH_2OR)]_2$ (R = Me, Et, ^{i}Pr), $[VOCl_2(mmp)]_2$ (**4**), $[VOCl_2(thffo)]_2$ (**5**), $[VOCl_2(OCH_2CH_2OCH_2CH_2OBu)]$ (**10**), and $[VOCl_2(OCH_2CH_2OPh)]$ catalyze the epoxidation of *cis*-cyclooctene to give moderate yields of cyclooctene oxide.

The focus of the work reported here has been the synthesis and characterization of oxovanadium complexes bearing alkoxide, ketone, and alcohol ligands as well as the catalysis in olefin polymerization and epoxidation.

A continuation of this work would be:

• Synthesis of oxovanadium(V) complexes with a combination of alkoxide and other ligand systems.

• Synthesis of oxovanadium(V) alkoxides containg vanadium-carbon bonds.

• Exploration of oxovanadium(V) alkoxides with enantiomerically pure chiral centers on the alkoxide ligand.

• Exploration of possible applications of the oxovanadium(V) complexes in organic synthesis and catalysis.

5 Appendix

5.1 Crystal Data and Refinement Details

	1	**2**	**3**
Emperical formula	$C_3H_{11}Cl_2O_4V$	$C_2H_6ClO_3V$	$C_{12}H_{28}Cl_2O_7V$
M/g·mol^{-1}	232.96	164.46	457.12
Temperature/°C	–100	–100	–100
Wavelength/Å	0.71073	0.71069	0.71073
Crystal system	monoclinic	triclinic	monoclinic
Space group	$P2_1/n$ (No. 14)	$P\bar{1}$ (No. 2)	$P2_1/c$ (No. 14)
a/Å	9.0797(2)	5.915(5)	8.4927(1)
b/Å	10.6658(1)	6.233(5)	11.0587(1)
c/Å	9.6127(1)	8.293(5)	22.0910(4)
α / °	90	83.341(5)	90
β / °	99.425(1)	75.780(5)	100.3000(1)
γ / °	90	81.307(5)	90
V/Å^3	918.35(2)	292.0(4)	2041.31(5)
Z	4	2	4
D_c/g·cm^{-3}	1.685	1.871	1.487
μ/mm^{-1}	1.624	2.056	1.203
F(000)	472	164	944
Crystal size/mm^3	0.18 · 0.48 · 0.16	0.58 · 0.28 · 0.26	0.44 · 0.44 · 0.28
θ range/°	2.86 to 27.49	2.54 to 27.50	1.87 to 25.00
hlk range	–10 to 11	–7 to 6	–10 to 10
	–13 to 11	–6 to 8	–9 to 13
	–12 to 12	–10 to 10	–26 to 26
No. reflns. collected	6769	2248	12153
No. indep. reflns. (R_{int})	2107 (0.0446)	1332 (0.0343)	3589 (0.0862)
T_{max}/T_{min}	0.8258/0.5319	0.6690/0.3773	0.7812/0.5026
No. data/restraints/params	2107/0/102	1332/0/66	3589/0/212
Goodness-of-fit on F^2	1.001	1.032	1.007
Final R indices [I>2σ (I)]	R_1 = 0.0352	R_1 = 0.0428	R_1 = 0.0618
	wR_2 = 0.0784	wR_2 = 0.1089	wR_2 = 0.1470
R indices (all data)	R_1 = 0.0477	R_1 = 0.0453,	R_1 = 0.0894
	wR_2 = 0.0831	wR_2 = 0.1110	wR_2 = 0.1603
$\Delta\rho_{max}$, $\Delta\rho_{min}$/e·Å^{-3}	0.391 and –0.591	0.576 and –0.993	0.872 and –0.744

	10	**14**	**$VOCl_2(O=PPh_3)_2 \cdot CH_2Cl_2$**
Emperical formula	$C_{16}H_{34}Cl_4O_8V_2$	$C_{30}H_{28}Cl_2NO_4V$	$C_{37}H_{32}Cl_4O_3P_2V$
M/g·mol^{-1}	598.11	574.36	432.12
Temperature/°C	–100	–100	–100
Wavelength/Å	0.71073	0.71073	0.71073
Crystal system	triclinic	monoclinic	monoclinic
Space group	$P\bar{1}$ (No. 2)	$C2/c$ (No. 15)	$P2_1/n$ (No. 14)
a/Å	7.4536(1)	14.0603(9)	9.5129(3)
b/Å	11.4397(2)	14.2943(10)	15.2796(4)
c/Å	15.3981(2)	16.4428(10)	13.9698(4)
α / °	96.650(1)	90	90
β / °	96.230(1)	114.854(2)	99.5052(2)
γ / °	91.864(1)	90	90
V/Å^3	1295.07(3)	2998.6(3)	2002.68(10)
Z	2	4	2
D_c/g·cm^{-3}	1.534	1.272	1.433
μ/mm^{-1}	1.170	0.540	0.763
F(000)	616	1188	882
Crystal size/mm^3	0.5 · 0.24 · 0.1	0.32 · 0.24 · 0.15	0.36 · 0.30 · 0.26
θ range/°	1.34 to 27.00	2.14 to 25.00	1.99 to 27.50
hlk range	–9 to 9	–15 to 16	–12 to 12
	–11 to 14	–16 to 10	–13 to 19
	–19 to 19	–19 to 19	–18 to18
No. reflns. collected	9497	9122	14875
No. indep. reflns. (R_{int})	5578 (0.0477)	2629 (0.1109)	4584 (0.0784)
T_{max}/T_{min}	0.9552/0.4970	0.9412/0.3948	0.8637/0.6097
No. data/restraints/params	5578/0/273	2629/0/169	4584/0/236
Goodness-of-fit on F^2	0.996	1.042	0.971
Final R indices [I>2σ (I)]	R_1 = 0.0511	R_1 = 0.0650,	R_1 = 0.0482
	wR_2 = 0.1362	wR_2 = 0.1644	wR_2 = 0.1014
R indices (all data)	R_1 = 0.0751	R_1 = 0.0922,	R_1 = 0.0856
	wR_2 = 0.1492	wR_2 = 0.1813	wR_2 = 0.1148
$\Delta\rho_{max}$, $\Delta\rho_{min}$/e·Å^{-3}	1.074 and –0.616	1.337 and –0.582	0.423 and –0.485

	15	**16**	**17**
Emperical formula	$C_{20}H_{44}ClO_{12}V_4$	$C_5H_{10}Cl_2NO_3V$	$C_5H_{11}Cl_2NO_3V$
M/g·mol^{-1}	822.11	253.98	254.99
Temperature/°C	–100	–100	–100
Wavelength/Å	0.71073	0.71073	0.71073
Crystal system	triclinic	orthorhombic	monoclinic
Space group	$P\bar{1}$ (No. 2)	$P2_12_12_1$ (No. 19)	$P2_1/c$ (No. 14)
a/Å	6.47150(10)	6.7749(3)	7.0730(6)
b/Å	9.39820(10)	11.0999(4)	12.4465(10)
c/Å	14.81330(10)	13.4468(5)	11.6856(10)
α / °	84.590(1)	90	90
β / °	87.6820(10)	90	94.073(2)
γ / °	1.7260(10)	90	90
V/Å^3	887.278(18)	1011.21(7)	1026.13(15)
Z	1	4	4
D_c/g·cm^{-3}	1.539	1.668	1.651
μ/mm^{-1}	1.370	1.478	1.457
F(000)	420	512	516
Crystal size/mm^3	0.62 · 0.30 · 0.28	0.50 · 0.35 · 0.18	0.50 · 0.48 · 0.24
θ range/°	1.38 to 27.50	2.38 to 30.00	2.89 to 22.49
hlk range	–8 to8	–8 to 9	–6 to 7
	–11 to 12	–14 to 15	–11 to 11
	–19 to 15	–18 to 18	–12 to 12
No. reflns. collected	6711	9164	2359
No. indep. reflns. (R_{int})	4020 (0.0369)	2954 (0.0711)	926 (0.0263)
T_{max}/T_{min}	0.7504/0.2949	0.8215/0.5434	0.7212/0.5295
No. data/restraints/params	4020/0/187	2954/0/111	926/0/115
Goodness-of-fit on F^2	1.068	1.005	1.043
Final R indices [I>2σ (I)]	R_1 = 0.0573	R_1 = 0.0377	R_1 = 0.0274
	wR_2 = 0.1519	wR_2 = 0.0716	wR_2 = 0.0821
R indices (all data)	R_1 = 0.0691	R_1 = 0.0484	R_1 = 0.0274
	wR_2 = 0.1602	wR_2 = 0.0752	wR_2 = 0.0821
$\Delta\rho_{max}$, $\Delta\rho_{min}$/e·Å^{-3}	2.386 and –0.695	0.345 and –0.409	0.344 and –0.423

	18	**19**
Emperical formula	$C_6H_{13}Cl_2NO_3V$	$C_7H_{13}Cl_2NO_3V$
M/g·mol^{-1}	269.01	281.02
Temperature/°C	–100	–100
Wavelength/Å	0.71073	0.71073
Crystal system	monoclinic	monoclinic
Space group	$P2_1/c$ (No. 14)	$P2_1/c$ (No. 14)
a/Å	7.15650(10)	8.0946(3)
b/Å	12.3024(2)	12.0495(4)
c/Å	13.2547(2)	12.4318(5)
α / °	99.9410(10)	90
β / °	90	102.3960(10)
γ / °	90	90
V/Å^3	1149.45(3)	1184.28(8)
Z	4	4
D_c/g·cm^{-3}	1.549	1.576
μ/mm^{-1}	1.305	1.271
F(000)	544	572
Crystal size/mm^3	0.36 · 0.26 · 0.18	0.40 · 0.36 · 0.28
θ range/°	2.27 to 27.50	2.38 to 25.00
hlk range	–9 to 8	–8 to 9
	–15 to 15	–13 to 14
	–16 to 17	–14 to 13
No. reflns. collected	8584	7327
No. indep. reflns. (R_{int})	2638 (0.0499)	2080 (0.0812)
T_{max}/T_{min}	0.8411/0.6018	0.7174/0.6304
No. data/restraints/params	2638/0/124	2080/6/175
Goodness-of-fit on F^2	1.016	1.053
Final R indices [I>2σ (I)]	R_1 = 0.0292	R_1 = 0.0523
	wR_2 = 0.0661	wR_2 = 0.1269
R indices (all data)	R_1 = 0.0362	R_1 = 0.0599
	wR_2 = 0.0685	wR_2 = 0.1324
$\Delta\rho_{max}$, $\Delta\rho_{min}$/e·Å^{-3}	0.325 and –0.718	0.498 and –0.662

5.2 Packing Diagrams of Single Crystals

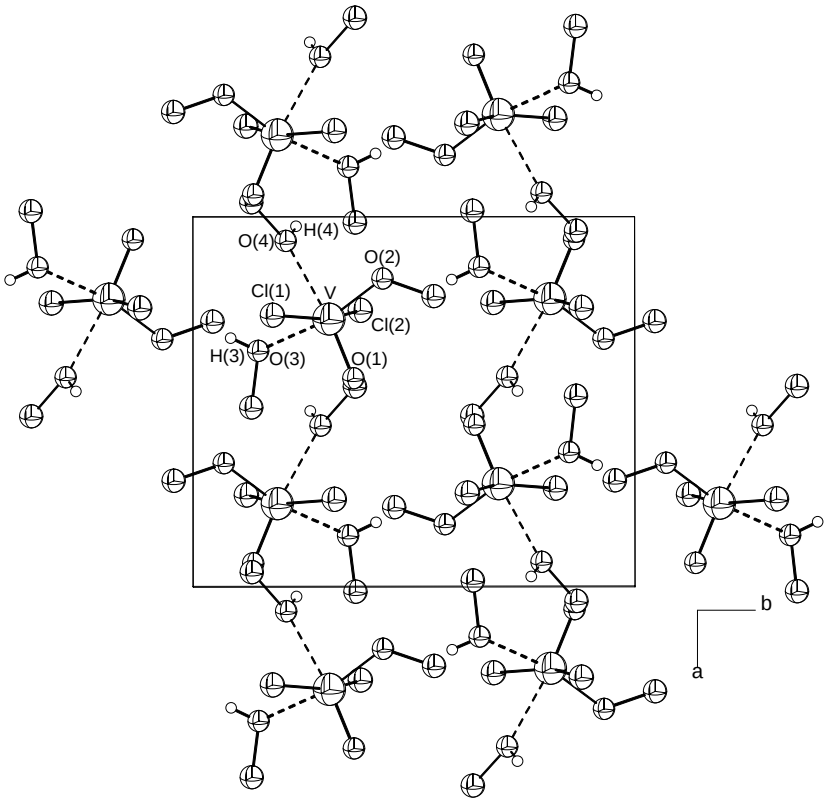

Fig. 5.1. Packing diagram for **1**.

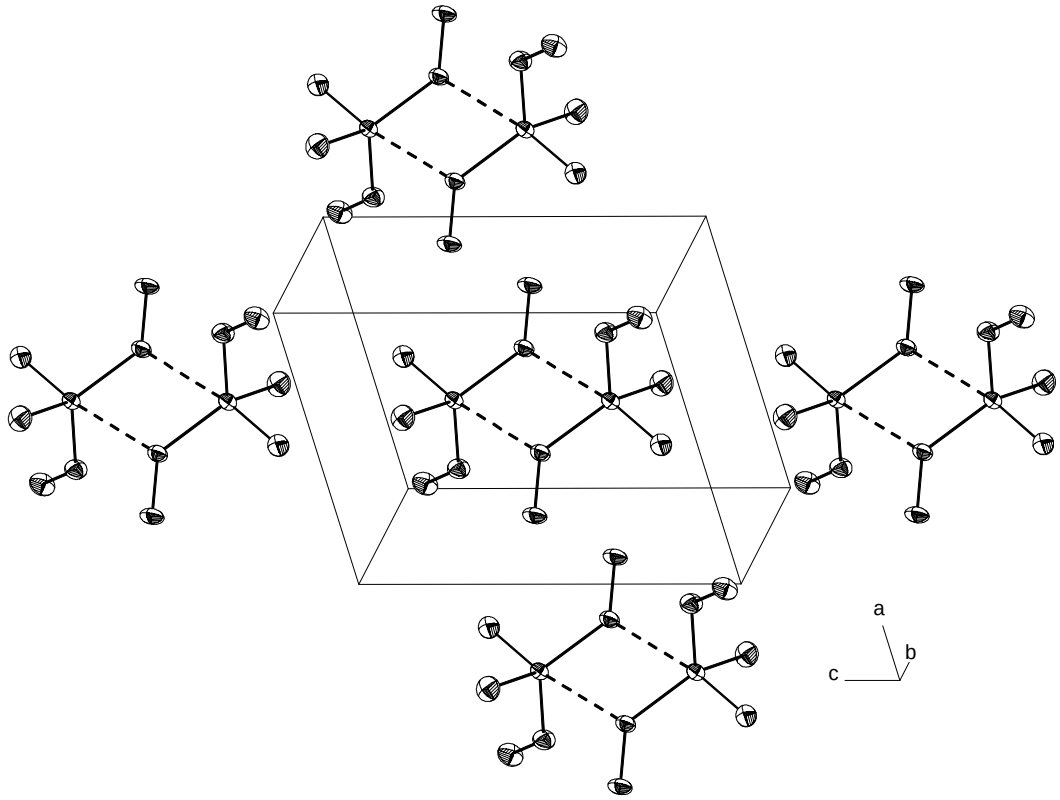

Fig. 5.2. Packing diagram for **2**.

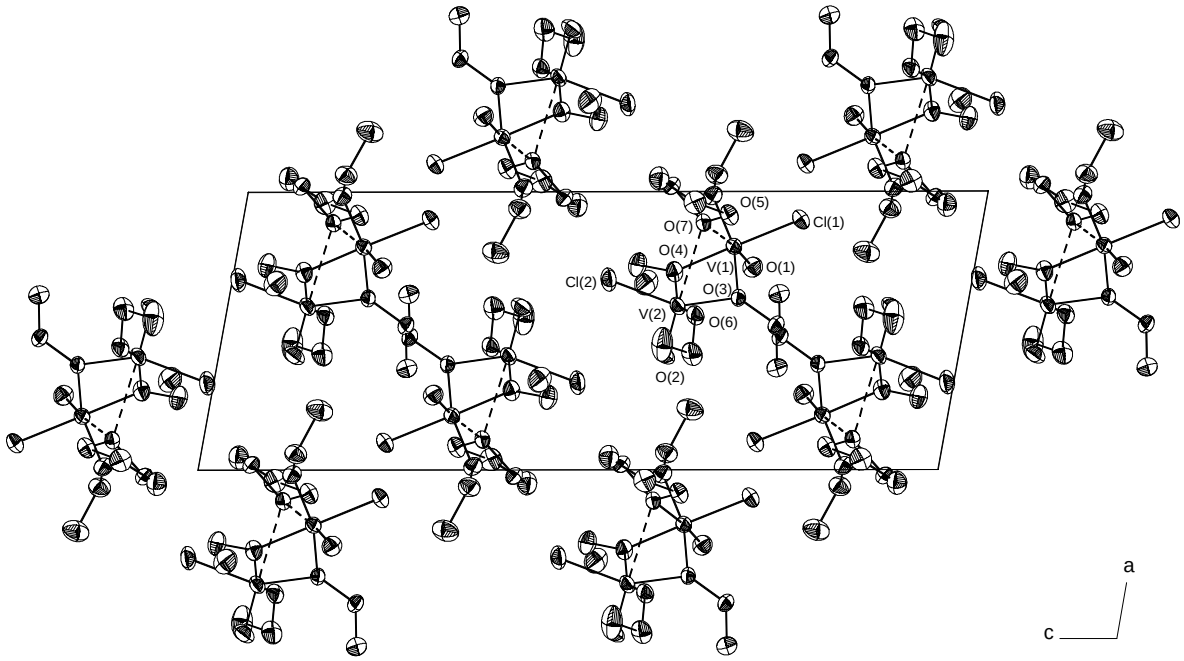

Fig. 5.3. Packing diagram for **3**.

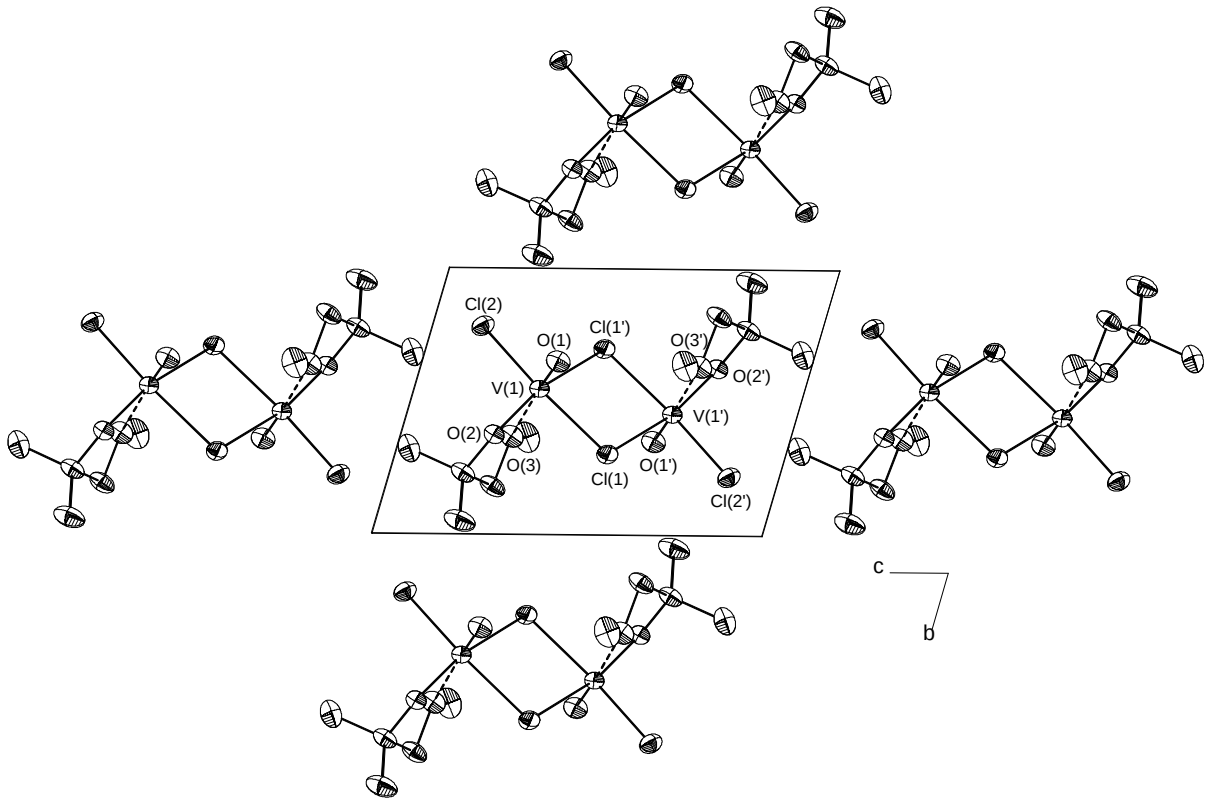

Fig. 5.4. Packing diagram for **4**. Symmetry transformations used to generate equivalent atoms: ' 1–x, 1–y, 1–z.

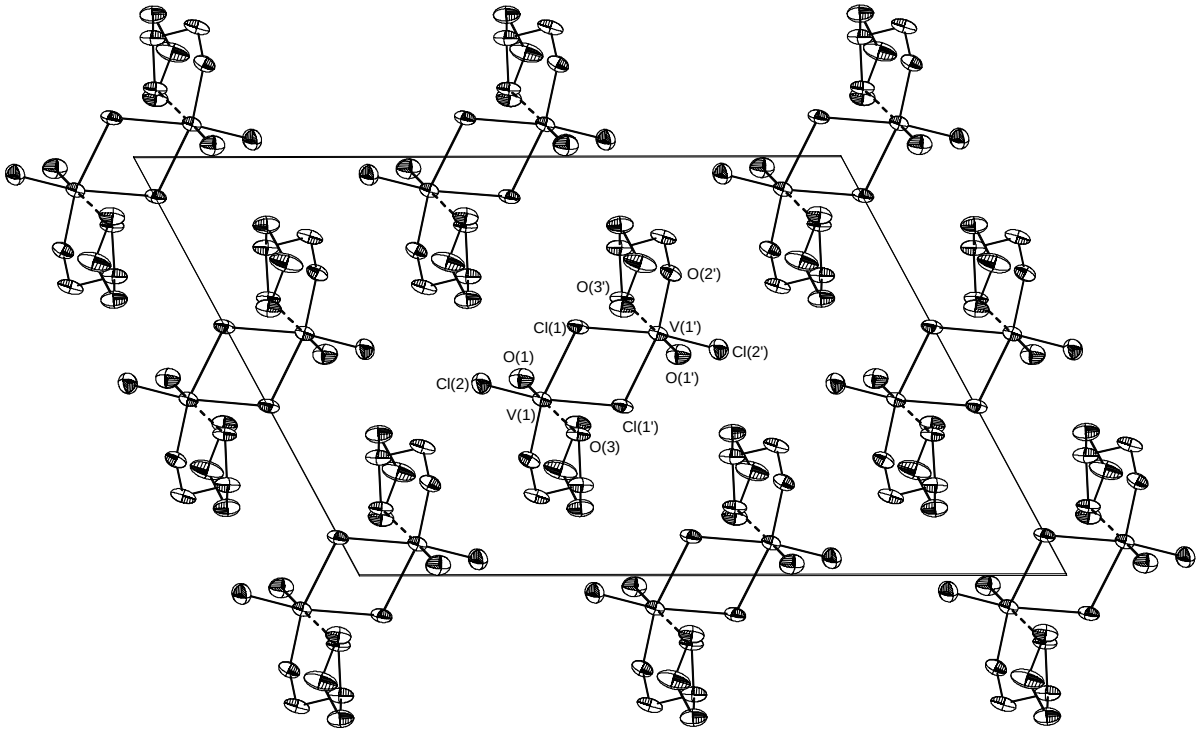

Fig. 5.5. Packing diagram for **5**.

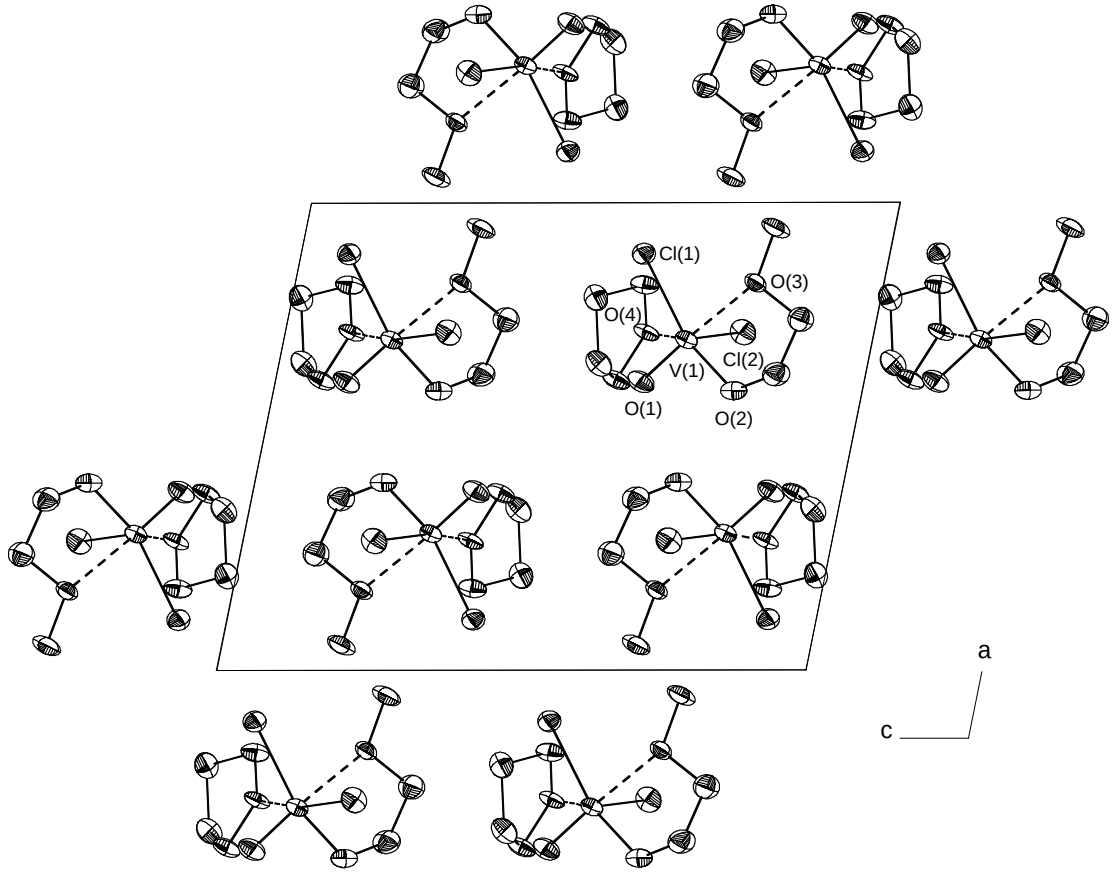

Fig. 5.6. Packing diagram for **6**.

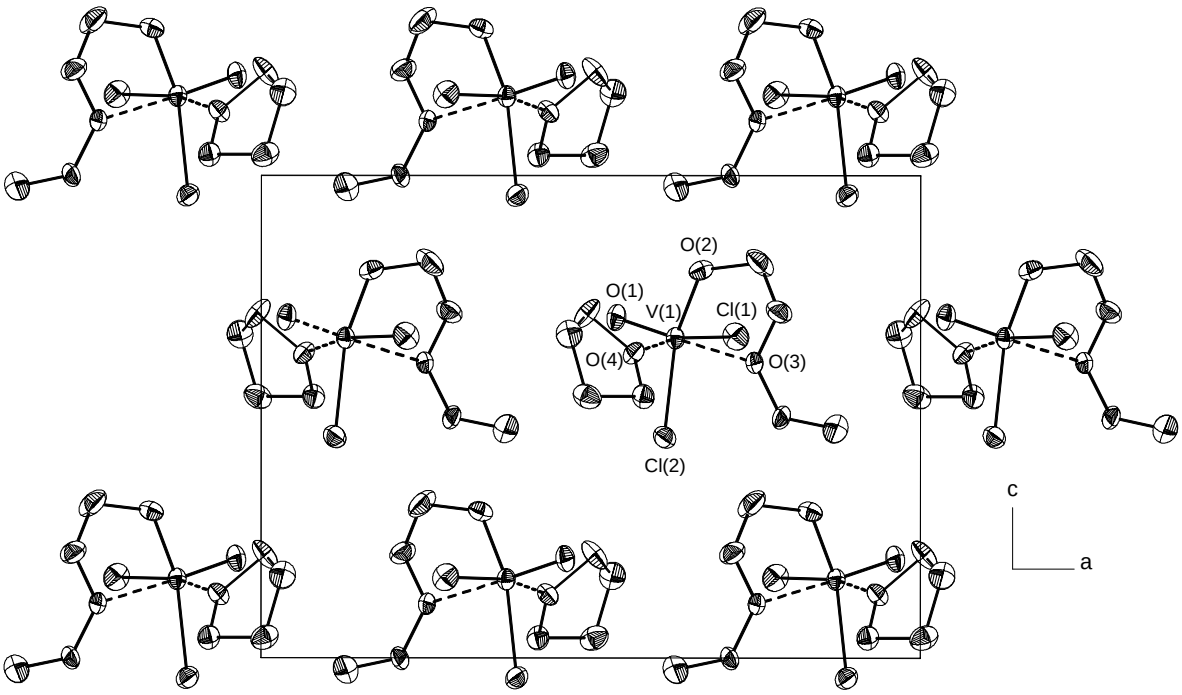

Fig. 5.7. Packing diagram for **7**.

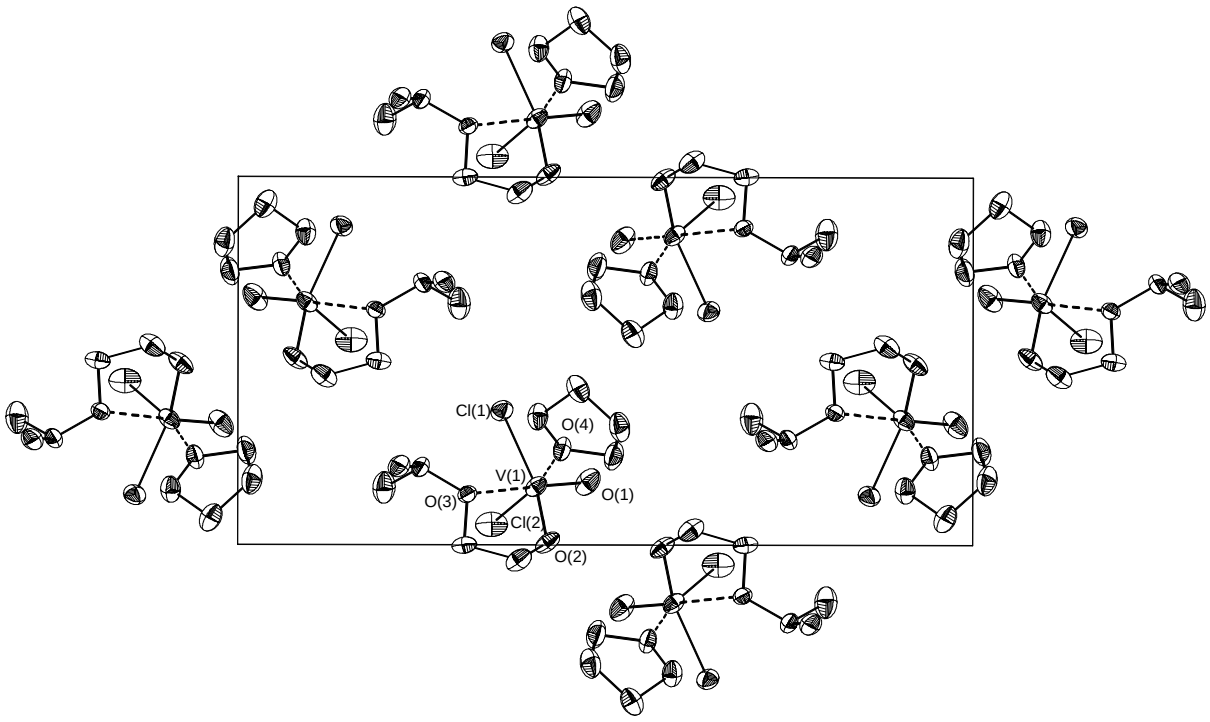

Fig. 5.8. Packing diagram for **8**.

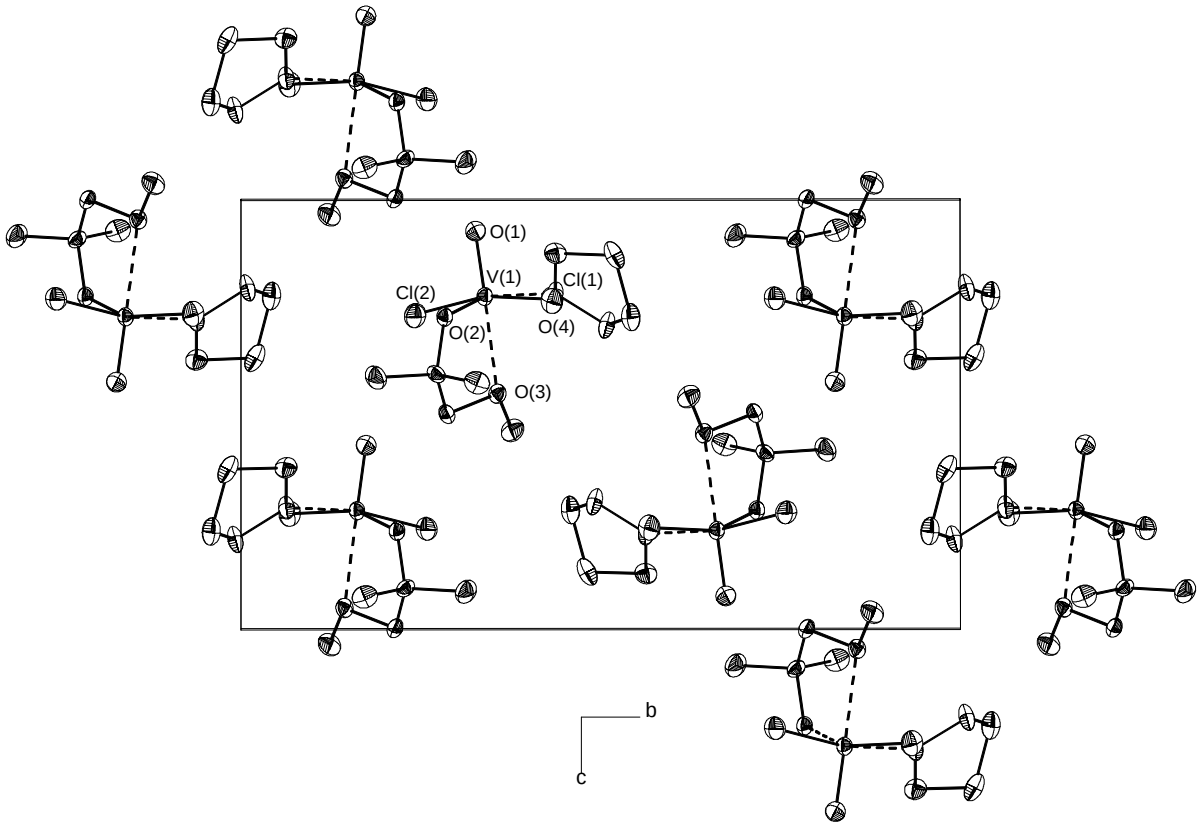

Fig. 5.9. Packing diagram for **9**.

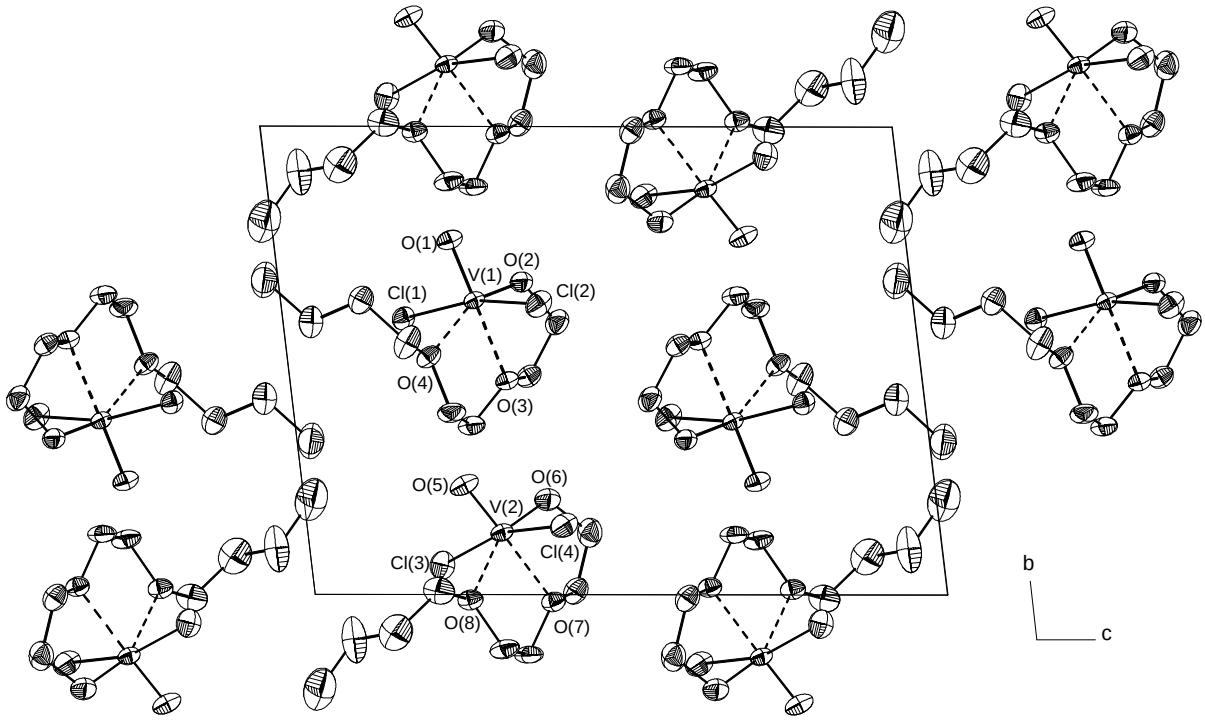

Fig. 5.10. Packing diagram for **10**.

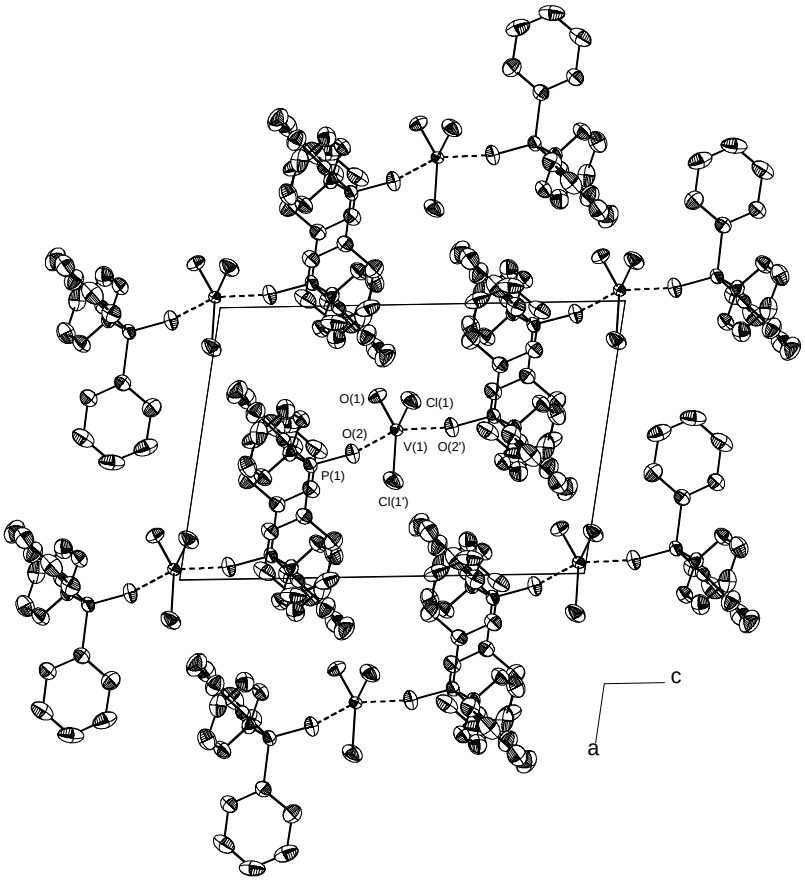

Fig. 5.11. Packing diagram for $VOCl_2(OPPh_3)_2$, lattice CH_2Cl_2 molecules are omitted for clarity. Symmetry transformations used to generated equivalent atoms: ' 1–x, –y, 1–z.

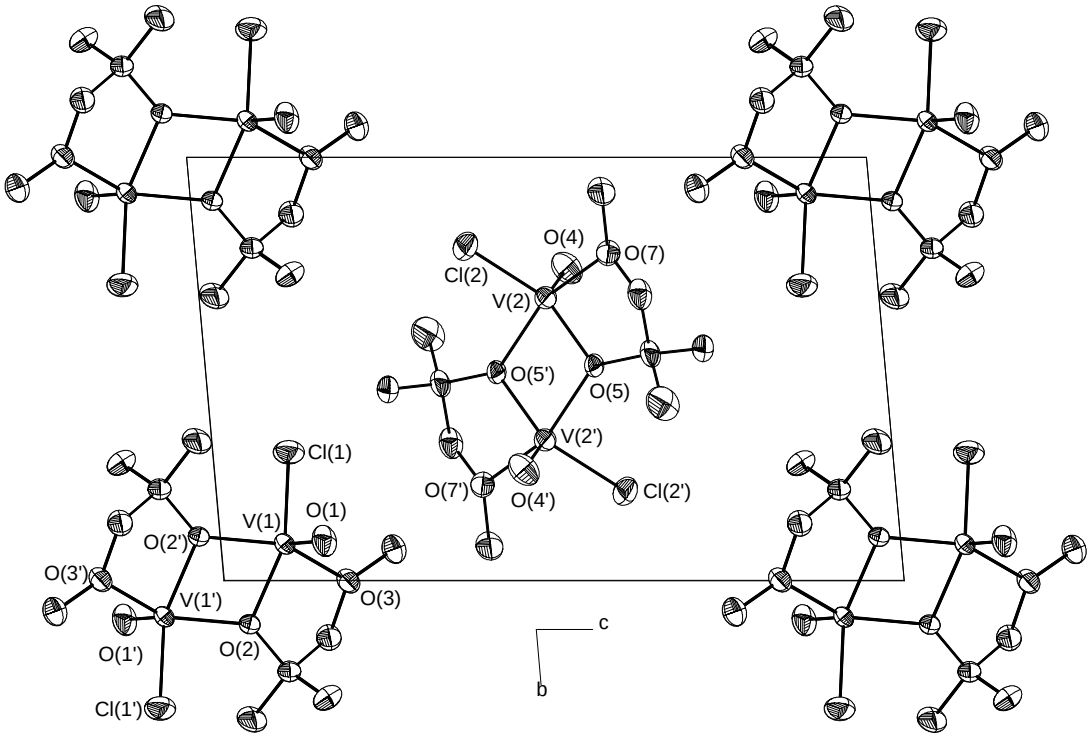

Fig. 5.12. Packing diagram for **15**. Symmetry transformations used to generate equivalent atoms: ' –x+2, –y, –z; " –x+1, –y–1, –z+1.

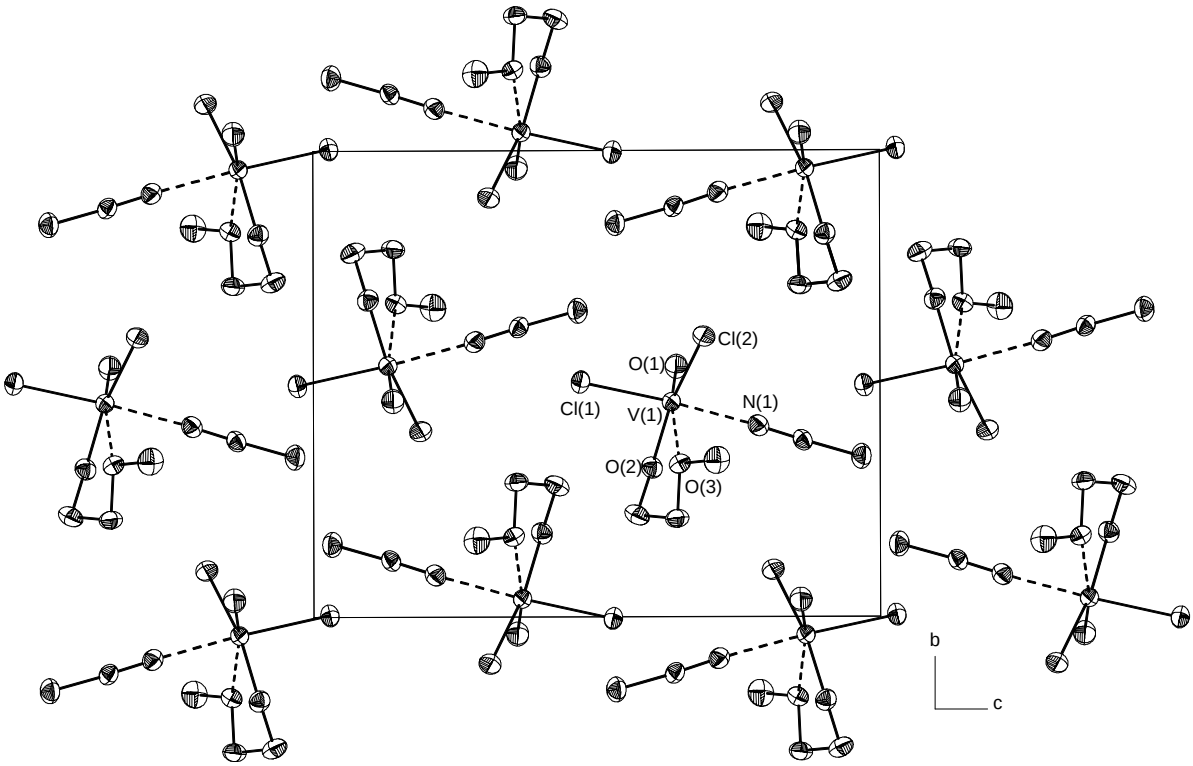

Fig. 5.13. Packing diagram for **16**.

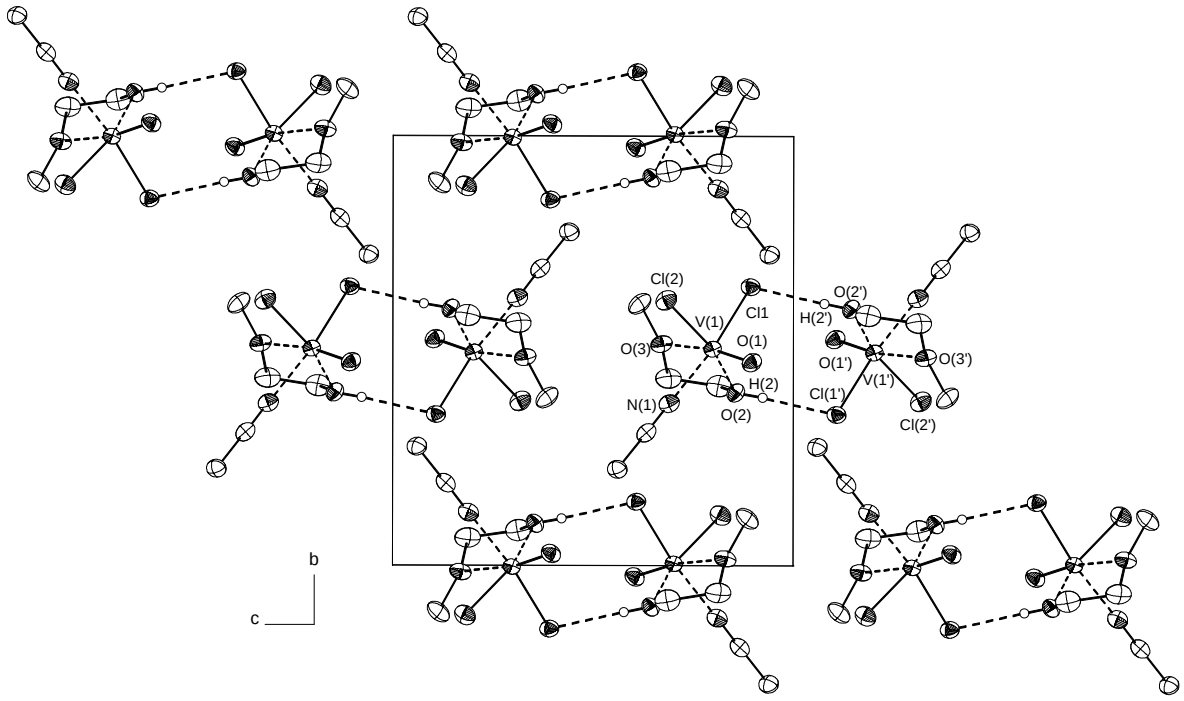

Fig. 5.14. Packing diagram for **17**. Symmetry transformations used to generate equivalent atoms: ' –x, 1–y, –z.

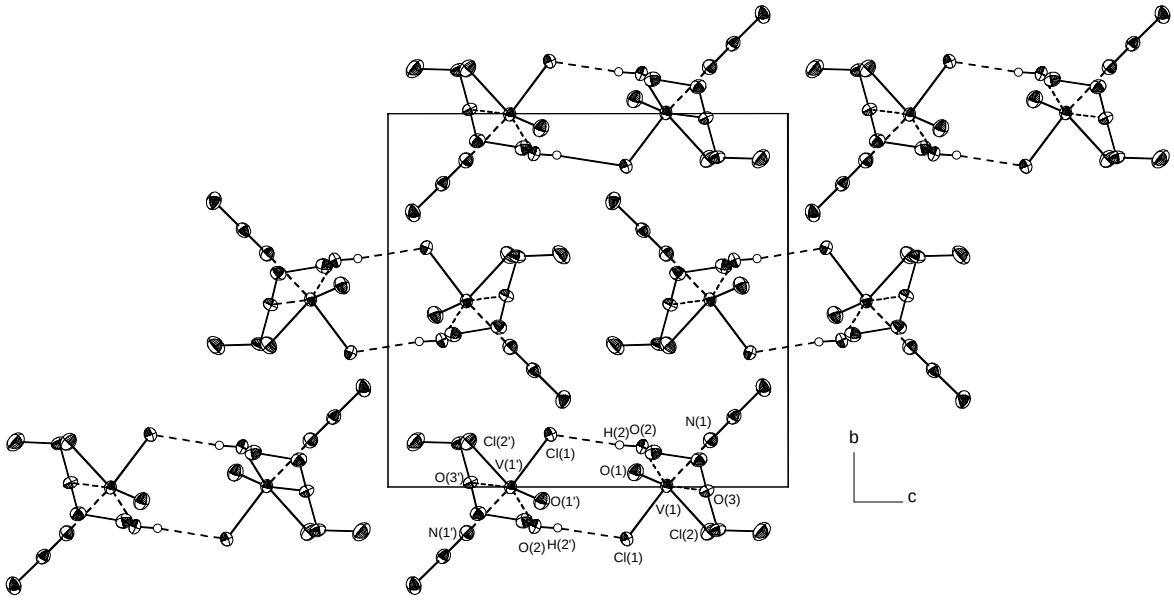

Fig. 5.15. Packing diagram for **18**. Symmetry transformations used to generate equivalent atoms: ' –x+1,–y+1,–z+1.

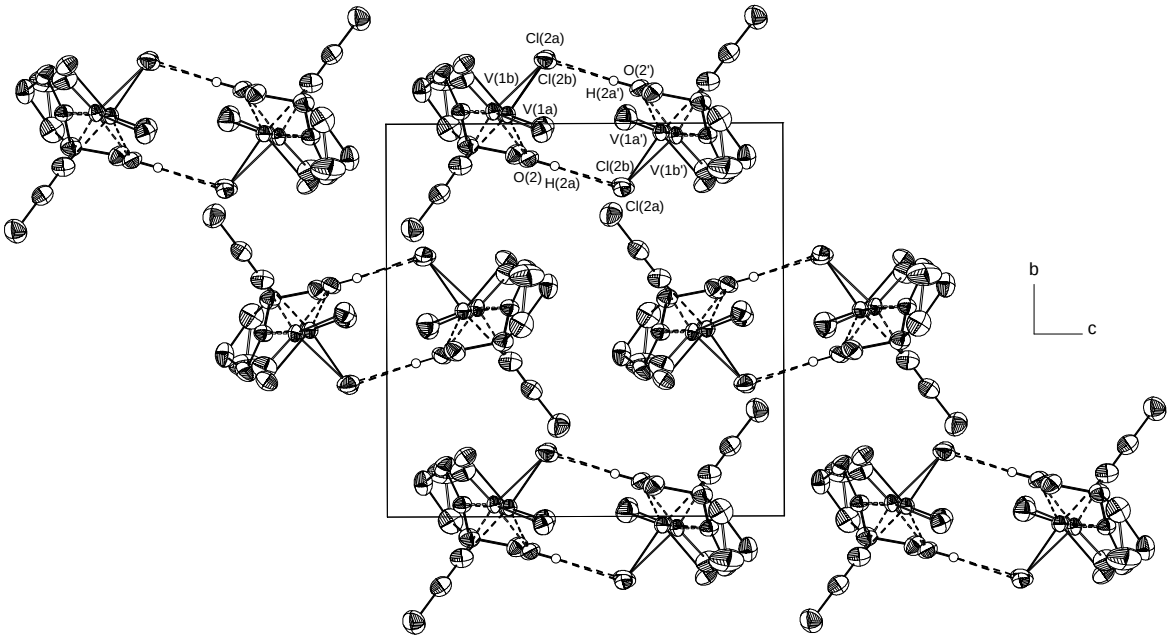

Fig. 5.16. Packing diagram for **19**, the second positions of the disordered atoms are denoted in dashed lines. Symmetry transformations used to generate equivalent atoms: ' 1–x, 1–y, –z.

5.3 Experimental Details for Ethylene Polymerization

Entry	Cocat.	c(V) mmol L^{-1}	Al:V	n(Al) mmol	MTCA mmol	t min	V mL	V(Tol) mL	Yield g	Activity[5]
1[1][3]	MAO	1.71	80	4	4	35		24	0.64	22
2[1][3]	MAO	1.33	80	2	2	45	20	17	1.07	55
3[1][3]	MAO	0.53	80	0.8	0.8	15	19	18	0.14	57
4[1][3]	MAO	1.28	80	2	2	22	20	17	0.48	52
5[1][3]	MAO	0.85	80	2	2	16	30	27	0.51	79
6[1][3]	MAO	0.85	80	2	2	60	30	27	0.65	26
7[1][3]	MAO	0.50	80	2	2	30	50	47	0.83	66
8[1][3]	MAO	0.20	80	0.8	2	30	50	49	0.51	102
9[1][3]	MAO	0.20	80	0.8	2	30	50	49	0.52	104
10[1][3]	MAO	0.10	510	2.6	2.5	30	50	47	0.12	48
11[1][4]	MAO	0.02	400	2.4	2.4	30	300	297	1.80	300
12[1][4]	MAO	0.02	400	2.4	2.4	30	300	297	0.40	67
13[1][4]	MAO	0.02	400	2.4	2.4	30	300	297	1.67	278
14[1][4]	MAO	0.03	400	2.4	2.4	30	200	197	0.47	78
15[1][4]	MAO	0.03	400	2.4	2.4	30	200	197	0.33	55
16[2][4]	MAO	0.10	1000	20	0	60	200	186	0	0
17[1][4]	MAO	0.10	1000	20	20	57	200	183	1.57	41
18[1][6][4]	MAO	0.10	1000	20	20	30	200	183	1.10	55
19[1][4]	MAO	0.10	1000	20	20	49	200	183	1.71	52
20[1][6][4]	MAO	0.10	1000	20	20	30	200	183	1.50	75
21[1][4]	MAO	0.05	1000	10	10	60	200	190	0.88	44
22[1][6][4]	MAO	0.05	1000	10	10	30	200	190	0.79	79
23a[1][4]	MAO	0.05	1000	10	10	60	200	190	0.87	44
24[1][6][4]	MAO	0.05	1000	10	10	30	200	190	0.79	79
25[2][4]	MAO	0.10	100	2	2	60	200	198	0.64	16
26[2][6][4]	MAO	0.10	100	2	2	30	200	198	0.58	29
27 [2][4]	MAO	0.10	100	2	2	60	200	198	0.77	19
28[2][4][6]	MAO	0.10	100	2	2	30	200	198	0.69	35
29[1][4]	DEAC	0.05	20	0.2	0	30	200	194	0	0
30[2][4]	DEAC	0.10	20	0.4	0.4	18	200	190	0.98	82
31[1][4]	DEAC	0.10	20	0.4	0.4	30	200	188	0.60	30
32[1][4]	DEAC	0.10	20	0.4	2	30	200	188	6.44	322

Entry	Cocat.	c(V) mmol L^{-1}	Al:V	n(Al) mmol	MTCA mmol	t min	V mL	V(Tol) mL	Yield g	Activity[5]
33[1][4]	DEAC	0.10	20	0.4	2	30	200	188	0	0
34[1][4]	DEAC	0.10	20	0.4	2	30	200	188	5.92	296
35[1][4]	DEAC	0.10	100	2	2	30	200	156	9.82	491
36[1][4]	DEAC	0.10	100	2	2	30	200	156	11.12	556
37[2][4]	DEAC	0.10	100	2	2	30	200	159	7.10	355
38[2][4]	DEAC	0.10	100	2	2	30	200	159	6.12	306
39[2][4]	MAO	0.02	400	1.7	2	30	200	198	0.01	3
40[2][4]	MAO	0.02	400	1.7	2	30	200	198	0.01	3
41[1][4]	MAO	0.10	100	2	2	30	200	195	0.10	5
42[1][4]	MAO	0.10	100	2	2	30	200	195	0.12	6
43[1][4]	DEAC	0.02	100	0.4	2	30	200	191	0	0
44[4]	DEAC	0.02	100	0.4	2	30	200	191	0	0
45[1]	DEAC	0.02	100	0.4	2	30	200	191	1.98	495
46[1]	DEAC	0.02	100	0.4	2	30	200	191	2.25	563
47[1]	MAO	0.02	1000	4.1	4	30	200	196	0.06	15
48[1]	MAO	0.02	1000	4.1	4	30	200	196	0.05	13
49[1]	MAO	0.10	400	8	8	30	200	191	0	0
50[1]	MAO	0.10	400	8	8	30	200	191	0	0
51[1]	DEAC	0.10	100	2	10	30	200	156	0	0
52[1]	DEAC	0.10	100	2	10	30	200	156	0	0

[1] Precatalyst $[VOCl_2(OCH_2CH_2OCH_3)]_2$.
[2] Precatalyst $VOCl_3$.
[3] Schlenk tube; *p*(ethylene) = 1 bar, at 22 °C; solvent: toluene.
[4] Glass autoclave; *p*(ethylene) = 2 bar, at 30 °C; solvent: toluene.
[5] [kg (mol [V])$^{-1}$ h^{-1} bar^{-1}].
[6] Feed of ethylene was calculated at a time of 30 min.

5.4 Experimental Details for Styrene Oligomerization

Entry[a]	T °C	Precatalyst	MAO mmol	Styrene mmol	Time h	Yield g	Conversion (%)
1	23	$[VOCl_2(OCH_2CH_2OMe)]_2$	2	26.2	20	2.72	99.6
2	40	$[VOCl_2(OCH_2CH_2OMe)]_2$	2	26.2	20	2.33	85.3
3	50	$[VOCl_2(OCH_2CH_2OMe)]_2$	2	26.2	20	1.94	71.1
4	60	$[VOCl_2(OCH_2CH_2OMe)]_2$	2	26.2	20	2.12	77.6
5	80	$[VOCl_2(OCH_2CH_2OMe)]_2$	2	26.2	20	1.67	61.2
6	80	$[VOCl_2(OCH_2CH_2OMe)]_2$	2	26.2	20	2.31	84.6
7	23	$[VOCl_2(OCH_2CH_2OMe)]_2$	2	39.3	1.5	2.09	76.6
8	23	$[VOCl_2(OCH_2CH_2OMe)]_2$	4	26.2	1.0	1.33	48.7
10	23	$[VOCl_2(OCH_2CH_2OPh)]$	2	39.3	1.5	2.08	76.2
11	22	$[VOCl_2(OCH_2CH_2OEt)]_2$	4	26.2	1	1.76	64.5
12	40	$[VOCl_2(OCH_2CH_2OEt)]_2$	4	26.2	1	1.94	71.1
13	60	$[VOCl_2(OCH_2CH_2OEt)]_2$	4	26.2	1	0.93	34.1
14	80	$[VOCl_2(OCH_2CH_2OEt]_2$	4	26.2	1	0.82	30.0

[a] Reaction conditions: [V] 0.05 mmol, 10 mL of toluene.

6 References

1 J. A. Hall, *J. Chem. Soc. London* **1887**, *51*, 751.

2 W. Prandtl, L. Hess, *Z. Anorg. Chem.* **1913**, *32*, 103.

3 D. C. Bradley, *Chem. Rev.* **1989**, *89*, 1317 and references cited therein.

4 W. Hemrika, R. Renirie, H. Dekker, R. Wever, in Vanadium Compounds, ed. A. S. Tracey, D. C. Crans, *ACS Symp. Ser. 711*, **1998**, 216.

5 For an overview of the biochemistry of vanadium, see: a) D. Rehder, *Inorg. Chem. Commun.* **2003**, *6*, 604; b) D. C. Crans, J. J. Smee, E. Gaidamauskas, L. Yang, *Chem. Rev.* **2004**, *104*, 849.

6 a) T. Hirao, *Chem. Rev.* **1997**, *97*, 2707; b) A. G. J. Ligtenbarg, R. Hage, B. L. Feringa, *Coord. Chem. Rev.* **2003**, *237*, 89; c) C. Bolm, *Coord. Chem. Rev.* **2003**, *237*, 245; d) T. Hirao, *Coord. Chem. Rev.* **2003**, *237*, 271; e) J. Iqbal, B. Bhatia, N. K. Nayyar, *Chem. Rev.* **1994**, *94*, 519.

7 W. L. Carrick, *J. Am. Chem. Soc.*, **1958**, *80*, 6455.

8 H. Hagen, J. Boersma, G. van Koten, *Chem. Soc. Rev.* **2002**, *31*, 357.

9 S. Gambarotta, *Coord. Chem. Rev.* **2003**, *237*, 229.

10 A. Lachowicz, W. Höbold, K.-H. Thiele, *Z. Anorg. Allg. Chem.* **1975**, *418*, 65.

11 W. Priebsch, D. Rehder, *Inorg. Chem.* **1990**, *29*, 3013.

12 J. Livage, *Coord. Chem. Rev.* **1999**, *190*, 391.

13 L. Albaric, N. Hovnanian, A. Julbe, G. Volle, *Polyhedron* **2001**, *20*, 2261.

14 H. Funk, W. Weiss, M. Zeising, *Z. Anorg. Allg. Chem.* **1958***, 296*, 36.

15 R. K. Mittal, R. C. Mehrotra, *Z. Anorg. Allg. Chem.* **1964**, *332*, 189.

16 D. C. Crans, H. Chen, R. A. Felty, *J. Am. Chem. Soc.* **1992**, *114*, 4543.

17 D. Gervail, R. Choukroun, *J. Inorg. Nucl. Chem.* **1974**, *36*, 3679.

18 B. S. Ault, *J. Phys. Chem.* **1999**, *A103*, 11474.

19 R. K. Mittal, R. C. Mehrotra, *Z. Anorg. Allg. Chem.* **1964**, *327*, 311.

20 D. C. Crans, R. A. Felty, O. P. Anderson, M. M. Miller, *Inorg. Chem.* **1993**, *32*, 247.

21 N. Sharma, A. K. Sood, S. S. Bhatt, S. C. Chaudhry, *Polyhedron* **1997**, *16*, 4055.

22 R. A. Henderson, D. L. Hughes, Z. Janas, R. L. Richards, P. Sobota, S. Szafert, *J. Organomet. Chem.* **1998**, *554*, 195.

23 a) D. Rehder, *Z. Naturforsch.,* **1977**, *B32*, 771; b) K. Paulsen, D. Rehder, *Z. Naturforsch.,* **1982**, *A37*, 139; c) W. Priebsch, D. Rehder, *Inorg. Chem.* **1985**, *24*, 3058.

24 K. Paulsen, D. Rehder, D. Thoennes, *Z. Naturforsch.* **1978**, *A33*, 834.

25 K. Witke, A. Lachowicz, W. Brüser, D. Zeigan, *Z. Anorg. Allg. Chem.* **1980**, *465*. 193.

26 B. Adler, I. Bieräugel, A. Lachowicz, K.-H. Thiele, *Z. Anorg. Allg. Chem.* **1977**, *431*, 227.

27 A. Lachowicz, K.-H. Thiele, *Z. Anorg. Allg. Chem.* **1977**, *434*, 271**.**

28 O. W. Howarth, J. R. Trainor, *Inorg. Chim. Acta* **1987**, *127*, L27.

29 F. Hillerns, D. Rehder, *Chem. Ber.* **1991**, 124, 2249.

30 F. Hillerns, F. Olbrich, U. Behrens, D. Rehder, *Angew. Chem.* **1992**, *104*, 479; *Angew. Chem., Int. Ed. Engl.*, **1992**, *31*, 447.

31 a) M. J. Gresser, A. S. Tracey, *J. Am. Chem. Soc***. 1986**, *108*, 1935; b) A. S. Tracey, M. J. Gresser, *Inorg. Chem.* **1988**, *27*, 2695; c) A. S. Tracey, M. J. Gresser, K. M. Parkinson, *Inorg. Chem.* **1987**, *26*, 629.

32 D. Rehder, C. Weidemann, A. Duch, W. Priebsch, *Inorg. Chem.* **1988**, *27*, 584.

33 C. N. Caughlan, H. M. Smith, K. Watenpaugh, *Inorg. Chem.* **1966**, *5*, 2131.

34 J. Spandl, I. Brüdgam, H. Hartl, *Z. Anorg. Allg. Chem.* **2000**, *626*, 2125.

35 F. J. Feher, J. F. Walzer, *Inorg. Chem.* **1991**, *30*, 1689.

36 P. J. Toscano, E. J. Schermerhorn, C. Dettelbacher, D. Macherone, J. Zubieta, *J. Chem. Soc., Chem. Commun.* **1991**, 933.

37 E. C. E. Rosenthal, F. Girgsdies, *Z. Anorg. Allg. Chem.* **2002**, *628*, 1917.

38 E. C. E. Rosenthal, H. Cui, K. C. H. Lange, S. Dechert, *Eur. J. Inorg. Chem.* **2004**, 4681.

39 E. C. E. Rosenthal, H. Cui, J. Koch, P. Escarpa Gaede, M. Hummert, S. Dechert, *Dalton Trans.* **2005**, 3108.

40 D. C. Crans, R. A. Felty, M. M. Miller, *J. Am. Chem. Soc.* **1991**, *113*, 265.

41 W. A. Nugent, R. L. Harlow, *J. Am. Chem. Soc.* **1994**, *116*, 6142.

42 H. Lütjens, G. Wahl, F. Möller, P. Knochel, J. Sundermeyer, *Organometallics* **1997**, *16*, 5869.

43 J. Y. Kempf, B. Maigret, D. C. Crans, *Inorg. Chem.* **1996**, *35*, 6485.

44 H. Glas, E. Herdtweck, G. R. J. Artus, W. R. Thiel, *Inorg. Chem.* **1998**, *37*, 3644.

45 H. Glas, K. Köhler, E. Herdtweck, P. Maas, M. Spiegler, W. R. Thiel, *Eur. J. Inorg. Chem.* **2001**, 2075.

46 F. Wolff, C. Lorber, R. Choukroun, B. Donnadieu, *Inorg. Chem.* **2003**, *42*, 7839.

47 B. Baruah, S. Das, A. Chakravorty, *Coord. Chem. Rev.* **2003**, *237*, 135.

48 F. A. Cotton, G. Wilkinson, C. A. Murillo, M. Bochmann, *Advanced Inorganic Chemistry*, 6th ed., John Wiley & Sons, New York, **1999**.

49 H.-L. Krauss, G. Gnatz, *Chem. Ber.* **1962**, *95*, 1023.

50 S. J. Miles, J. D. Wilkins, *J. Inorg. Nucl. Chem.* **1975**, *37*, 2271.

51 G. Beindorf, J. Straehle, W. Liebelt, K. Dehnicke, *Z. Naturforsch.* **1980**, *B35*, 522.

52 J. C. Daran, Y. Jeannin, G. Constant, R. Morancho, *Acta Crystallogr.* **1975**, *B31*, 1833.

53 A. Gourdon, Y. Jeannin, *Acta Crystallogr.* **1980**, *B36,* 304.

54 J.-C. Daran, A. Gourdon, Y. Jeannin, *Acta Crystallogr.* **1980**, *B36*, 309.

55 K. Tarama, S. Yoshida, H. Kanai, S. Osaka, *Bull. Chem. Soc. Jpn.* **1968**, *41*, 1271.

56 H. Kanai, S. Osaka, *React. Kinet. Catal. Lett.* **2000**, *70*, 105.

57 F. A. Cotton, J. Lu, *Inorg. Chem*. **1995**, *34*, 2639.

58 R. A. Henderson, A. Hills, D. L. Hughes, D. J. Lowe, *J. Chem. Soc., Dalton Trans.* **1991**, 1755.

59 a) K. Ziegler, E. Holzkamp, H. Breil, H. Martin, *Angew. Chem.* **1955**, *67*, 426; b) G. Natta, P. Pino, P. Corradini, F. Danusso, E. Mantica, G. Mazzanti, G. Moraglio, *J. Am. Chem. Soc.* **1955**, *77*, 1708.

60 A. Zambelli, A. Lety, C. Tosi, I. Pasquon, *Makromol. Chem.* **1968**, *115*, 73.

61 G. Natta, I. Pasquon, A. Zambelli, *J. Am. Chem. Soc.* **1962**, *84*, 1488.

62 Y. Doi, S. Suzuki, K. Soga, *Makromol. Chem., Rapid Commun.* **1985**, *6*, 639.

63 Y. Ma, D. Reardon, S. Gambarotta, G. Yap, H. Zahalka, C. Lemay, *Organometallics* **1999**, *18*, 2773.

64 A. Zambelli, G. Natta, I. Pasquon, R. Signorini, *J. Poly. Sci.* **1967**, *C16*, 2485.

65 G. Natta, A. Zambelli, G. Lanzi, I. Pasquon, E. R. Mognaschi, A. L. Segre, P. Centola, *Makromol. Chem.* **1965**, *81*, 161.

66 a) M. H. Lehr, *Macromolecules*, **1968**, *1*, 178; b) D. L. Christman, G. I. Keim, *Macromolecules*, **1968**, *1*, 358; c) M. H. Lehr, C. J. Carman, *Macromolecules* **1969**, *2*, 217.

67 a) A. Gumbolt, J. Helberg, G. Schleitzer, *Makromol. Chem.* **1967**, *101*, 229; b) Y. Doi, S. Suzuki, K. Soga, *Macromolecules* **1986**, *19*, 2896; c) T. Ouzumi, K. Soga, *Makromol. Chem.* **1992**, *193*, 823.

68 a) D. L. Christman, *J. Poly. Sci.* **1972**, *A10*, 471; b) S. Cesca, *J. Poly. Sci. Macromol. Rev.* **1975**, *10*, 1.

69 W. Kaminsky, F. Renner, *Makromol. Chem., Rapid Commun.* **1993**, *14*, 239.

70 C. Wang, S. Friedrich, T. R. Younkin, R. T. Li, R. H. Grubbs, D. A. Bansleben, M. W. Day, *Organometallics* **1998**, *17*, 3149.

71 D. J. Tempel, L. K. Johnson, R. L. Huff, P. S. White, M. Brookhart, *J. Am. Chem. Soc.* **2000**, *122*, 6686.

72 G. Natta, M. Peraldo, G. Allegra, *Makromol. Chem.* **1964**, *75*, 215.

73 Y. Doi, M. Takada, T. Keii, *Makromol. Chem.* **1979**, *180*, 57.

74 A. Zambelli, I. Pasquon, R. Signorini, G. Natta, *Makromol. Chem.* **1968**, *112*, 160.

75 J. Boor, Jr., E. A. Youngman, *J. Poly. Sci.* **1966**, *A4*, 1861.

76 A. Zambelli, G. Allegra, *Macromolecules* **1980**, *13*, 42.

77 P. Corradini, G. Guerra, R. Pucciariello, *Macromolecules* **1985**, *18*, 2030.

78 P. Cossee, *J. Catal.* **1964**, *3*, 80.

79 E. J. Arlman, P. Cossee, *J. Catal.* **1964**, *3*, 99.

80 P. Margl, L. Deng, T. Ziegler, *Organometallics* **1998**, *17*, 933.

81 P. Sobota, J. Ejfler, S. Szafert, T. Glowiak, I. O. Fritzky, K. Szczegot, *J. Chem. Soc., Dalton Trans.* **1995**, 1727.

82 P. Sobota, J. Ejfler, S. Szafert, K. Szczegot, W. Sawka-Dobrowolska, *J. Chem. Soc., Dalton Trans.* **1993**, 2353.

83 Z. Janas, L. B. Jerzykiewicz, R. L. Richards, P. Sobota, *Chem. Commun.* **1999**, 1015.

84 Z. Janas, L. B. Jerzykiewicz, S. Przybylak, R. L. Richards, P. Sobota, *Organometallics* **2000**, *19*, 4252.

85 K. Takaoki, T. Miyatake, *Macromol. Symp.* **2000**, *157*, 251.

86 C. Redshaw, L. Warford, S. H. Dale, M. R. J. Elsegood, *Chem. Commun.* **2004**, 1954.

87 H. Hagen, J. Boersma, M. Lutz, A. L. Spek, G. van Koten, *Eur. J. Inorg. Chem.* **2001**, 117.

88 H. Hagen, C. Bezemer, J. Boersma, H. Kooijman, M. Lutz, A. L. Spek, G. van Koten, *Inorg. Chem.* **2000**, *39*, 3970.

89 a) M. P. Coles, V. C. Gibson, *Polym. Bull.* **1994**, *33*, 529; b) S. Scheuer, J. Fischer, J. Kress, *Organometallics* **1995**, *14*, 2627; c) M. C. W. Chan, J. M. Cole, V. C. Gibson, J. A. K. Howard, *Chem. Commun.* **1997**, 2345; d) M. C. W. Chan, K. C. Chew, C. I. Dalby, V. C. Gibson, A. Kohlmann, I. R. Little, W. Reed, *Chem. Commun.* **1998**, 1673; e) M. P. Coles, C. I. Dalby, V. C. Gibson, I. R. Little, E. L. Marshall, M. H. Ribeiro da Costa, S. Mastroianni, *J. Organomet. Chem.* **1999**, *591*, 78.

90 C. Lorber, B. Donnadieu, R. Choukroun, *J. Chem. Soc., Dalton Trans.* **2000**, 4497.

91 K. Nomura, A. Sagara, Y. Imanishi, *Chem. Lett.* **2001**, 36.

92 K. Nomura, A. Sagara, Y. Imanishi, *Macromolecules* **2002**, *35*, 1583.

93 J. Yamada, M. Fujiki, K. Nomura, *Organometallics* **2005**, *24*, 2248.

94 a) Y. Nakayama, H. Bando, Y. Sonobe, Y. Suzuki, T. Fujita, *Chem. Lett.* **2003**, *32*, 766; b) Y. Nakayama, H. Bando, Y. Sonobe, T. Fujita., *J. Mol. Catal.* **2004**, *A213*, 141.

95 Z. Janas, P. Sobota, M. Kasprzak, T. Glowiak, *Chem. Commun.* **1996**, 2727.

96 Z. Janas, P. Sobota, M. Klimowicz, S. Szafert, K. Szczegot, L. B. Jerzykiewicz, *J. Chem. Soc., Dalton Trans.* **1997**, 3897.

97 a) P. H. M. Budzelaar, A. B. van Oort, A. G. Orpen, *Eur. J. Inorg. Chem.* **1998**, 1485; b) W.-K. Kim, M. J. Fevola, L. M. Liable-Sands, A. L. Rheingold, K. H. Theopold, *Organometallics* **1998**, *17*, 4541.

98 a) E. A. C. Brussee, A. Meetsma, B. Hessen, J. H. Teuben, *Organometallics*, **1998**, *17*, 4090; b) E. A. C. Brussee, A. Meetsma, B. Hessen, J. H. Teuben, *Chem. Commun.* **2000**, 497.

99 M. J. R. Brandsma, E. A. C. Brussee, A. Meetsma, B. Hessen, J. H. Teuben, *Eur. J. Inorg. Chem.* **1998**, 1867.

100 a) F. J. Feher, R. L. Blanski, *J. Am. Chem. Soc.* **1992**, *114*, 5886; b) M. Motevalli, D. Shah, S. A. A. Shah, A. C. Sullivan, *Organometallics*, **1994**, *13*, 4109; c) C. Lorber, B. Donnadieu, R. Choukroun, *Organometallics*, **2000**, *19*, 1963; d) P. T. Witte, A. Meetsma, B. Hessen, *Organometallics*, **1999**, *18*, 2944; e) D. Reardon, F. Conan, S. Gambarotta, G. Yap, Q. Wang, *J. Am. Chem. Soc.*, **1999**, *121*, 9318; f) S. Millione, G. Cavallo, C. Tedesco, A. Grassi, *J. Chem. Soc., Dalton Trans.* **2002**, 1839.

101 V. Conte, F. Di Furia, S. Moro, *J. Phys. Org. Chem.* **1996**, *9*, 329.

102 A. Butler, M. J. Clague, G. E. Meister, *Chem. Rev.* **1994**, *94*, 625.

103 H. Mimoun, L. Saussine, E. Daire, M. Postel, J. Fischer, R.Weiss, *J. Am. Chem. Soc.* **1983**, *105*, 3101.

104 D. J. Berrisford, C. Bolm, K. B. Sharpless, *Angew. Chem.* **1995**, *107*, 1159; *Angew. Chem., Int. Ed. Engl.* **1995**, *34*, 1059.

105 H. Mimoun, M. Mignard, P. Brechot, L. Saussine, *J. Am. Chem. Soc.* **1986**, *108*, 3711.

106 P. Chaumette, H. Mimoun, L. Saussine, J. Fischer, A. Mitschler, *J . Organomet. Chem.* **1983**, *250,* 291.

107 a) H. Mimoun, *J . Mol. Catal.* **1980**, *7*, 1; b) H. Mimoun, *Angew. Chem.* **1982**, *21*, 1303; *Angew. Chem., Int. Ed. Engl.* **1982**, *2,* 734; c) H. Mimoun, *Isr. J. Chem.* **1983**, *23*, 451.

108 H. Mimoun, P. Chaumette, M. Mignard, L. Saussine, J. Fischer, R. Weiss, *Nouv. J. Chim.* **1983**, *7*, 467.

109 M. R. Maurya, S. Khurana, W. Zhang, D. Rehder, *Eur. J. Inorg. Chem.* **2002**, 1749.

110 J. Salta, J. Zubieta, *Inorg. Chim. Acta* **1997**, *257*, 83.

111 C. Weidemann, W. Priebsch, D. Rehder, *Chem. Ber.* **1989**, *122*, 235.

112 W. Mowat, A. Shortland, G. Yagupsky, N. J. Hill, M. Yagupsky, G. Wilkinson, *J. Chem. Soc., Dalton Trans.* **1972**, 533.

113 F. J. Feher, R. L. Blanski, *Organometallics* **1993**, 12, 958.

114 a) M. R. Caira, B. J. Gellatly, *Acta Crystallogr.* **1980**, *B36*, 1198 and references therein; b) D. Collison, B. Gahan, C. D. Garner, F. E. Mabbs, *J. Chem. Soc., Dalton Trans.* **1980**, 667; c) B. Gahan, F. E. Mabbs, *J. Chem. Soc., Dalton Trans.* **1983**, 1713.

115 D. Rehder, *Bull. Magn. Reson.* **1982**, *4*, 33.

116 C. Sanchez, M. Nabavi, F. Taulelle, *Mater. Res. Soc. Symp. Proc.* **1988**, *121*, 93.

117 M. Zviely, A. Goldman, I. Kirson, E. Glotter, *J. Chem. Soc., Perkin Trans. 1* **1986**, 229.

118 a) S. R. Cooper, Y. B. Koh, K. N. Raymond, *J. Am. Chem. Soc.* **1982**, *104*, 5092; b) M. E. Cass, D. L. Greene, R. M. Buchanan, C. G. Pierpont, *J. Am. Chem. Soc.* **1983**, *105*, 2680; c) M. E. Cass, N. Gordon, C. G. Pierpont, *Inorg. Chem.* **1986**, *25*, 3962.

119 G. Foulon, J.-D. Foulon, N. Hovnanian, *Polyhedron* **1993**, *12*, 2507.

120 J.-P. Brunette, R. Heimburger, M. J. F. Leroy, *C. R. Acad. Sci.* **1971**, *C272*, 2147.

121 A. A. Konovalova, S. V. Bainova, V. D. Kopanev, Yu. A. Buslaev, *Russ. J. Coord. Chem.* **1983**, 661.

122 *Gmelins Handbuch der Anorganischen Chemie*, 8th edn., Verlag Chemie, Weinheim, **1967**, *48B*, 88.

123 W. Prandtl, B. Bleyer, *Z. Anorg. Chem.* **1910**, *67*, 152.

124 G. M. Sheldrick, *Acta Crystallogr.* **1990**, *A46*, 467.

125 G. M. Sheldrick, SHELXS-97-*Program for Crystal Structure Determination*, Universität Göttingen **1997**.

126 G. M. Sheldrick, SADABS-*Program for Empirical Absorption Correction of Area Detector Data*, Universität Göttingen **1996**.

127 K. Brandenburg, DIAMOND 2.1, Universität Kiel **1999**.

128 D. D. Perrin, W. L. F. Armarego, *Purification of Laboratory Chemicals*, 3rd edn., Butterworth-Heinemann, Oxford **1988**, 115.

129 K. B. Sharpless, T. R. Verhoeven, *Aldrichim. Acta* **1979**, *12*, 63.

130 R. J. Kern, *J. Inorg. Nucl. Chem.* **1962**, *24*, 1105.

131 J. G. H. Du Preez, M. L. Gibson, *J. S. Afr. Chem. Inst.* **1970**, *23*, 184.

132 C.-C. Su, H.-Y. Kang, *Proc. Natl. Sci. Counc. B, ROC* **1982**, *6*, 157.

Lebenslauf

Huiling Cui

Geburtstag:	19.11.1975
Geburtsort:	Botou, Hebei Province, P. R. China
Staatsangehörigkeit:	Chinesisch
Familienstand:	verheiratet

Schulausbildung

Aug. 1981 – Jul. 1987	Fu-Zhen Grundschule, Botou, China
Aug. 1987 – Jul. 1990	Fu-Zhen Junior Middle School, Botou, China
Aug. 1990 – Jul. 1994	Jiao-He Senior Middle School, Botou, China

Hochschulausbildung

Sep. 1994 – Jul. 2001	Studium Chemie am Fachbereich Chemie der Nankai Universität, Tianjin, China
Juli 2002– April 2006	Anfertigung der Dissertation unter Anleitung von Dr. Esther C. E. Rosenthal (in der Arbeitsgruppe von Prof. Dr. Herbert Schumann) am Institut für Chemie der Technischen Universität Berlin

Publications and Posters

E. C. E. Rosenthal, H. Cui, K. C. H. Lange, S. Dechert

"Synthesis, molecular structure, and olefin polymerisation activity of an oxovanadium(V) alkoxide with unprecedented chloride bridging ligands."

Eur. J. Inorg. Chem. **2004**, 4681.

E. C. E. Rosenthal, H. Cui, J. Koch, P. Escarpa Gaede, M. Hummert, S. Dechert

"Chloride-bridged oxovanadium(V) complexes with alkoxyalkoxide ligands. Synthesis, structure, electrochemistry and reactivities."

Dalton Trans. **2005**, 3108.

E. C. E. Rosenthal, H. Cui

"Oxovanadium alkoxides: The search for efficient polymerization catalyst an addition to the quest."

Tag der Chemie, Berlin, **2003**.

E. C. E. Rosenthal, H. Cui

"Oxovanadium alkoxides: structures with versatile coordination environment."

Tag der Chemie, Berlin, **2004**.

E. C. E. Rosenthal, H. Cui

"Oxovanadium alkoxides: solvent participation in the formation of novel derivatives."

Tag der Chemie, Berlin, **2005**.